This dissertation has been
microfilmed exactly as received

67-8360

WARNER, Charles Young, 1934-

TURBULENT NATURAL CONVECTION IN AIR ALONG A VERTICAL FLAT PLATE.

The University of Michigan, Ph.D., 1966
Engineering, mechanical

University Microfilms, Inc., Ann Arbor, Michigan

TURBULENT NATURAL CONVECTION IN AIR ALONG A VERTICAL FLAT PLATE

Charles Young Warner

A dissertation submitted in partial fulfillment
of the requirements for the degree of
Doctor of Philosophy in the
University of Michigan
1966

Doctoral Committee:

Professor Vedat S. Arpaci, Chairman
Professor Arthur G. Hansen
Professor Arnold M. Kuethe
Associate Professor Herman Merte, Jr.

TURBULENT NATURAL CONVECTION IN AIR ALONG A VERTICAL FLAT PLATE

Charles Young Warner

ABSTRACT

Extensive measurements of temperature and heat transfer were obtained from the two-dimensional natural convection of air past a vertical flat plate at uniform temperature, for Grashof Numbers up to 10^{12}. The design, fabrication, and operation of an experimental facility for this case is described.

Local heat flux measurements at twenty-four stations along the vertical coordinate of the plate are reported for four plate temperature levels. Measured temperatures within the boundary layer are presented for plate-to-probe distances ranging from 0.0005 to 12 inches, in both the laminar and turbulent regimes of the flow.

The temperature measurements indicate a very poor agreement with the 1/7 power law customarily assumed for the turbulent case, and evidence is given for the inaccuracy of the early measurements on which it was based. A strong similarity between the inner portion of the laminar and turbulent temperature profiles is noted, when plotted on natural coordinates.

The local heat flux measurements confirm the correlation of Bayley:

$$Nu = 0.010\ (Gr\ Pr)^{1/3}.$$

A discussion of problems and suggested techniques relative to the measurement of the velocity field is given. It is shown that the small magnitude of the velocities encountered, coupled with the presence of the temperature field and large fluctuations in all properties, puts this flow beyond the reach of present anemometry techniques.

To the memory of my father, Charles Arthur Warner, whose personal dedication to principles of individual freedom and responsibility has been an elusive example and a continuing inspiration.

ACKNOWLEDGEMENTS

It is a pleasure to acknowledge aid received from a great many sources in the completion of this work. To my committee: Professor Kuethe for well-timed instructions on turbulence, Professor Merte for special help on instrumentation and calibration, and for his interest and many helpful experimental suggestions, Professor Hansen for inspiration and support, and to Professor Arpaci, whose technical guidance and analytical expertise has been consistently matched with selfless service to his students. Special thanks is due the Department of Mechanical Engineering for extra-mile financial support, and to the National Science Foundation, National Aeronautics and Space Administration, and Ford Foundation whose financial backing allowed the author to devote full time to this work. To the staff of the Fluids Laboratory a special gratitude for friendly suggestions and helping hands. To Messrs. Blake, Scott, and Savkar for friendship and for their important role as sounding-boards, and to my wife and family, gratitude for the hardships indured in common that our family horizons might be broader, and a personal pledge of greater attention henceforth, as we pursue those horizons together.

TABLE OF CONTENTS

		Page
DEDICATION		ii
ACKNOWLEDGEMENTS		iii
LIST OF TABLES		v
LIST OF ILLUSTRATIONS		vi
LIST OF APPENDICES		viii
NOMENCLATURE		ix
I	INTRODUCTION	1
II	LITERATURE SURVEY	6
III	EXPERIMENTAL SETUP AND VERIFICATION	14
	A. Configuration of Heated Plate	14
	B. Plate Surface Preparation	14
	C. Heating Arrangements	17
	D. Probe Position Control Apparatus	17
	E. Enclosure Design	27
	F. Boundary Layer Temperature Instrumentation	27
	G. Wall Temperature Instrumentation	32
	H. Thermocouple Calibration	33
	I. Apparatus Checkout and Verification	35
IV	EXPERIMENTAL RESULTS	44
	A. Temperature Profiles in the Boundary Layer	45
	B. Results Relative to Boundary Layer Thickness	57
	C. Results of the Heat Flux Measurements	59
	D. Remarks Concerning the Measurement of Velocity	66
V	CONCLUSIONS AND RECOMMENDATIONS	71
VI	BIBLIOGRAPHY	73
	APPENDICES BEGIN ON PAGE 77	

LIST OF TABLES

Table		Page
1	Verification of the Two-Dimensionality Within the Turbulent Boundary Layer	42
A1	Temperature Field in Boundary Layer, Degrees Fahrenheit	79
A2	Nondimensional Temperature Field, θ / θ_{wall}	81
A3	Heat Flux Measurements	83
A4	Heat Flux Data Reduction Results	84
A5	Thermocouple Calibration Data	91
A6	Probe Positioning Mechanism Calibrations ...	92
A7	Plate Emissivity Distribution	93
A8	Typical Plate Temperature Distribution	101
A9	Experimental Equipment Listing	102

LIST OF ILLUSTRATIONS

Figure		Page
1	Velocity and Temperature Profiles in the Natural Convection Boundary Layer	3
2	Turbulent Results of Eckert and Diagula(14)	10
3	Photograph of Emissivity Measuring Apparatus	16
4	Plate Section Heating Schematic	18
5	Photograph of Typical Plate Section	19
6	Power Control and Measurement Circuits	20
7	Photograph of Probe Carriage Assembly	21
8	Probe Position Control: Schematic of Carriage Mounted Equipment	23
9	Probe Position Control: Instrument Panel Schematic	24
10	Photograph of Positioner Control Panel	25
11	Sketch of Fine-Position Indication System ..	26
12	Sketch of Enclosure	28
13	Temperature Boundary Layer Probe Schematic .	30
14	Photograph of Thermocouple Switching Panel .	34
15	Thermocouple Calibration Schematic	36
16	Verification Data: Laminar Temperature Data Compared with Theoretical Profile ..	39
17	Sketch of Leading Edge Configuration	40
18	Experimental Turbulent Temperature Profiles.	46
19	Laminar and Transitional Temperature Field Very Near Wall	47

LIST OF ILLUSTRATIONS (Continued)

Figure		Page
20	Turbulent Temperature Field Very Near Wall .	48
21	Comparison of Experimental Turbulent with Data of Fujii(20)	49
22	Laminar Data of Griffiths and Davis(24)	52
23	Comparison of Normalized Experimental and Power-Law Profiles	54
24	Turbulent and Laminar Profiles at Moderate Distances from the Wall	56
25	Enthalpy Thickness vs. x	58
26	Experimental Heat Transfer Data	61
27	Comparison of Heat Transfer Data with Correlations and Data from the Literature	62
28	Local Heat Flux vs. Plate Distance, θ_w= 46°F	71
29	Local Heat Flux vs. Plate Distance, θ_w= 65°F.	72
A1	Geometry of Tables A1 and A2	78
A2	Geometry for Probe Heat Flow Analysis	89
A3	Representation of Plate for Thermometry Analysis	95
A4	Plate Temperature Distribution: One-Dimensional Model	97
A5	Wall Temperature Distribution Under Uniform Heat Flux Conditions	100
A6	Forced-Free Convection Interaction Data for Hot Wires (Collis and Williams(8)).	106

LIST OF APPENDICES

Appendix		Page
I	Experimental Temperature and Heat Flux Data.	77
II	Thermocouple Probe Design Considerations ...	88
III	Thermocouple Fixed-Point Calibrations	91
IV	Probe Positioning Mechanism Calibrations ...	92
V	Wall Emissivity Data	93
VI	Analysis of Plate Temperature Variations ...	94
VII	Typical Plate Temperature Distributions	99
VIII	Equipment List	102
IX	Velocity Measurement in Natural Convection .	103

NOMENCLATURE

Symbol	Usage
b, c, C, d, D	Constants with variable local meaning
C_p	Specific heat at constant pressure
g	Acceleration of gravity
Gr	Grashof number based on length x
h	Heat transfer coefficient
k	Thermal conductivity
l	Length
m	Exponent, group of variables
N	Group of variables
Nu	Nusselt number
Pr	Prandtl number
q	Local heat flux
Q	Average heat flux
Ra	Rayleigh number based on length x
T	Temperature
u	Velocity parallel to plate
v	Velocity perpendicular to plate
x	Vertical displacement parallel to plate
y	Horizontal displacement perpendicular to plate
z	Horizontal displacement parallel to plate

NOMENCLATURE (Continued)

GREEK LETTERS

Symbol	Usage
α	Molecular diffusivity of heat
β	Coefficient of volumetric expansion
δ	Boundary layer thickness
Δ	Difference operator
ζ	Dimensionless distance
θ	Excess temperature above ambient
η	Dimensionless distance
μ	Dynamic viscosity
ν	Kinematic viscosity
ρ	Density

SUBSCRIPTS, etc.

c	Thermocouple
w	Wall condition
e	End condition
f	Fluid property
M	Main section
G	Guard section
x	Local value
*	Critical value
T	Temperature, thermal
h	Enthalpy

I. INTRODUCTION

To even the most casual observer, the phenomenon of natural convection has empirical meaning. A plume of cigarette smoke, rising through a short laminar trajectory, degernerates in a very visual manner into the random disorder to which scientists have attached the name of turbulence.

The physics of laminar motion lends itself conveniently to mathematical description in most cases of practical importance. The treatment of turbulence has consistently been more difficult. Approaches of a purely analytical nature are indeed rare. Even today, it can be justly said that from an analytical point of view, hardly a beginning has been made upon the study of turbulence.

Being unable to grasp the whole of the turbulence problem, investigators have grappled with its grosser dimensions, and a structure of empirical laws has evolved for each geometrical model; to a degree of refinement largely dependent upon the practical importance of the model. From this background have come not only the foundation for the statistical theories of turbulence, but also such far-reaching empirical summaries as the logarithmic law of the wall for turbulent boundary layers.

The historical development of the literature of natural convection boundary layers has been true to form.

Although early work provided a fine, proven theory for the laminar case, relatively little attention has been given to the more frequently encountered turbulent layer.

The topic of turbulent natural convection has received consideration from time to time over this long historical development. In the past two decades it has been pursued with a periodic vigor imposed by necessity. In the late forties and early fifties, gas turbine applications incited a flurry of attention, which revived itself a decade later in response to the urgency of liquid rocket stratification and agitation problems.

Despite the practical importance of the turbulent natural convection boundary layer, the attention devoted to it to date has provided little basic information about it. In addition to the absence of satisfactory analytical techniques, there is a lack of complete data relative to the local properties (and to a lesser extent the overall effects as well). Little more than the general shape of the velocity and temperature profiles may be gleaned from the literature (see Figure 1). The few authors who have published experimental data relative to the grosser effects such as the heat transfer are not in agreement. As a result of a survey of the literature, it becomes apparent that there is room for improvement of the experimental foundation upon which the turbulent heat transfer correlations are based.

Accordingly, the first objective of the present work

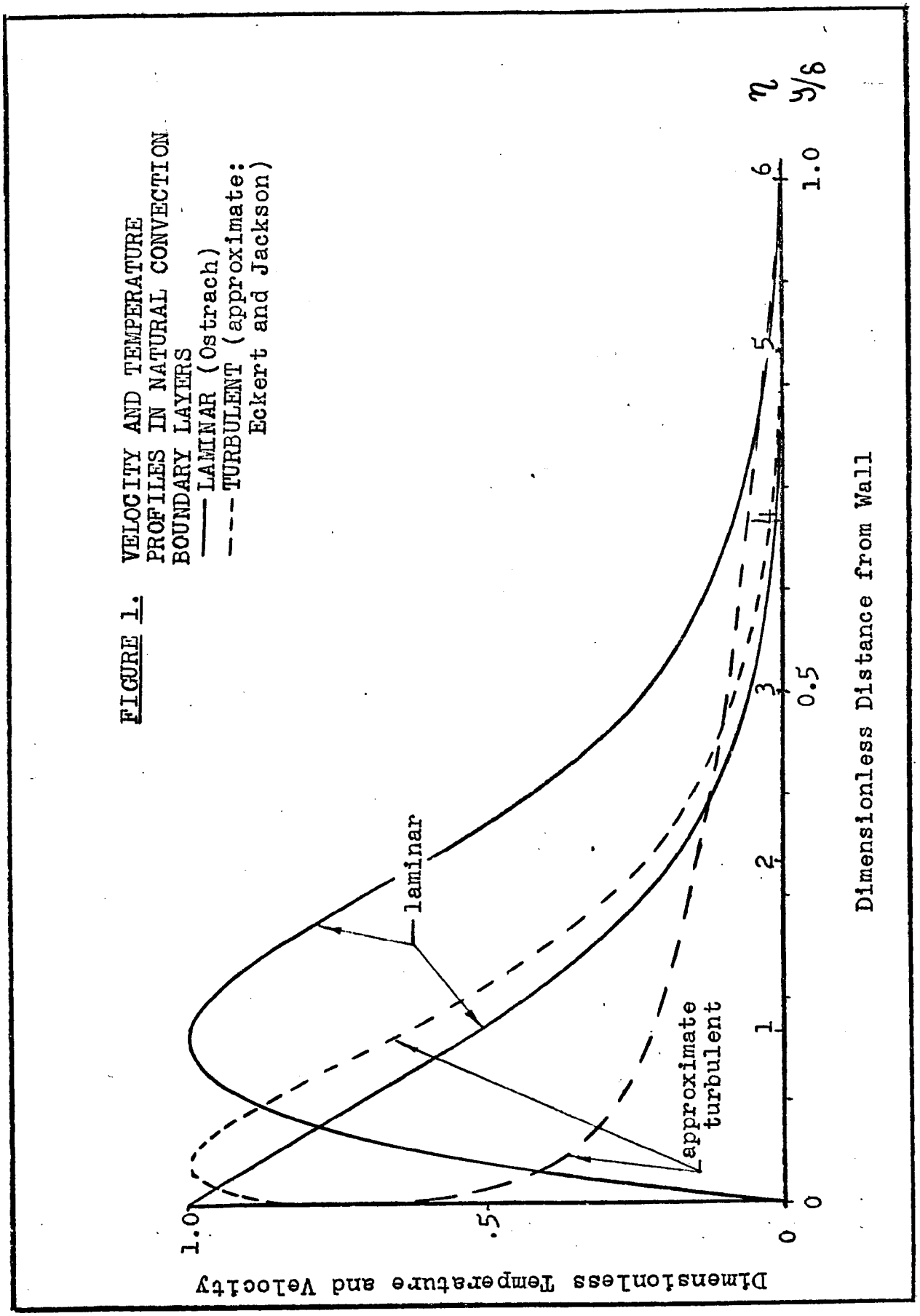


FIGURE 1. VELOCITY AND TEMPERATURE PROFILES IN NATURAL CONVECTION BOUNDARY LAYERS
—— LAMINAR (Ostrach)
– – – TURBULENT (approximate: Eckert and Jackson)

was that of accumulating data relative to the magnitude and distribution of heat flux in the developing turbulent layer. This was intended to be a means of support for the present literature. A basic aim was to prpvide either verification of one of the existing correlations, or the foundation upon which an improved correlation might be based.

The desirability of having more precise information relative to the local parameters of the flow certainly suggests itself. Both the temperature and velocity profiles present unique and challenging measurement problems, however. The problem of temperature measurement within the boundary layer gave early promise of an economical solution, whereas the velocity problem remained formidable. Of the several anemometry techniques which presented themselves, none was suitable to the problem. The combined challenge of low velocities, poor probe-to-fluid communication, large turbulent fluctuations, and large temperature gradients makes accurate velocity measurements very difficult within the limits of established techniques.

Hence the second major objective of the present work was the accurate experimental determination of the turbulent temperature profiles. Accordingly, an experimental program was designed to determine the heat transfer and temperature profiles of the turbulent layer in natural convection.

A third goal of gaining precise empirical information about the velocity field proved to be incapable of fulfillment, using the tools and techniques available at present.

In the sections which follow, a literature survey brings into focus the dearth of experimental data now contained in the literature, while attempting to present the essence of the work done to date. An experimental program is described, and the results are presented and compared with the literature.

II. LITERATURE SURVEY

The theoretical background for natural convection is discussed at some length by McAdams (33) and by Jakob (27), where are cited the works of Lorenz, Boussinesq, Polhausen, Schmidt and Beckmann, Ostrach (37), and others. The earliest work of any importance relative to the turbulent case appears to have been that of Griffiths and Davis (24), who measured and reported temperature and velocity fields near a vertical heated plate of uniform temperature. In their measurements, temperatures and velocities were recorded in the laminar and turbulent regimes by the use of a platinum wire exposed to the flow. Their work remains, however approximate it may be, the only source of velocity measurements, and until recently the sole source of temperature profiles in turbulent natural convection. The profile data obtained is based upon measurements at rather wide geometrical spacings, making intrepretation somewhat difficult. The general trend of the heat-flux data reported is correct by the standards of later investigators; the local heat flux being uniformly distributed in the turbulent regime. The actual magnitudes of the heat transfer are possibly high, however. Their results are called most critically to task in the literature on the ground of possible three-dimensionality in the supposed two-dimensional flow, presumably attributable to the finite width of the

heated plate used in their work, and the attendant lateral inflow of cooler air from the sides. These results will be more fully discussed in comparing them to the present experiment in a later section. The laminar experimental work of many authors is discussed in the references cited above. Measurements of heat transfer over a wide range of Rayleigh number were reported by Saunders[40]. His experiments, performed in air under pressure, were quite carefully taken. His turbulent results are discussed in detail in a later section, and quantitative comparisons are made at that point.

McAdams[33] and Jakob and Linke[28] summarized the experimental work of many researchers, and recommended correlations for turbulent flow given approximately by

$$\bar{N}u = 0.13\,(Gr\,Pr)^{1/3} \tag{1}$$

It has already been noted that the work of Griffiths and Davis suggested a near-uniform distribution of local heat flux in the turbulent regime. That this result is consistent with Equation (1) may be demonstrated as follows. If

$$\bar{N}u = C\,(GrPr)^{m} \tag{2}$$

and by definition

$$Q = b\,\bar{N}u\,k_f\,\Delta T = \int_0^L b\,q_x\,dx,$$

$$Gr = \frac{\beta \Delta T x^3}{\nu^2} g,$$

and

$$q_x = h_x \Delta T = Nu_x k_f \Delta T / x,$$

the average Nusselt number may be written as

$$\bar{Nu} = \int_0^L (Nu_x / x)\, dx$$

Thus the local Nusselt number is given by

$$Nu_x = x \frac{d}{dx}(\bar{Nu}) = 3m\, C\, (GrPr)^m, \tag{3}$$

and the local heat flux is

$$q_x = C_1 x^{3m-1} \tag{4}$$

It is now easily seen that a value of m = 1/3 agrees exactly with a length-independent heat flux.

The development and success of integral methods introduced in forced convection by Polhausen and von Kármàn is impressive in its application to turbulent boundary layers. Eckert and Jackson[15] extended this technique to the case of turbulent natural convection. Using the rough profiles suggested by the data of Griffiths and Davis (see Figure 1), and carrying over successful relations for wall shear and heat flux from the Blasius formula for forced convection in smooth tubes, they produced an analytical correlation for Nusselt number which differs considerably from that of the earlier investigators. Their correlation is

$$\bar{Nu} = 0.0210\, (GrPr)^{2/5}, \tag{5}$$

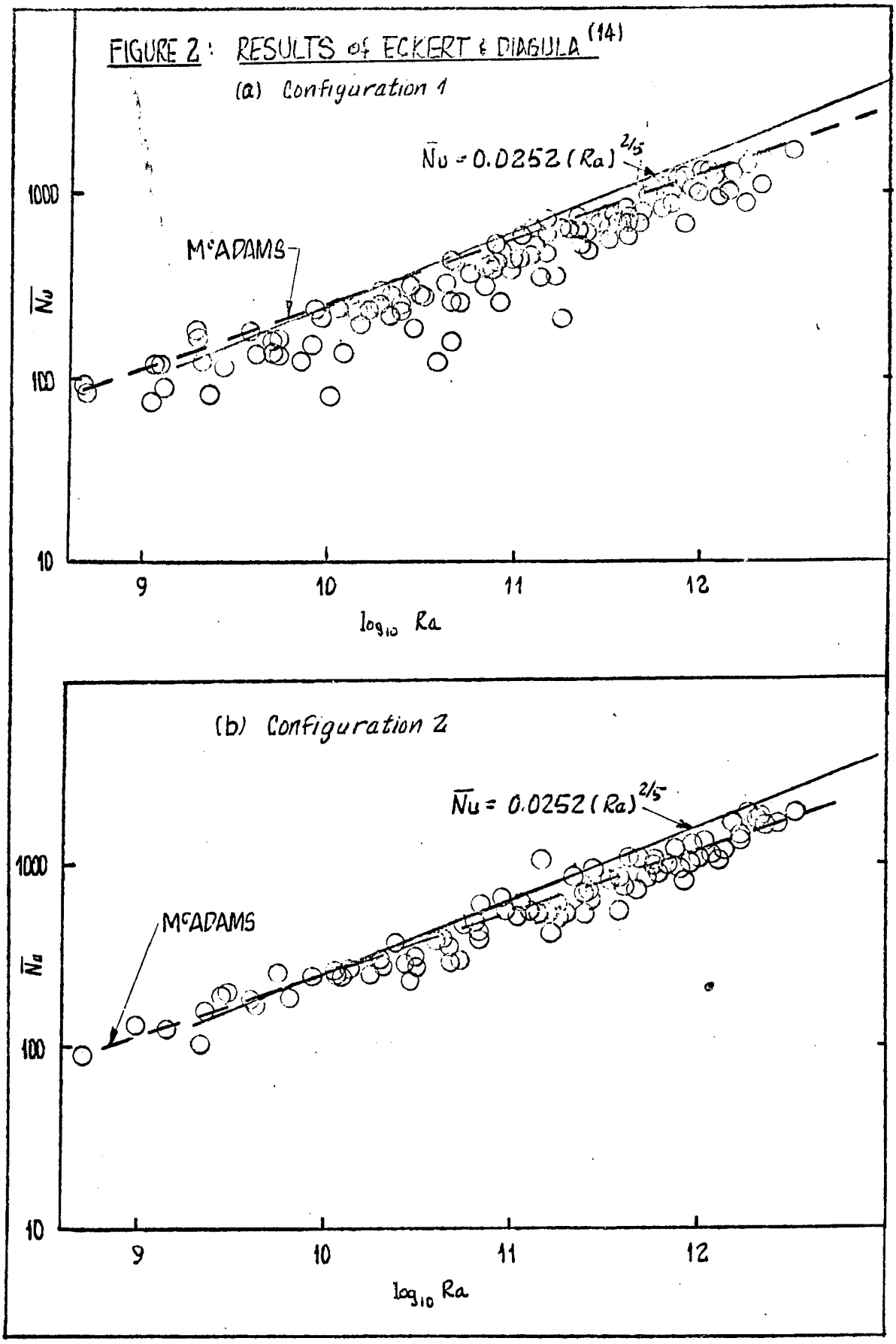
Figure 4 of their paper records this correlation and the data chosen by them for comparison (This figure has been reproduced in some textbooks.) It will be noted from their figure that the turbulent experimental data is somewhat scattered, allowing a reasonable correlation with either of Equations (1) or (5). Following the reasoning outlined above shows that their correlation suggests a local heat flux dependence of the form

$$q_{vx}(x) = C_2 x^{6/5}, \tag{6}$$

which is certainly not in agreement with reported experimental trends. A second look at their figure indicates that while the 2/5 power correlation appears to agree moderately well with the data of Saunders[40] and that summarized by Jakob and Linke[28] taken together, it deviates considerably from either set taken individually, being too steep in slope. On the other hand, both sets of data have better slope correlation with the expression given in Equation (1).

Later experimental work related to turbulent natural convection inside turbine blade passages was taken by Eckert and Diagula[14], from flow inside a large, steam-jacketed pipe. Their results for two configurations are replotted here as Figure 2, together with two correlations. It will be noted from the figure that a correlation closely resembling the one of Equation (5) is suggested by the authors of the work. However, much better agree-

FIGURE 2 : RESULTS of ECKERT & DIAGULA [14]



ment is obtained with the earlier recommendation of McAdams, which is given by equation (1).

In recent experiments employing a hot vertical cylinder surrounded by liquid, Fujii[20] showed a decrease in local heat flux beyond the transition region. This led him to postulate a "transient" turbulent regime where a 1/4 power correlation for Nusselt number seemed to satisfy. Fujii's theory[19] for the fully turbulent regime is essentially that of Eckert and Jackson, however, and he also recommended a 2/5 power correlation. It is impossible to say whether this was by conviction or convention.

In the light of the poor agreement with experimental data, one is led to discard the 2/5 power correlation of Equation (5) in favor of the better-verified empirical law of Equation (1).

The rather poor correlation with experiment achieved by the Eckert and Jackson result is an indication that something physically unsound has been introduced into the theoretical approach. A reevaluation of the underlying assumptions is suggested. Those whose merits come immediately under scrutiny are the following: (a) carryover of Blasius' resistance formula from forced convection, (b) the applicability of Reynolds' analogy to the natural convection case, in spite of the mathematical inconsistency involved, and (c) the approximation entailed in the use of the 1/7 power velocity and temperature profiles. The

1/7 power profiles, as introduced by Eckert and Jackson, are attributed to be a good representation of the Griffiths and Davis data, the latter having been first reduced to an arbitrary scale by a similarity assumption. That the temperature profiles actually do not obey the 1/7 power law will be shown in a later section.

The results of another application of the integral theory give a very interesting contrast. Bayley(3), improving the method employed by Eckert and Jackson, also applied the integral procedure to the natural convection boundary layer, but with a model which was expanded to include a temperature profile differing from the 1/7 power law. His temperature profile was derived indirectly from the physics of turbulent forced convection. Adopting as a first approximation a constant value of eddy diffusivity, estimated from the Blasius resistance formula, which he assumed to be uniformly distributed throughout the boundary layer, Bayley was able to derive from the integral boundary layer equations the relation

$$\overline{Nu} = 0.10\ (Gr\,Pr)^{1/3}, \tag{7}$$

the slope of which agrees exactly with the recommended correlation of McAdams given above*. The success achieved by Bayley in predicting the proper trend for heat transfer must be attributed to his better representation of the physical model in the temperature profile used.

* Reference to Figure 2 shows that Equation (7) is an improvement over Equation (1) for the data shown there.

The success of Bayley's model will be further demonstrated during the analysis of the present experimental work, below.

Information of value relative to the local parameters of the boundary layer was contributed to the literature by the optical studies of Eckert and Soehngen[16], Goldstein[22], and others. Photointerferograms published by them give an indication of the magnitude and frequency of the fluctuations encountered in this boundary layer, and thus provide insight into the nature of the flow itself. It will be appropriate to discuss some of the flow characteristics shown by these studies in a later section; at that point the peculiarities of natural convection turbulence will be in sharper focus.

Later works relative to turbulent natural convection are primarily devoted to enclosed spaces and propellant stratification (See Clark[7], and Vliet[53].). As no new analytical techniques or experimental data relative to the most basic flat plate case is reported there, they will only be mentioned here.

The following sections describe the apparatus used in the present experiment. Thereafter follows a discussion of results in which some of the work cited above will again be discussed.

III. EXPERIMENTAL SETUP AND VERIFICATION

The experimental apparatus, test equipment, and verification procedures employed in this investigation are discussed below.

A. Configuration of Heated Plate

The vertical test surface was constructed of a single plate of Pioneer #901 Aluminum, of dimensions 1/2 by 24 by 144 inches, the long side being aligned with the vertical. The plate was sectioned by slots 3/8 inch wide by 7/16 inch deep cut from the heated side such that the central foot of width was isolated over the full length of the plate from the outer sections. The outer sections served as stiffening and as guard-heating areas. The central test area was further subdivided by similar slots cut horizontally across it, giving twenty-four 6 by 12 inch subsections. This partitioning of the plate allowed accurate control of the heat transferred into each section of the boundary layer. An analysis of the flow of heat from the heaters into the plate and boundary layer is contained in Appendix VI.

B. Plate Surface Preparation

After the plate was mounted in its support frame, the test surface was polished to a nominal roughness of less than 15 microinches rms by a sequence of treatments with very fine sandpaper and a cloth wheel contain-

ing Tripoli compound and diamond paste. The roughness was determined after polishing by means of an electronic profilometer. To facilitate radiation corrections, the emissivity distribution over the surface was measured by a simple comparitive technique. As is elaborated in Appendix V., the objective of the emissivity measurements was to ascertain that a uniform distribution of emissivity existed over the entire surface. The mathematical treatment of the heat flux data depended upon a uniform emissivity distribution.

A radiation thermopile was exposed for calibration to a laboratory blackbody, and then to a sheet of commercial aluminum foil, both at the intended plate temperature. The blackbody consisted of a 12° thick-walled copper cone of rectangular cross-section, artificially blackened on the inner surfaces with acetylene smoke. The cone was heated by means of electrical strip heaters fastened to its outer surface, the entire assembly being encased in glass-fiber insulation. The measured emissivity of the foil was used as a qualitative check of the procedure. The relative output of the thermopile when exposed to the heated plate was then a measure of the plate emissivity. Apparatus used in this and other phases of the experiment is described in the Equipment List, Appendix VIII. Appendix V reports the data pertinent to emissivity measurements. Figure 3 shows the apparatus employed in this phase of the setup procedure.



Figure 3. Photograph of Emissivity Measurement Apparatus

C. Heating Arrangements

Each section of the plate test area was heated by two electrical strip heaters, together covering one-half of the area of the section. The guard-heating section on either side was equipped with twelve strip heaters which together composed a heating element extending full-length. Heaters were wired in pairs; the current to the pair of heaters on each six-inch test section was controlled by an adjustable autotransformer. The two guard heaters for each square foot of test section were likewise wired and controlled in unison. Figure 4 shows a typical area of the plate with several sections and the heaters and wiring involved. (Heaters have been shaded slightly to aid in interpretation.) Figure 5 is a photograph of a similar area from the hardware. The wiring scheme and locations and lead paths of the twisted lead thermocouples are indicated in the figures. Figure 6 illustrates the control wiring schematically. The power input to each set of heaters could be measured individually at the wattmeter jacks. The wattmeter could be easily switched from one plate circuit to another.

D. Probe Position Control Apparatus

The position of the probe was remotely controllable in the three rectangular coordinates by means of a carriage designed for this purpose. The complete carriage assembly is shown in Figure 7. Probe position

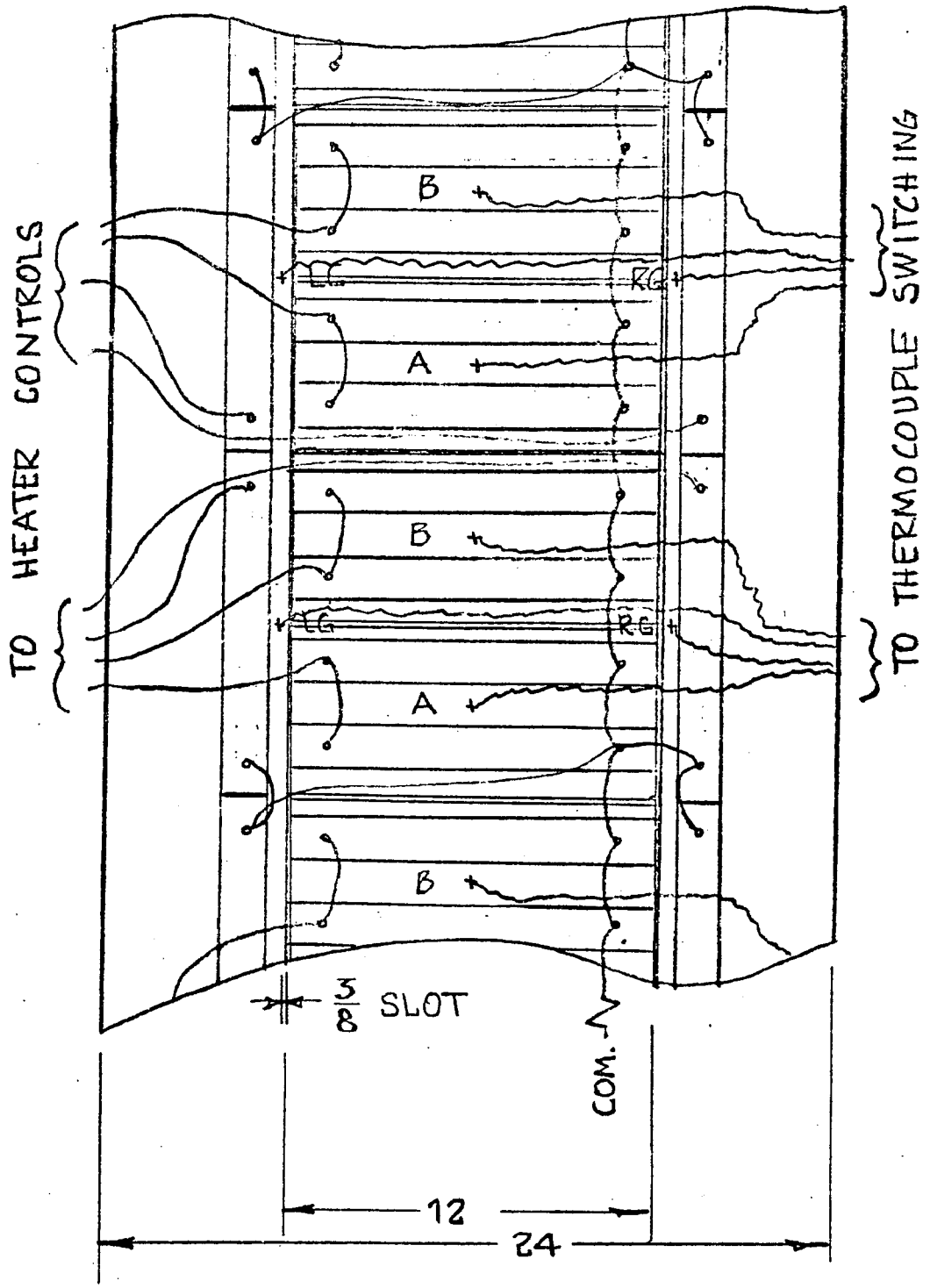


Figure 4. Plate Section Heating Schematic

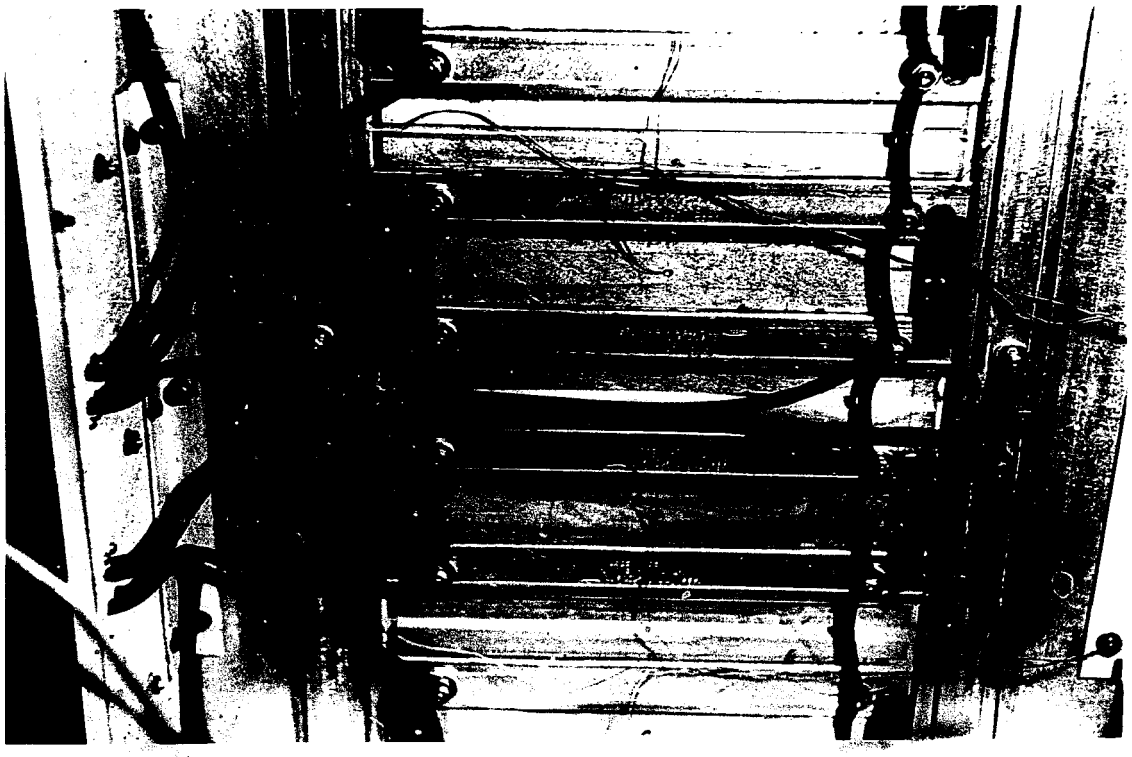


Figure 5. Photograph of Typical Plate Section

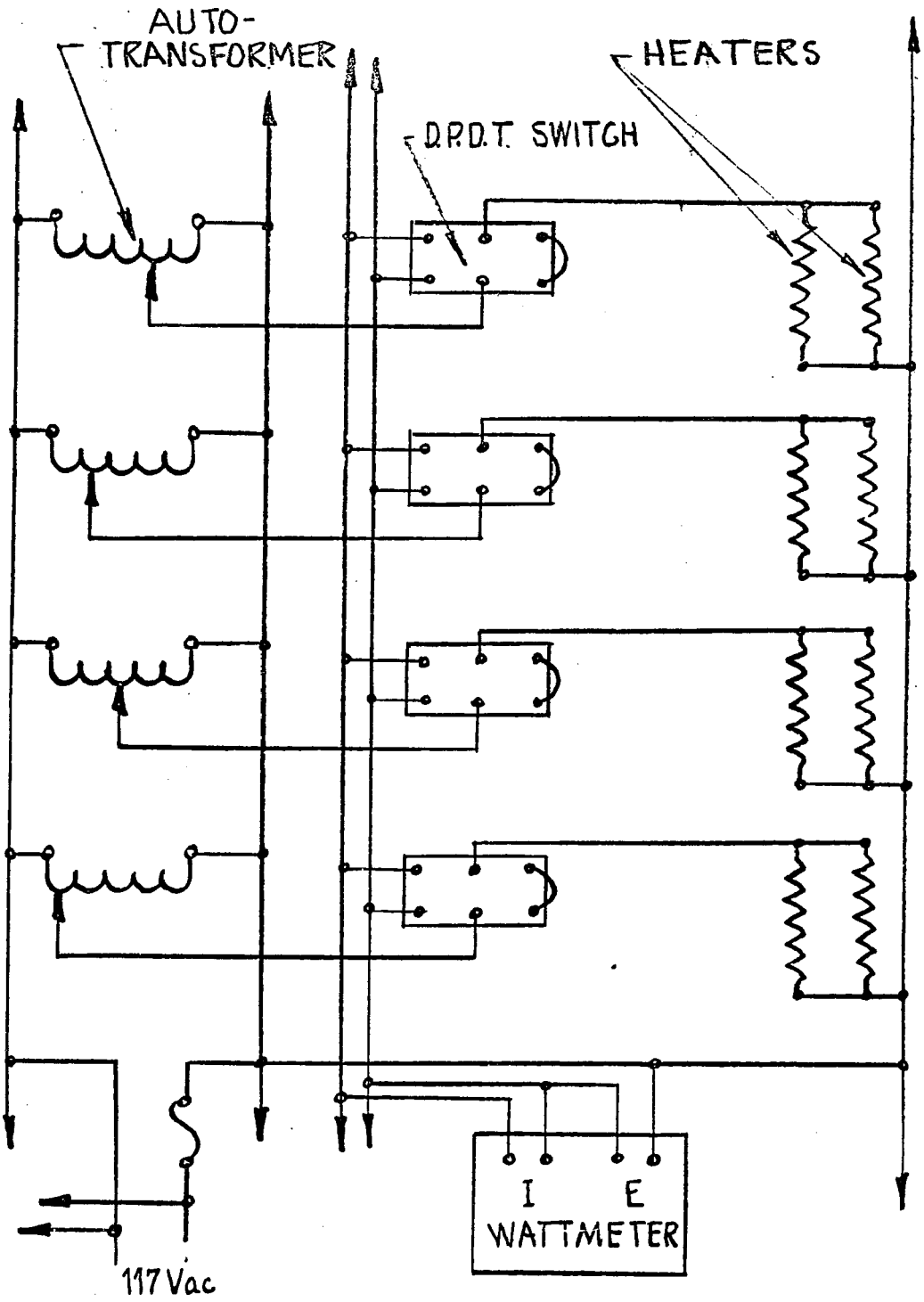


Figure 6. Power Control and Measurement Circuits

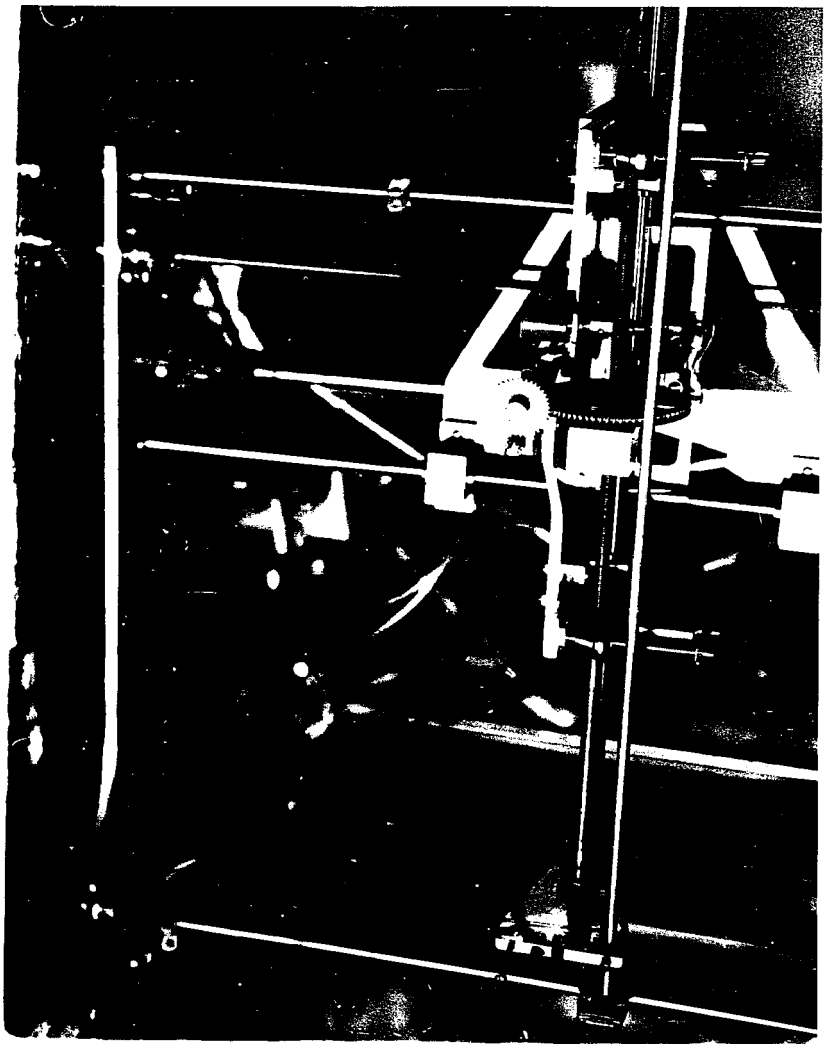


Figure 7. Photograph of Probe Carriage Assembly

in the y and z directions (horizontally normal to and parallel to the plate, respectively) was remotely adjusted through gear trains driven by direct current electric motors. Position was measured using precision potentiometers connected to the gear trains. Figures 8, 9, and 10 illustrate the control and measurement circuitry and the control panel. In addition to the coarse measurements provided by the potentiometer circuitry (accurate to the nearest 1/16 inch), the y-direction displacement was indicated on a fine scale in the inch of travel nearest the wall. In this important range, a dial indicator, mounted on the probe clamp outside the boundary layer and kept in contact with the wall through a spring-loaded extension plunger, gave position readings. A telescope was used to read the dial indicator, which could in this way be interpolated to the nearest 0.0002 inch. This system is illustrated in Figure 11. The coarse position indicating apparatus was calibrated by setting a desired position as determined by direct measurement, while the corresponding indication was taken from the panel potentiometer with the galvanometer in null position. The position calibration included in Appendix IV is the result of repeated application of this process. Subsequent checks of the calibration gave a reproducibility of better than 0.05 inch.

The x position was directly measurable to the nearest 1/8 inch by visual reference to markings on

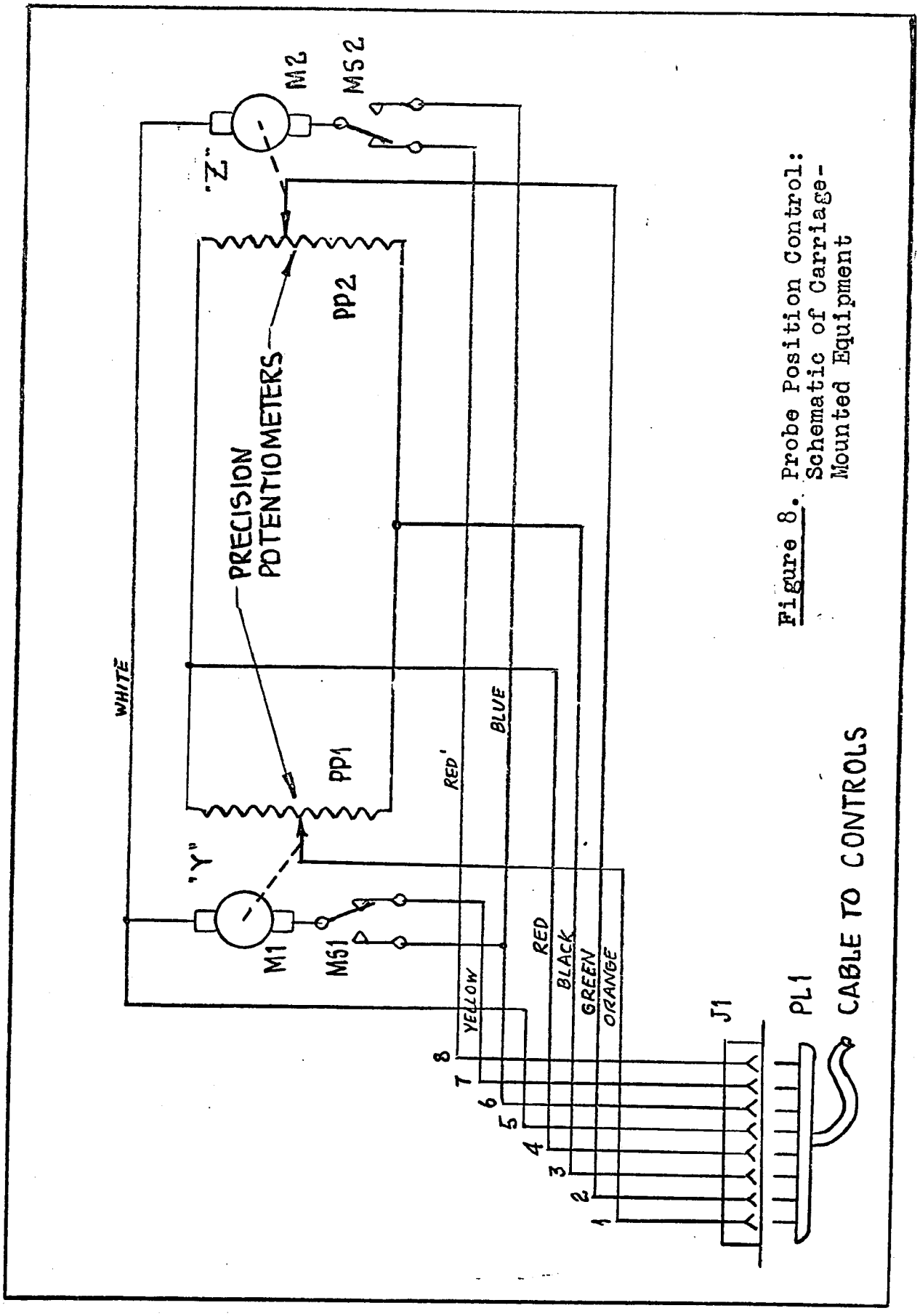


Figure 8. Probe Position Control: Schematic of Carriage-Mounted Equipment

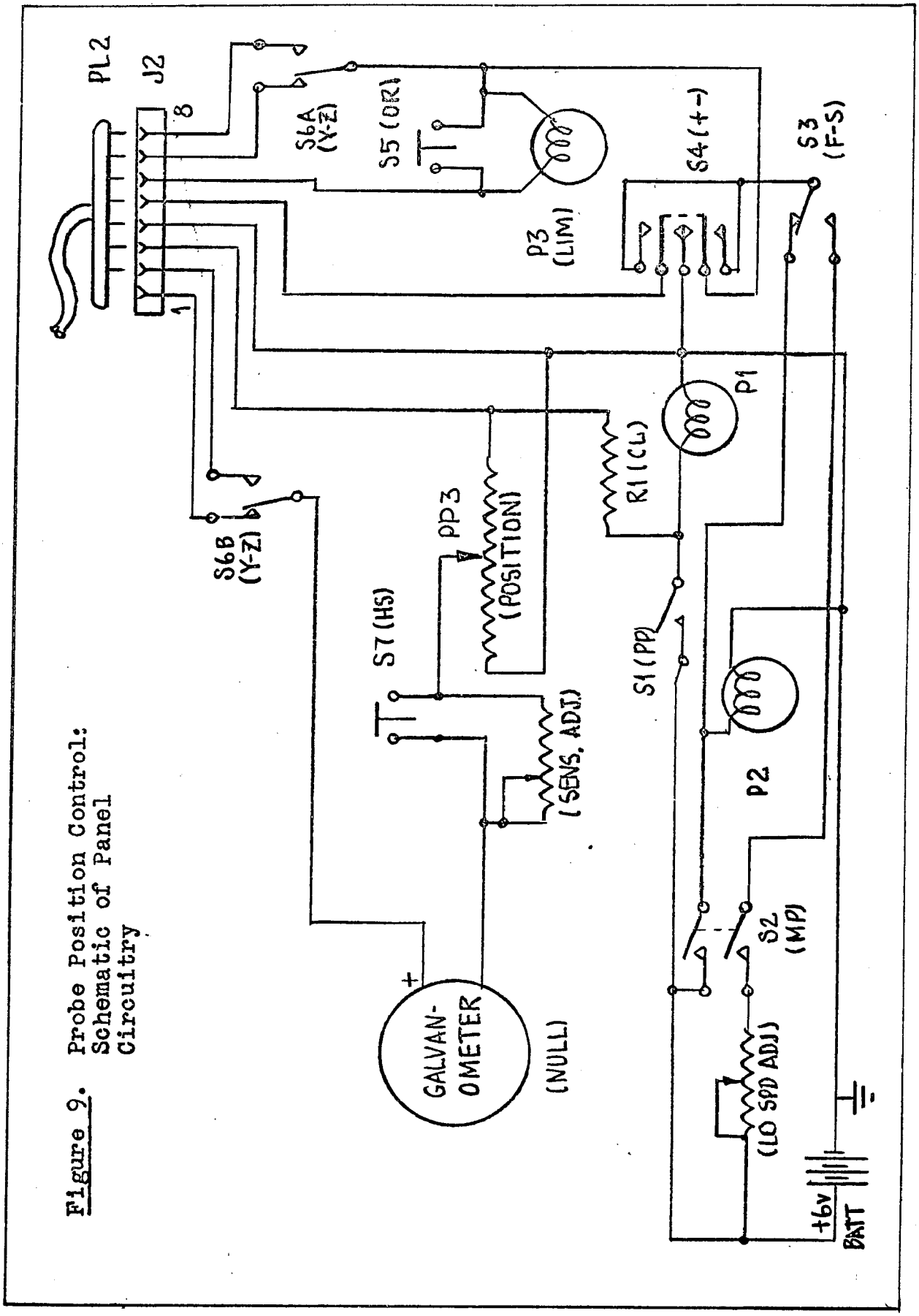


Figure 9. Probe Position Control: Schematic of Panel Circuitry

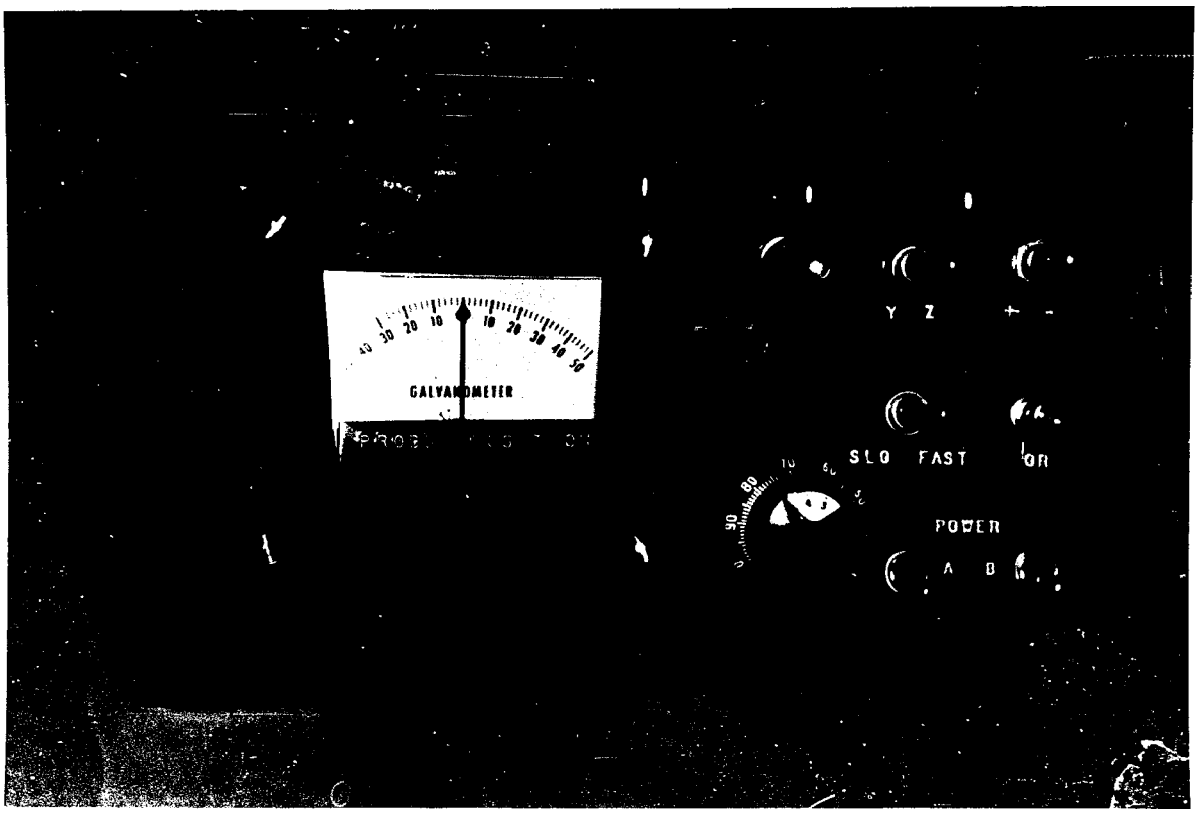


Figure 10. Photograph of Positioner Control Panel

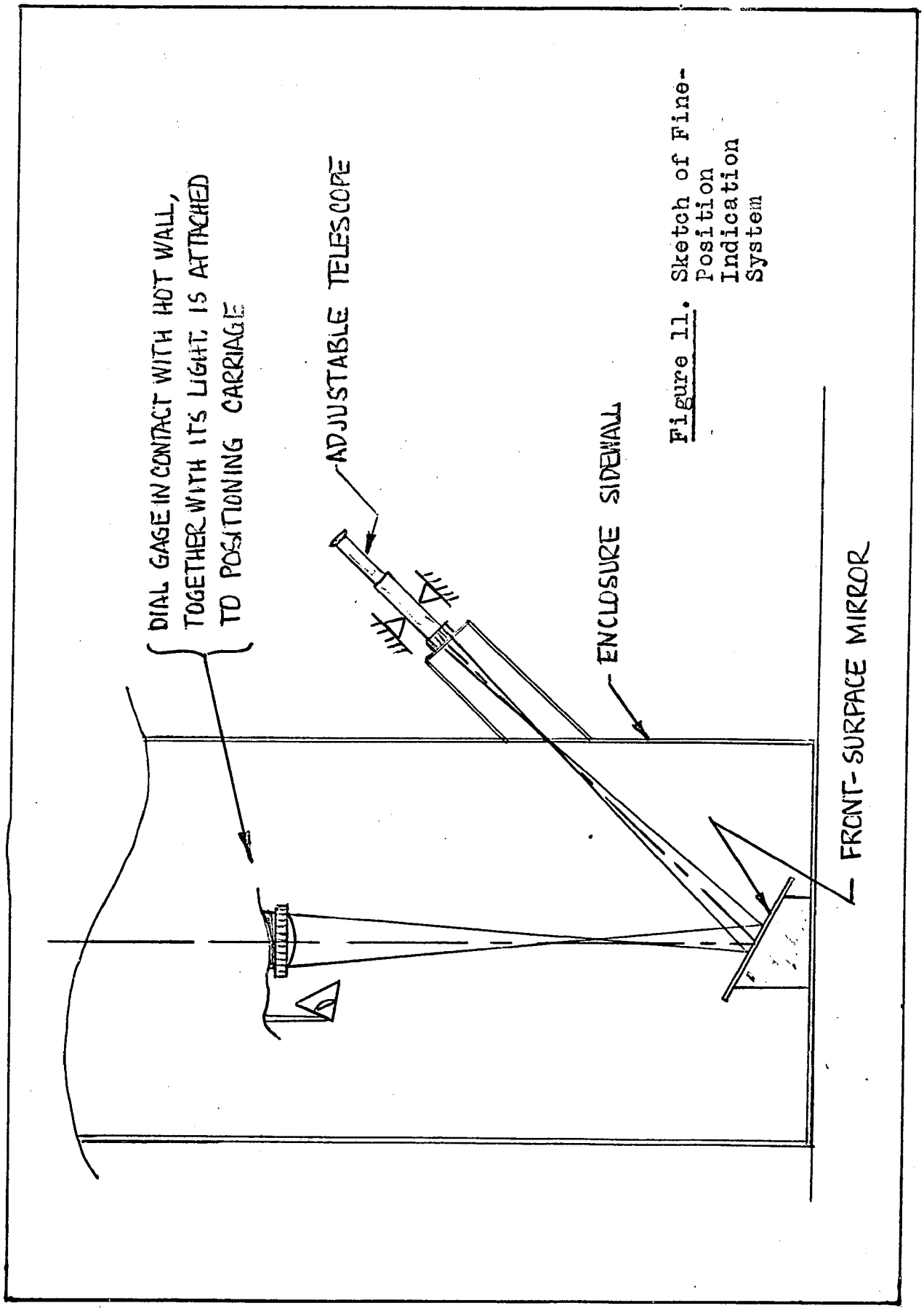


Figure 11. Sketch of Fine-Position Indication System

the viewing window attached to the plate supports.

E. Enclosure Design

To simulate, insofar as possible, a two-dimensional flow field, an enclosure was constructed of light plywood fastened to a wood and metal framework. It was parallelpiped in shape, roughly 2 by 8 by 12 feet, as shown in Figure 12. The inner surface was lined with reflective aluminum foil, and the end nearest the heated plate was joined to the plate supports by a 14 inch plexiglas window extending from top to bottom. X-position marks were painted on this window to allow the operator to fix the position of the probe by alignment of the probe carriage visually with the marks.

The end of the enclosure furthest from the plate was provided with slots baffled with several alternate layers of wire screen and gauze, extending over the full height, to allow ambient air to be drawn into the enclosure in an orderly manner. The top of the enclosure was open full width for approximately two feet nearest the plate to allow the entire boundary layer to exit without disturbing the enclosed fluid. Enclosure surface temperatures were recorded by means of thermocouples imbedded in the foil liner.

F. Boundary Layer Temperature Instrumentation

Consistent with the objective of accurate determination of the temperature field within the boundary layer, local measurements were made by means of a

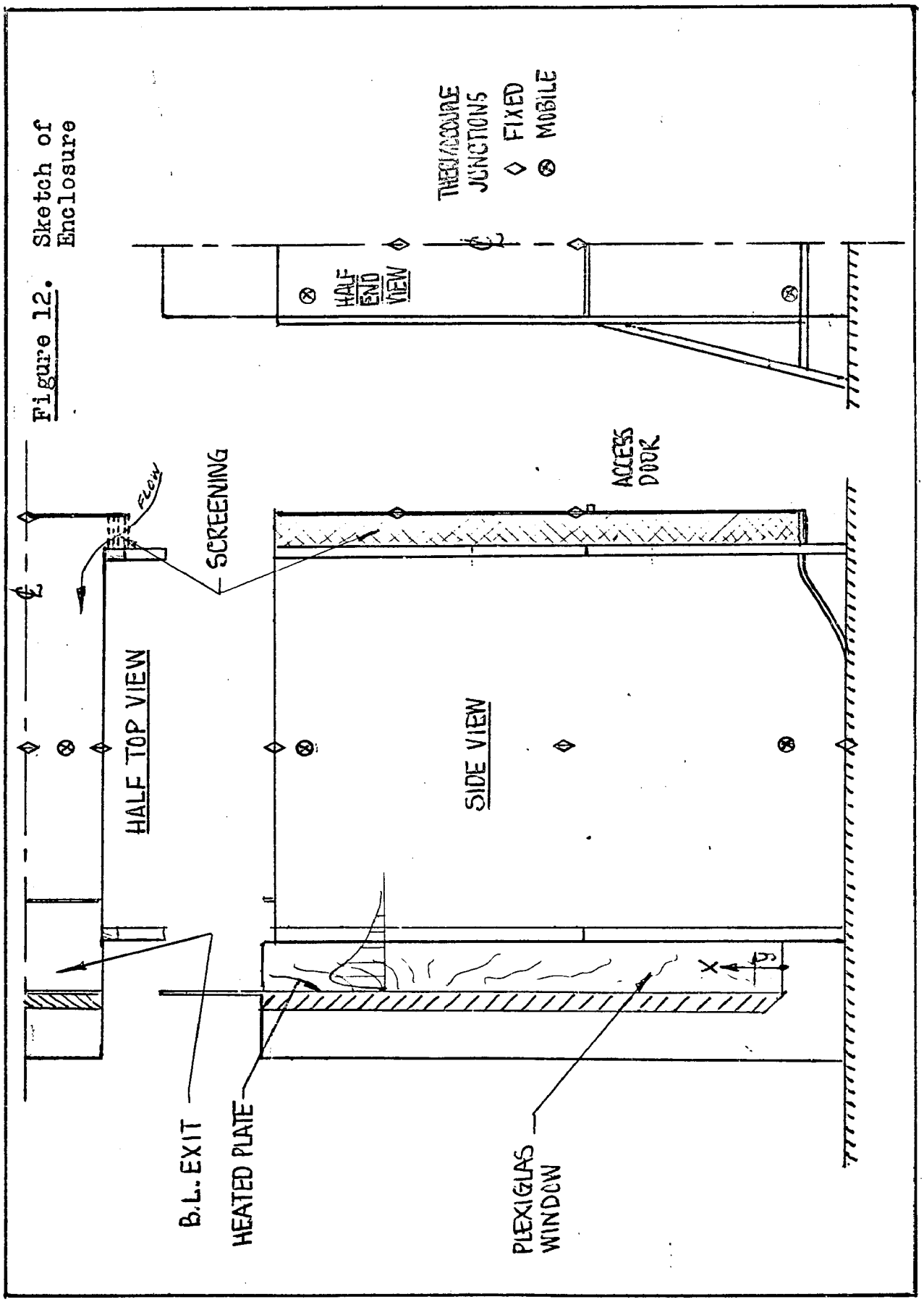


Figure 12. Sketch of Enclosure

thermocouple probe designed for this purpose.

Consideration of the physical situation existing near the wall in turbulent free convection reveals a challenging thermometry problem. The relatively high temperature gradients and low heat transfer coefficients, combined with the large relative fluctuations in all local properties of the flow in this region, constitute a difficult set of design restrictions. The primary problem is the limitation of the conduction of heat away from the sensitive element of the thermometer. This problem is elaborated in Appendix II, where an analytical approach is suggested.

The probe configuration which was adopted for use in this work is shown in Figure 13. It consisted of a stiff metal tube supporting a bakelite block into which two 0.070 inch ceramic capillaries were cemented. Twenty-eight gauge chromel and constantan wires from a standard glass-wound pair were then appropriately stripped of insulation and threaded through the tubes. These leads were then bent through 90° and cut to form a support fork. A sensitive element of similar materials 0.0005 inch in diameter was to be soldered across the fork tips. The soldering points were sanded flat and tinned with solder to prepare the fork for this process. To be sure that the probe element would be parallel to the plane of the heated wall, the support fork was then mounted in the positioner and brought into contact with the wall.

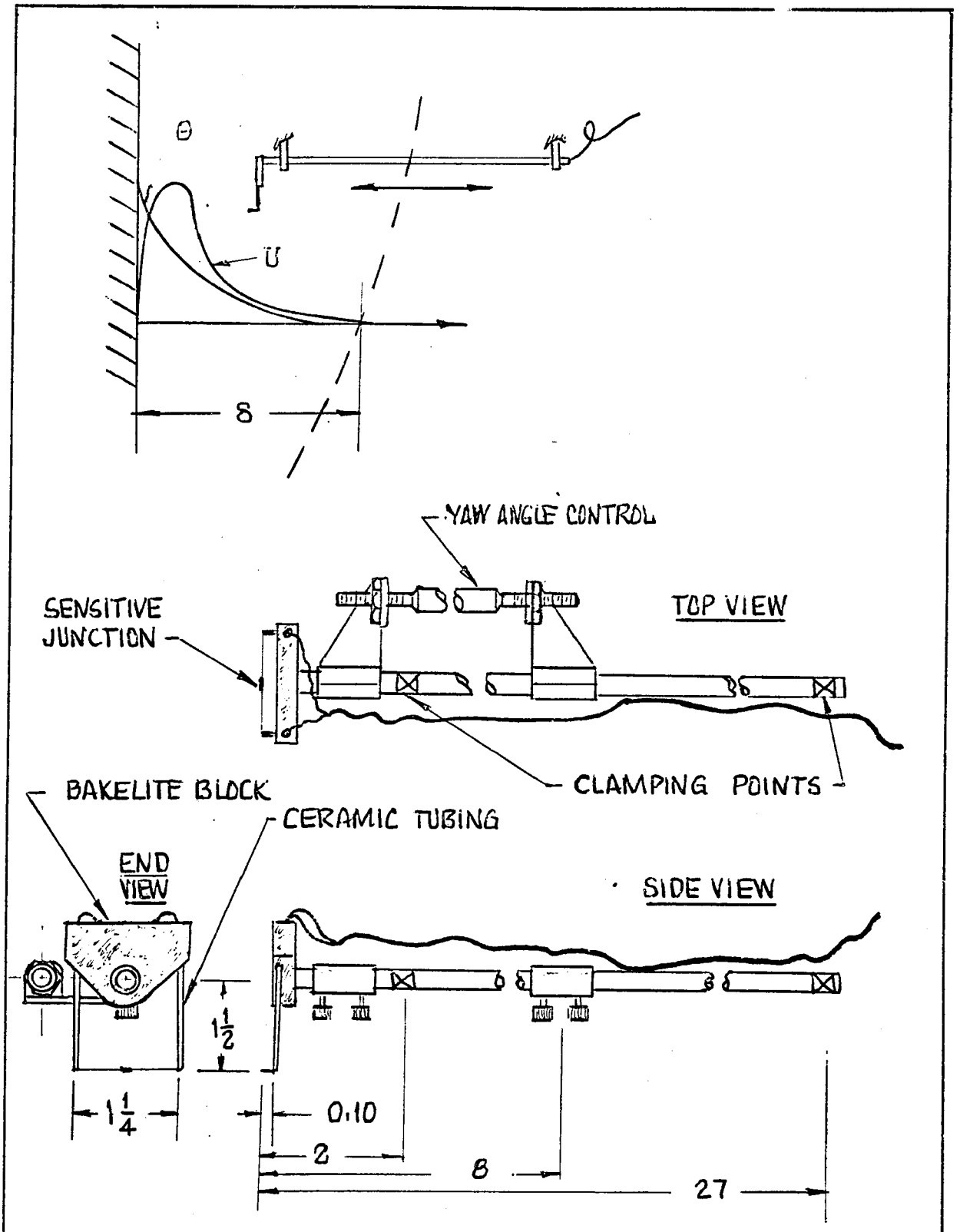


Figure 13. Temperature Boundary Layer Probe Schematic

Contact with the wall was determined by completion of a simple electrical circuit between the thermocuple lead wires and the heated plate, as indicated by a sensitive galvanometer. To ensure that both fork points contacted the wall simultaneously, each probe tip was individually brought into contact with a gage block taped to the wall. The relative position of the two points of the fork was then adjusted by means of a yaw positioner until contact occurred at the same point. The probe body was then dismounted from the positioner and set aside for the mounting of the sensitive element.

The element itself was constructed of chromel and constantan wire of 0.5 mil diameter, as supplied by the Omega Corporation. Elements were assembled by taping two lengths of wire to separate cardboard forks, aligning the wires, and clamping the forks for soldering. After placing this assembly under a microscope, one fork tip was cut, and the resulting loose wire was wound around the remaining wire. The two wires thus brought into close physical contact were then fluxed and soldered over a length of about 1/10 inch near their centers. Alternate wires were then trimmed from either end, leaving an element of less than 0.0011 inches in nominal diameter. This completed element was stretched across the probe fork, soldered in place, and inspected carefully. After final trimming, the probe assembly was removed from the microscope and mounted on the positioner as before. The

positioner was carefully zeroed by bringing the probe into electrical contact with the wall and setting the dial indicator to zero.

Temperature readings could then be taken from the thermocouple by comparison to an ice bath temperature. A Leeds and Northrup K-2 precision potentiometer was employed for these measurements. Temperatures were measured within the boundary layer at the positions indicated in Appendix I. Each repositioning of the probe in the vertical direction was followed by a new electrical determination of the point at which the probe contacted the wall. This position was assigned the value of y = 0.0005 inch, in accordance with the diameter of the probe element, and the remaining positions were measured relative to it.

G. Wall Temperature Instrumentation

The steadywall temperature was evaluated for uniformity by means of forty-eight copper-constantan thermocouples. Each thermocouple was provided with an individual ice junction, and each could be connected independently to the Leeds and Northrup 8662 precision potentiometer by means of switching in the copper path. Thirty gauge thermocouple wire was used.

The wall temperature could be determined from this system to the nearest half-degree Fahrenheit. The positions of thermocouples in the plate sections have already been given in Figure 4. Thermocouple hot junctions

were peened into holes in the aluminum plate, drilled so that the junctions could be positioned very close to the test surface. After the junctions were fixed in position, the remainder of each hole was filled with an aluminum plug. All cold junctions were thermally connected to the ice bath by means of silicone oil inside a small-diameter glass sheath.

Enclosure surface temperatures were measured with similar thermocouples fastened to the sides, top, bottom, and end of the enclosure, and ambient air temperatures by shielded thermocouples suspended in the air. The geometry of these couples is shown in Figure 12. The switchboard and reference junction arrangement for the copper-constantan thermocouple system is given in Figure 14.

H. Thermocouple Calibration

The magnitude of the turbulent fluctuations expected within the boundary layer suggested that very-high precision measurements would be out of the question. It was expected, however, to obtain an accuracy in the time-mean temperature of the same order as that obtained in the plate temperature measurements. A three-point calibration procedure was sufficient to meet these requirements. This served to determine the set of constants of the calibration equation

$$\Delta T = A + BT + CT^2 \tag{8}$$

for each of the thermocouple materials employed. ΔT

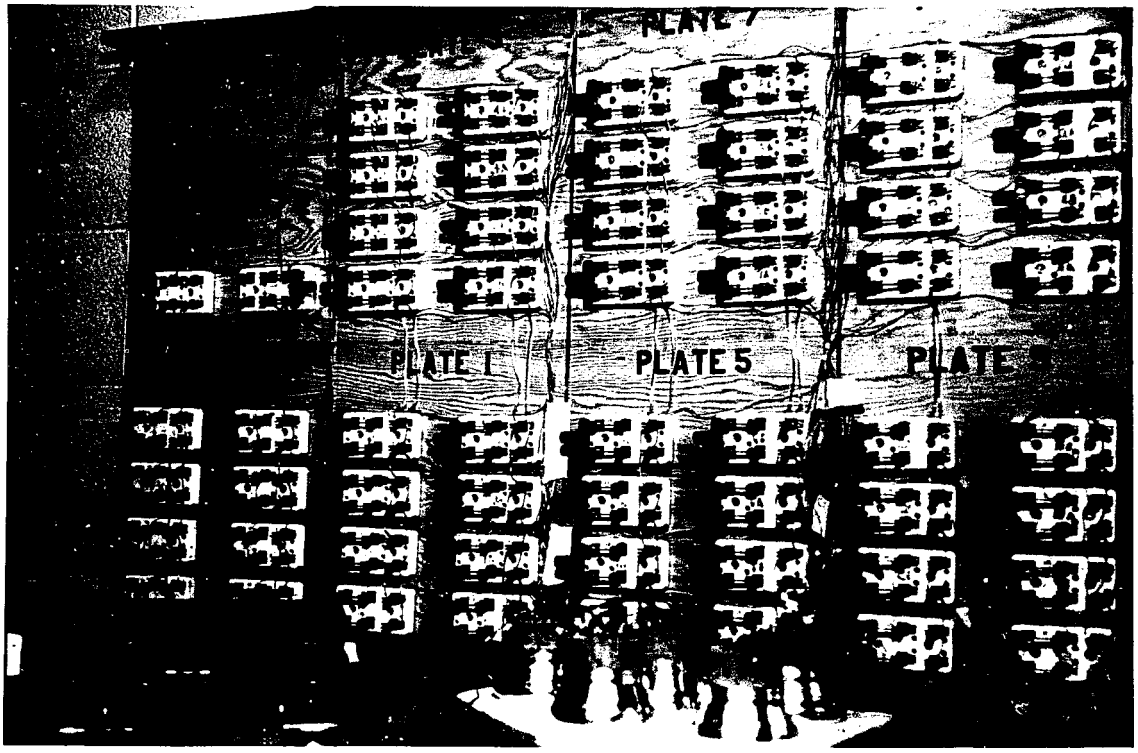


Figure 14. Photograph of Thermocouple Switching Panels

represents here the difference between the actual and the indicated temperatures. The three points chosen were the ice and steam points and a room temperature secondary point. Because of the use of a very fragile wire in combination with a stronger support wire in the boundary layer probe, a special calibration thermocouple was prepared. It is shown in Figure 15.

The ice point temperature was taken from a saturated water-ice bath, the steam point from a distilled-water hypsometer. The third point, measured by means of a precision platinum resistance thermometer, was the equilibrium temperature of a large, well insulated copper block. During the calibration, the thermocouple outputs were measured with the same respective instruments to be used during the actual tests. Appendix III gives the details of the measurements and calculations performed to specify the deviation equations. These equations were included in the data reduction programs as subroutines. The temperature results reported in Appendix I have thus been corrected for thermocouple calibration.

I. Apparatus Checkout and Verification

One of the early objectives of the experimental work was necessarily that of a system-wide "calibration". Several items were open to question, requiring satisfactory verification before the desired data could be treated with confidence. Among these were the following.

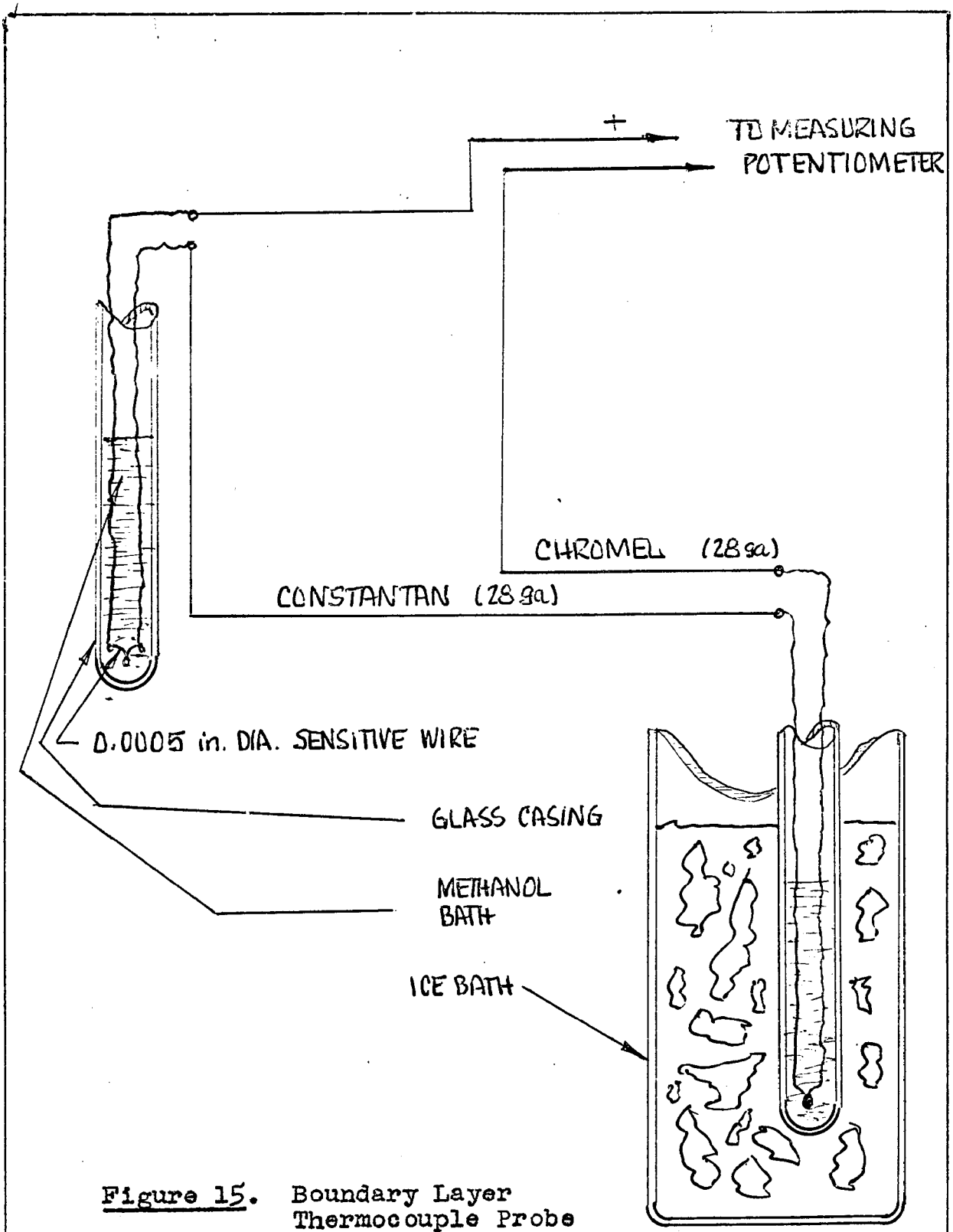


Figure 15. Boundary Layer Thermocouple Probe Calibration Schematic

First, it was necessary to determine that the enclosure design had no appreciable effect upon the representation of the infinite-media model which the experiment was intended to simulate. Secondly, several modifications were required before an acceptable leading-edge configuration was found; one which would supress the tendency of the apparatus toward early transition. It was therefore necessary to verify that the laminar layer was indeed present and stable in the ranges predicted by the theory. A third topic which required verification was the assumed existence of an essentially two-dimensional flow field over the test sections of the plate. The design of the air temperature probe was a fourth point requiring experimental support. It was necessary to verify that the probe operated properly, particularly in the troublesome region near the wall. These problems are treated individually in the following discussion.

The central goal of the verification procedure was set as a reproduction of the laminar theory in the appropriate region. The standard for this was the Pohlhausen-Ostrach similarity solution, already amply verified by experiment. Although the satisfactory behavior of the experimental boundary layer in the laminar range cannot be treated as a foolproof verification of the turbulent layers beyond it, it does provide necessary reassurance regarding the appropriateness of comparing the present turbulent data with that reported

by other workers. Further, because the boundary layer thermometer used was subject to its own forced-convection problem (see Appendix II), its verification in the laminar range is a highly reliable test of suitability for measurement accuracy in the turbulent range, since the convection coefficient of the probe will be higher there.

Analytical data points for this comparison were generated by a special Runge-Kutta computer program based on the Ostrach solutions. The results of measurements in the laminar range are compared with this analytical solution in Figure 16. Very good agreement is evident. This gave a high degree of confidence in the thermometer system, and partial confirmation that the flow was indeed laminar where it was expected to be.

With regard to the treatment of the leading edge, early design attempts confirmed the result of Dotson(13), which was later brought to the author's attention. In fact, some evidence was found to support the proposition that the minimum floor-to-leading edge distance data reported by Dotson was actually subject to change with changing plate overheat. However, no extensive investigation of this was made. A floor-to-leading edge distance of one foot was found to be satisfactory for the present configuration. The leading edge contour was faired to a sharp edge by a short guard heater as sketched in Figure 17. This was found to be necessary after preliminary experiments with blunt

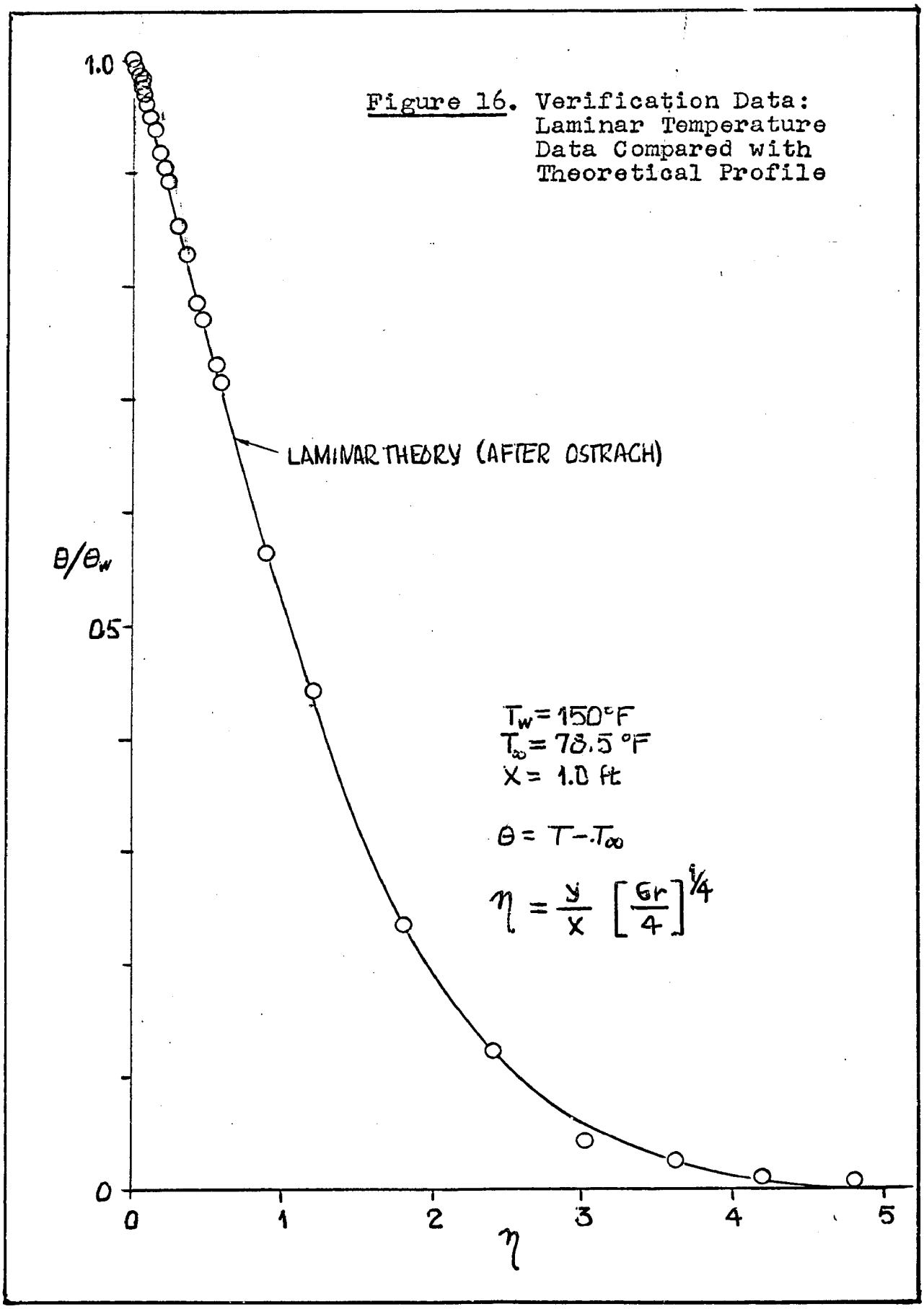


Figure 16. Verification Data: Laminar Temperature Data Compared with Theoretical Profile

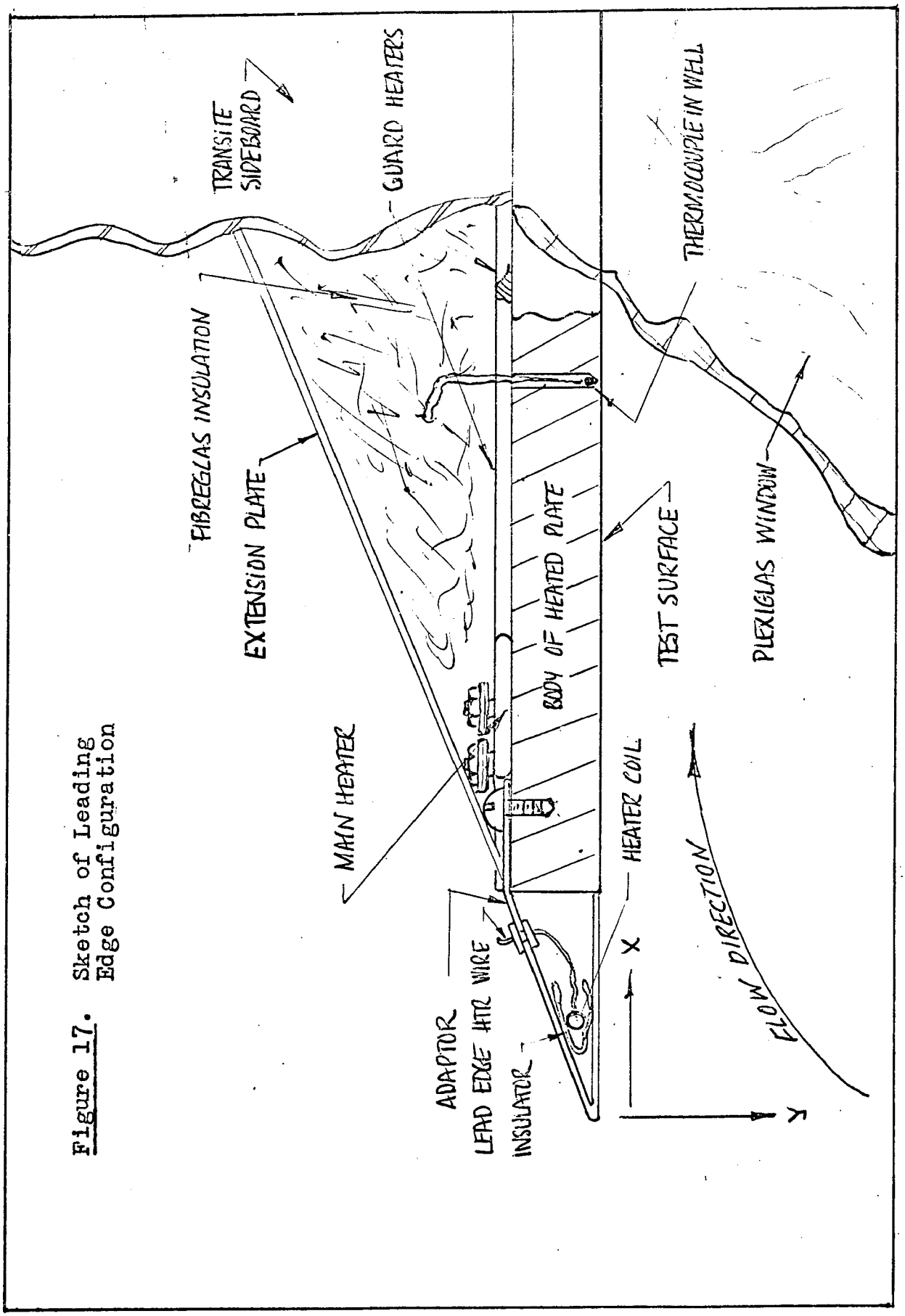


Figure 17. Sketch of Leading Edge Configuration

leading edges proved unsuccessful. Flow disturbances caused by the blunt edges led to early transition. The entire configuration was studied thoroughly by means of smoke visualization techniques. These confirmed the other indications of laminar flow, and were accepted as sufficient proof of adherence to the the laminar model in the appropriate range.

The question of three-dimensional effects was of real concern from the inception of the project, since similar troubles had plagued earlier investigators (see Eckert and Jackson[15], page 6). Although the overall design was based on a very conservative approximation, still the lack of any precise design data for this configuration left room for doubt. As a means of verification of the two-dimensionality of the flow, temperature traverses parallel to the plate were made at several distances from the plate, and at several values of Grashof number. The results are shown in Table 1. As can be seen, no appreciable difference in fluid temperature was recorded within the center test area. The total excursion in no case exceeded 0.03 millivolts, or roughly one degree Fahrenheit. The temperature deviations from the mean are apparently random.

One of the most commonly encountered problems in experimental research involving boundary layers is that of early transition due to vibration, random currents,

TABLE 1.

VERIFICATION OF THE TWO-DIMENSIONALITY WITHIN THE TURBULENT BOUNDARY LAYER

Thermocouple readings in millivolts.

$x = 11.75$ feet, $T_w = 2.70$, $T_\infty = 1.33$

y, inches	z, inches 6	3	2	1	0	-1	-2	-3	-6
11	1.32	1.33	1.33	1.33	1.33	1.33	1.33	1.33	1.33
7	1.34	1.35	1.33	1.33	1.34	1.33	1.33	1.34	1.34
4	1.37	1.37	1.37	1.37	1.37	1.37	1.37	1.37	1.37
2	1.45	1.42	1.43	1.45	1.43	1.43	1.43	1.43	1.43
½	1.62	1.62	1.62	1.62	1.61	1.61	1.61	1.60	1.61

$x = 5.0$ feet, $T_w = 2.70$, $T_\infty = 1.22$

4	1.23	1.23	1.22	1.22	1.22	1.23	1.23	1.23	1.24
1¼	1.38	1.40	1.38	1.39	1.39	1.39	1.39	1.38	1.41
½	1.55	1.50	1.56	1.54	1.55	1.55	1.55	1.53	1.53

$x = 2.0$ feet, $T_w = 2.72$, $T_\infty = 1.15$

2	1.15	1.16	1.16	1.16	1.16	1.16	1.16	1.15	1.15
1	1.15	1.16	1.16	1.16	1.16	1.15	1.15	1.15	1.15
½	1.23	1.23	1.23	1.23	1.23	1.22	1.23	1.25	1.28

or other disturbances in the environment. To evaluate the magnitude of these effects, special trial runs were made with all heavy machinery in the laboratory shut down. The operating vibration and noise of these had no noticeable effect upon the transition in the boundary layer, as verified by smoke observations. It was found that the ambient turbulence caused by workaday laboratory operations had a large effect upon the air in the test space. To eliminate this, the entire apparatus was isolated from the rest of the laboratory by a special partition, and readings were taken when disturbances were at a minimum. The partition proved to be a satisfactory answer to the problems introduced by random currents, again verified by smoke visualizations.

After the satisfactory completion of the verification procedures outlined above, the apparatus was employed for extensive heat flux and temperature measurements. These are described and evaluated in the following sections.

IV. EXPERIMENTAL RESULTS

Significant data were gathered relating to the local and surface parameters of the natural convection turbulent convection turbulent boundary layer.

Temperature was measured at very closely-spaced intervals, especially near the wall. These measurements serve at least three important functions. First, they demonstrate conclusively that the 1/7 power law does not apply to the natural convection case, as is widely assumed in the literature. Second, they give ample evidence of prominent contrasts between natural and forced convection turbulence. Thirdly, they provide a standard against which new analytical attempts may be measured.

The temperature measurements are first compared among themselves and with early analyses, and thereafter with other measurements from the literature.

Although local parameters of the flow are seldom reported, much heat transfer information has been published, as discussed above. As has been seen above, this data is usually reported on logarithmic coordinates. However, even with the use of this smoothing process, discrepancies nearing twenty percent are commonly found in the literature. Further, very little work has been published in which it was possible to measure the dependence of heat flux upon distance up the plate. Both techniques of reporting are included below, where good agreement with the analytical

result of Bayley is demonstrated.

A. Temperature Profiles in the Boundary Layer

Appendix I presents tables in which the measured boundary layer temperatures are listed. Table A1 presents the measured temperature in degrees Fahrenheit, while Table A2 gives the normalized temperature, $(T - T_\infty)/(T_w - T_\infty)$.

Figure 18 shows several of the measured profiles. Figure 19 gives the temperature field very near the wall. Note that laminar, as well as transitional turbulent profiles are shown here. Figure 20 shows the turbulent profiles in the same near-plate region. The transition regime for this data can be deduced from Figure 28, page 67, which shows wall heat flux data for the same θ_w.

Fujii[20] reported temperature profiles on universal coordinates resulting from his experiments near a vertical heated cylinder in water and ethylene glycol. His temperature profile is shown in Figure 21, together with the present data at a corresponding value of Rayleigh number. The comparison provided in the figure shows poor agreement of the present data with the profile of Fujii. This may be partly attributable to the values of Nu_x used by Fujii in preparing the abscissa values for his curves. Considering the possible effects of Prandtl number, especially in relation to the onset and character of the turbulent flow, the lack of agreement is not surprising. Other contributory causes of this poor agreement may be found in the highly specialized

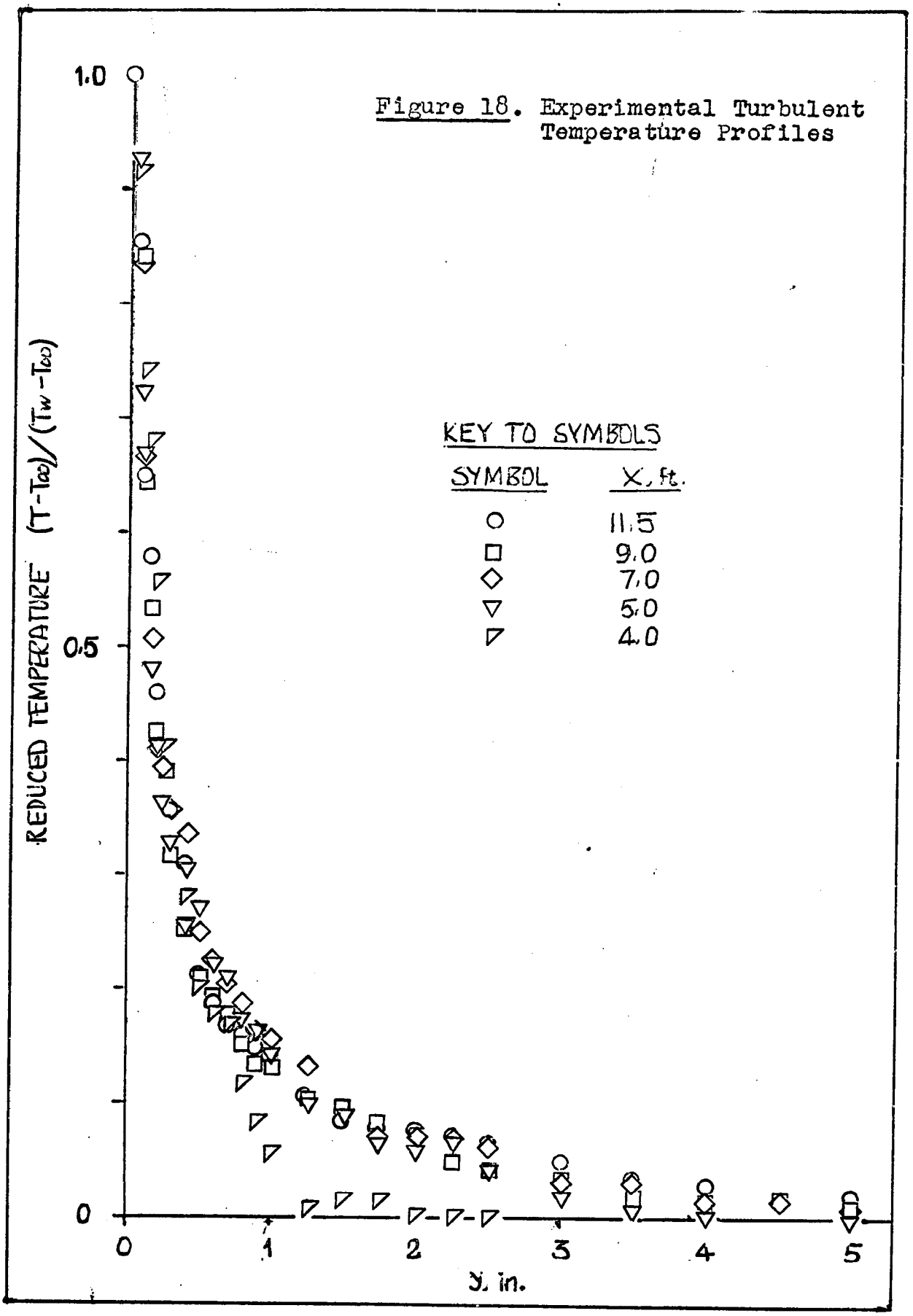


Figure 18. Experimental Turbulent Temperature Profiles

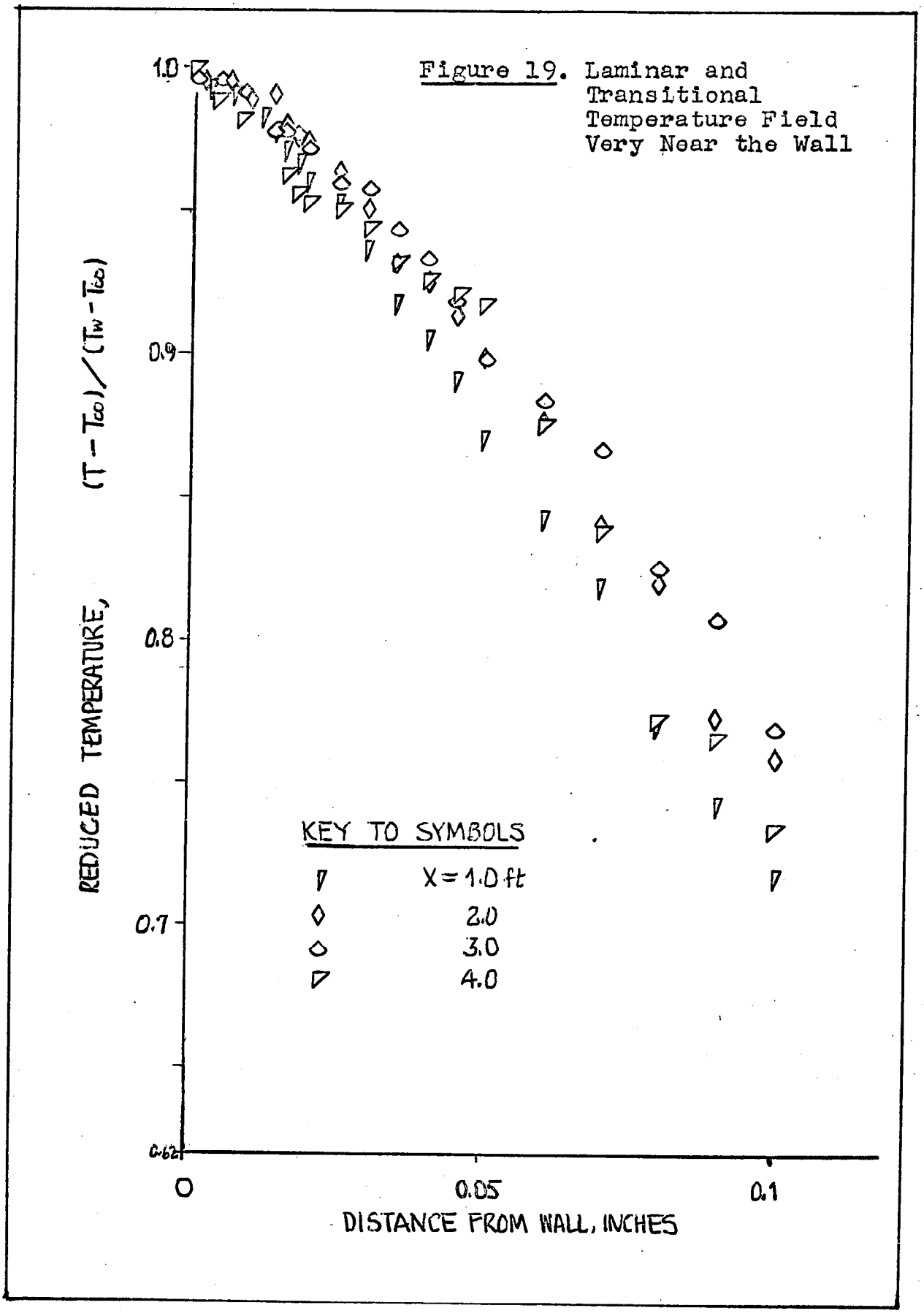


Figure 19. Laminar and Transitional Temperature Field Very Near the Wall

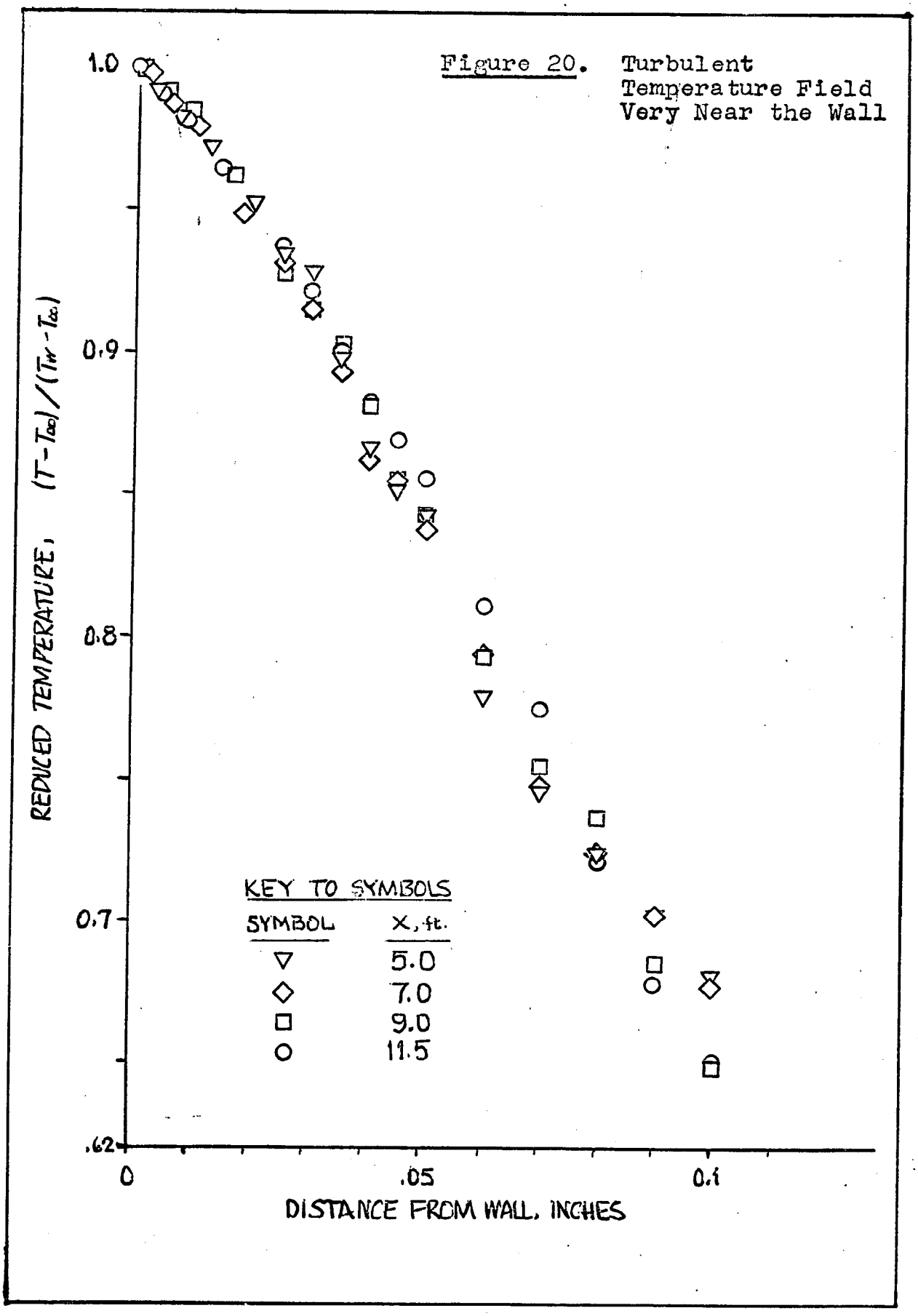


Figure 20. Turbulent Temperature Field Very Near the Wall

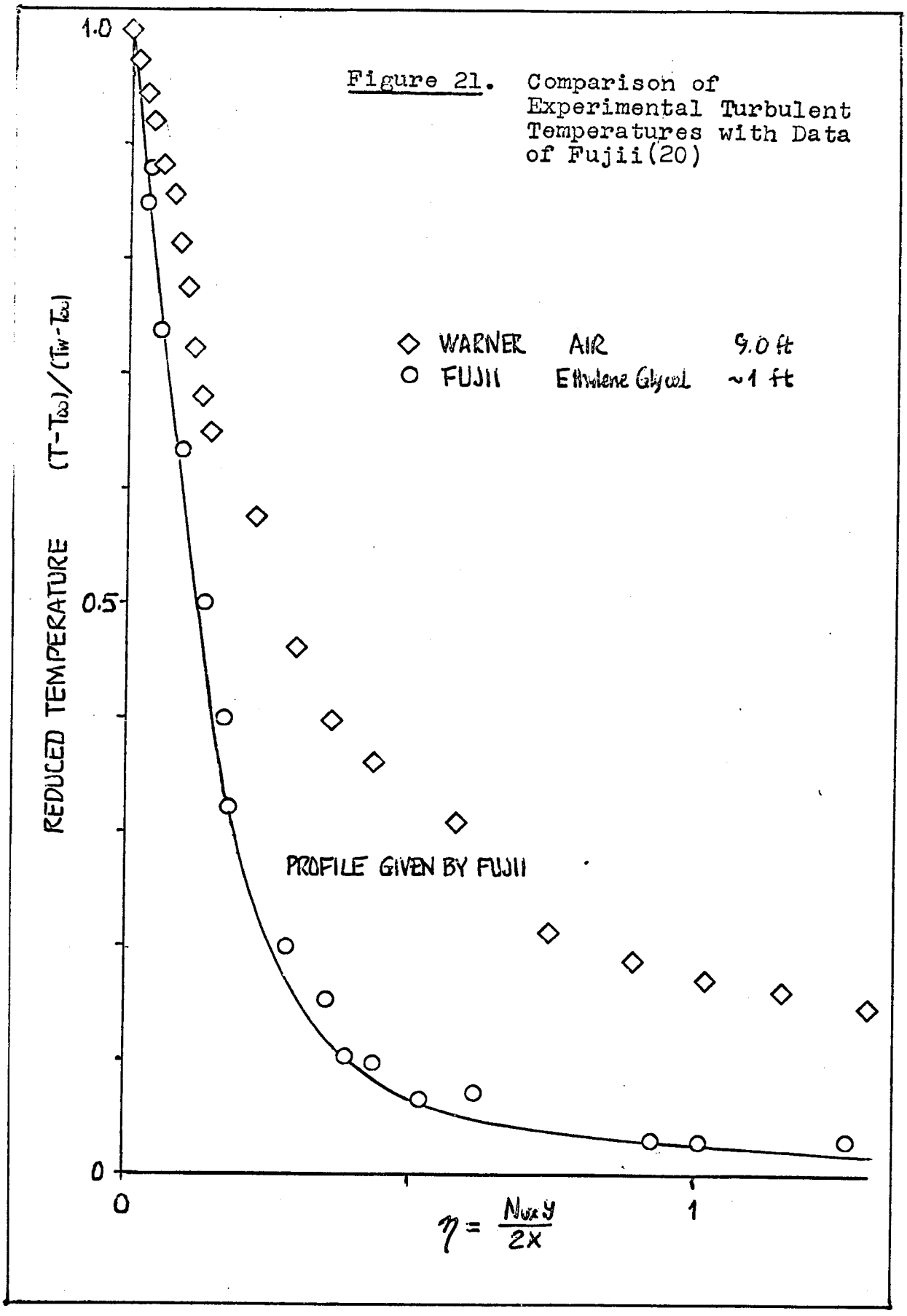


Figure 21. Comparison of Experimental Turbulent Temperatures with Data of Fujii(20)

experimental model used by Fujii. His small-diameter cylinder and relatively small enclosure both may have given rise to significant physical departure from the flat plate case.

The pioneering work of Griffiths and Davis[24], using a vertical flat plate in air, provided a significant first step toward an understanding of natural convection. However, the scale of the graphs used to present their data and the wide separation between data points makes comparison difficult. Some comments regarding their work are probably appropriate before such a comparison is undertaken. Besides the possibility of three-dimensionality in the flow already alluded to above, the instrument used by Griffiths and Davis for their measurements of local parameters deserves careful consideration. Both velocity and temperature were measured in their work by means of a hot-wire anemometer, the temperature being deduced from the unheated wire resistance. The sensitive element of the instrument was a 0.006 inch platinum wire. The wire length was not stated.

From the discussion of probe design given above it will be recalled that conduction into and through the support prongs from the hot sensing element into the cooler ambient air adjoining the support prongs can give a significant error in a thermocouple probe. Certainly the same can be said for a platinum resistance thermometer. Indeed, for the instrument in question, both the design

of the support prongs and the conduction characteristics of the sensitive element would be expected to aggravate the problem. For the particular probe used by Griffiths and Davis, conduction was certainly important. This conduction error caused a response that underestimated the temperature, especially near the wall where temperature gradients are large and heat transfer by convection is hampered by low velocities.

A comparison of the Griffiths and Davis laminar results with the Ostrach-Polhausen theory is given in Figure 22. This indeed shows the trend to be expected from thermometer conduction errors. The calibration of the Griffiths and Davis instrument for both velocity and temperature took place in a uniform-temperature stream. The nonuniform temperature and velocity fields, significant sources of error, although present in the actual measurements, were not accounted for in the calibration procedure. (The present author became cognizant of the conduction loss errors when a simple thermocouple probe of the type commonly employed in forced convection measurements failed to respond properly in the laminar range. See Appendix II for an analysis of this problem.) The response of the probe to velocity may have been relatively much improved; the conduction in that case was somewhat simulated by the effect of overheat in the wire, and may have been within the accuracy of the velocity calibrations.

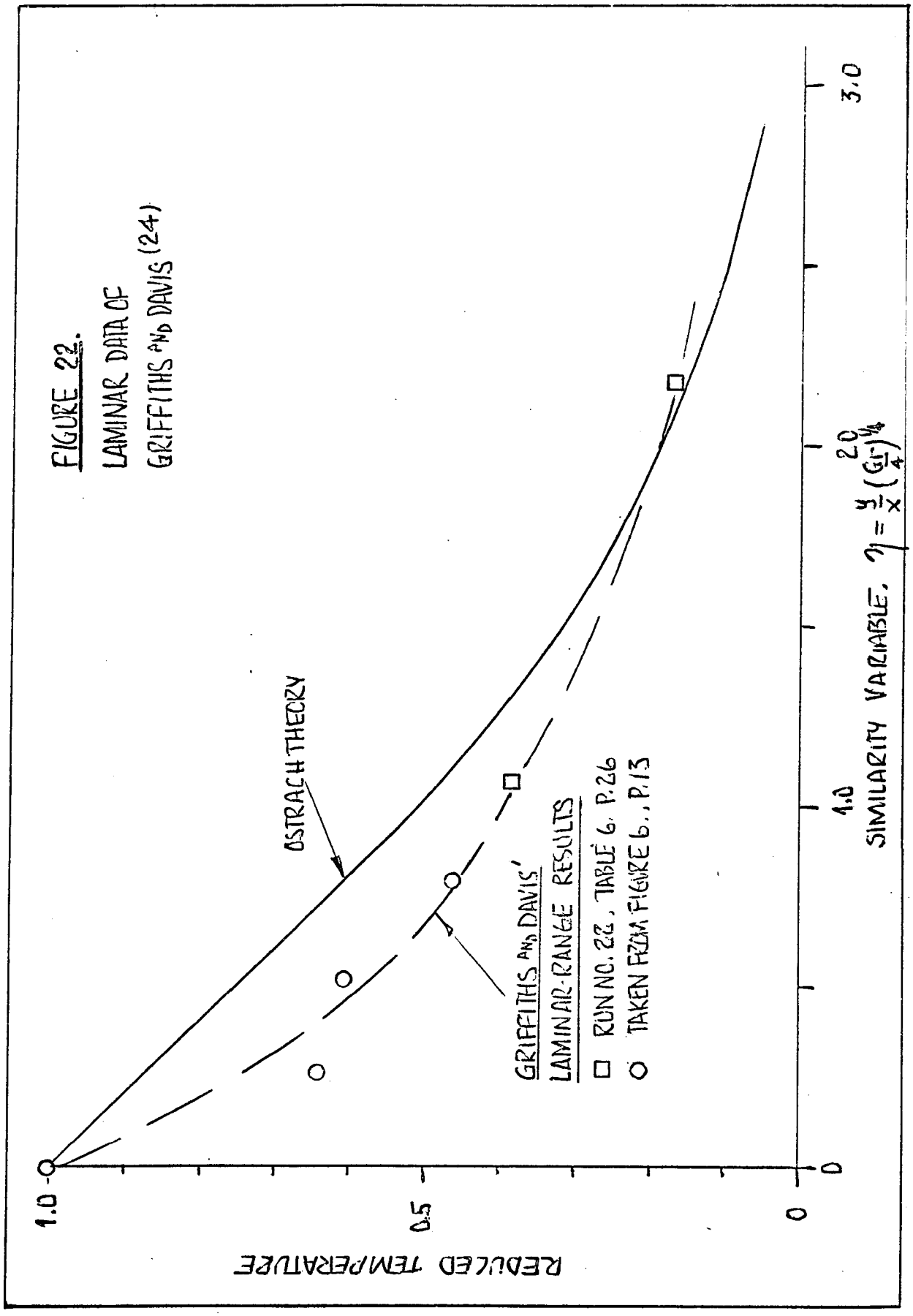


FIGURE 22.
LAMINAR DATA OF GRIFFITHS AND DAVIS (24)

The Griffiths and Davis instrument thus underestimated the actual temperatures near the wall, giving rise to a fair agreement with the power law profiles later recommended by other authors. This is strikingly illustrated in Figure 23, where the data of Figure 18 is compared to the power law profile recommended by Eckert and Jackson(15). Those authors apparently developed the 1/7 power profile from experience with forced convection, and from the data of Griffiths and Davis. The comparison of Figure 23 is based upon the equality of a quantity which was named the "enthalpy thickness" for convenience. That is the quantity

$$\delta_h = \frac{1}{(T_w - T_\infty)} \int_0^\infty (T - T_\infty)\, dy \tag{9}$$

was used to normalize the curves. Hence the abscissa is $\eta = y/\delta_h$ in each case shown. Figure 23 gives dramatic proof that the 1/7 power profile is a poor model for turbulent natural convection in air.

As an extension of this study, further power-law profiles were calculated. Satisfactory representation of the experimental data was not given by 1/5, 1/9, or 1/11 power laws, and no trend was seen that gave promise of success for any similar law. It can of course be shown that no power law is adequate at the wall. It was concluded that local parameters such as the temperature calculated from the power law would very probably be in error.

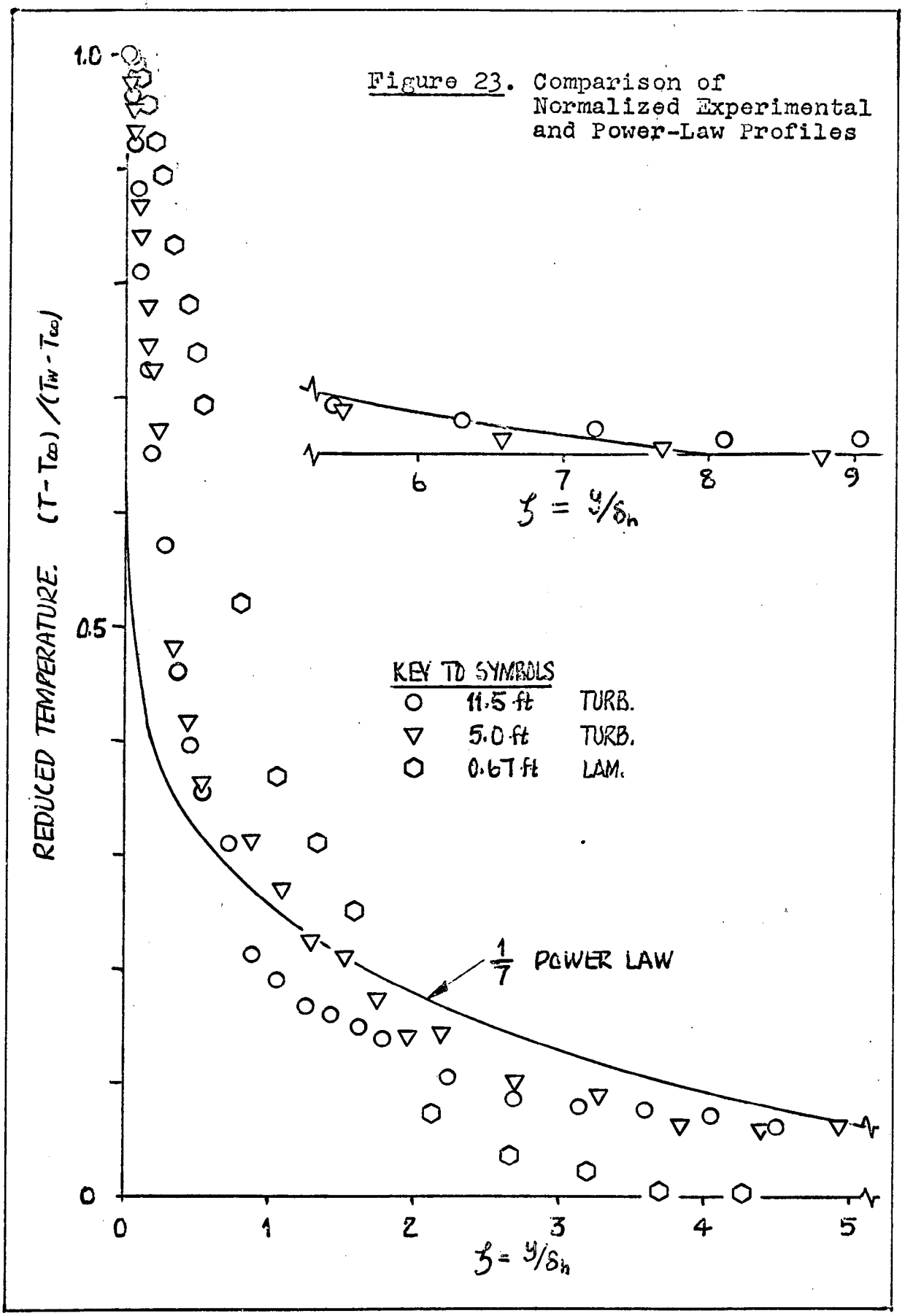


Figure 23. Comparison of Normalized Experimental and Power-Law Profiles

The grosser properties of the boundary layer, on the other hand, can be expected to depend only mildly upon the overall shape of the temperature profile, and may not respond poorly to the power-law assumption. It may be safely concluded that the power-law representation is a poor one, however.

Figure 24 shows a large portion of several selected experimental profiles from Figure 18, here on a somewhat expanded scale. A typical laminar profile has been included. Comparison of this figure with those given earlier reveals a striking contrast. While the expected dissimilarities very near the wall and far from the wall are evident, there is demonstrated in Figure 24 a significant intermediate-range similarity in the natural coordinate y. Insofar as can be discerned from this figure, any one of the profiles shown might be adequately represented by the laminar theory in this intermediate range.

This trend is evidently the result of the unique nature of the natural convection layer. Because the potential for flow is greatly reduced relative to a forced convection layer, the contrasts between the laminar and turbulent profiles would not be expected to be as sharp for natural convection. Although large fluctuations were observed in the instantaneous temperatures, the time-average temperature profile varies little from the laminar one except very near and very far from the wall. It appears that the primary effect of turbulence in this

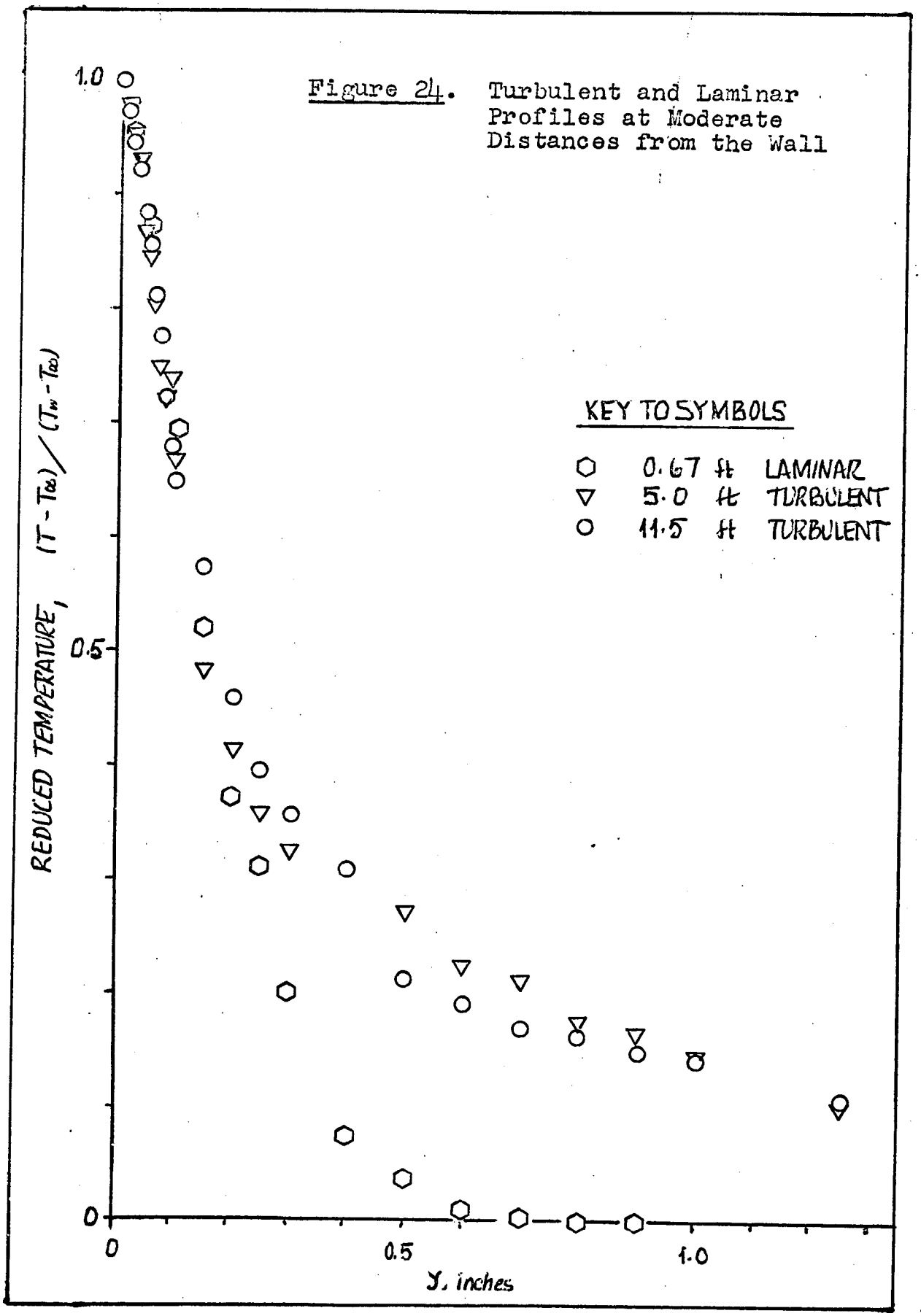


Figure 24. Turbulent and Laminar Profiles at Moderate Distances from the Wall

case is to transfer heat from the wall into the ambient, without a great effect on the already-established portions of the turbulent layer. Hence the most significant changes in the turbulent profiles with distance up the plate are seen in the outer portion of the profiles. This is a striking witness to the unique nature of natural convection turbulence. Reference has already been made to this in introducing the interferometric results of Eckert and Soehngen[16] in an earlier section. The larger scale and lower frequencies than would be expected in forced convection help one to understand why such abrupt contrasts can exist in the temperature fields.

B. Results Relative to Boundary Layer Thickness

Figure 25 shows some experimental results concerning the behavior of the enthalpy thickness of the boundary layer with increasing distance up the plate. The laminar thickness (normalized to the experimental values at $x = 0.67$ and 1.0 feet) is shown as a solid line. The enthalpy thicknesses predicted by the analyses of Eckert and Jackson[15] and Bayley[3], transformed to the present coordinates, are also shown. The heavy dashed line is an estimate of the actual behavior, as exhibited by the data points shown. Rapid growth of the boundary layer at transition and subsequent slow growth in the turbulent range are suggested here. The increased agreement obtained by Bayley over the other analysis shown

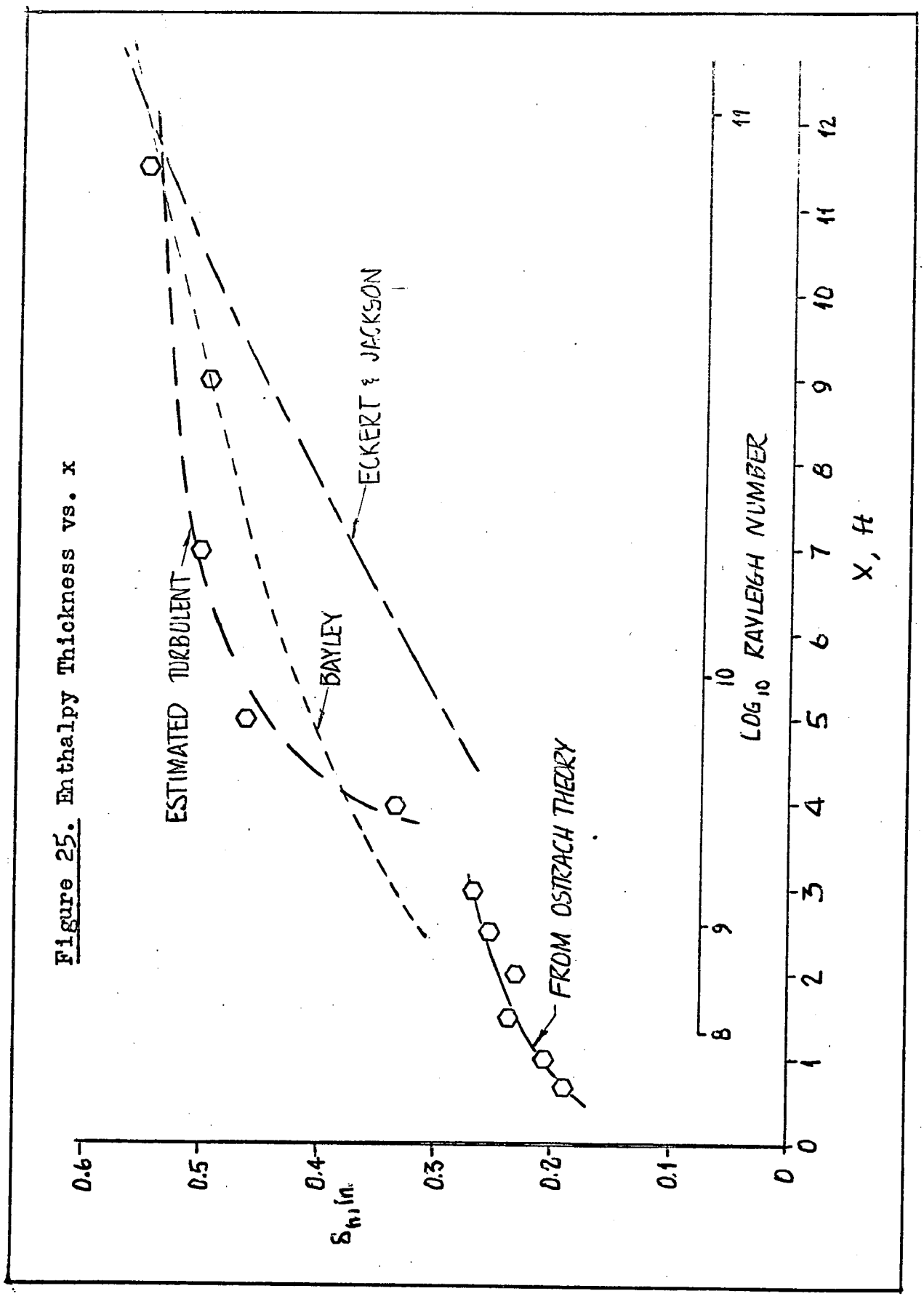


Figure 25. Enthalpy Thickness vs. x

is expected in the light of what has been seen of the physics introduced into the two analyses, although neither was expected to be accurate at low values of Rayleigh number. The rather poor agreement obtained here is not too surprising, in view of the limited nature of the analyses. Although insufficient information was obtained to verify a general correlation of data on this subject, it is felt that the trends shown here are realistic.

C. Results of the Heat Flux Measurements

Table A3 of Appendix I records the uncorrected heat flux data taken during these experiments. Power input to each six-inch section of plate height was measured independently. Baffles and guard heating sections assured a two-dimensional flow field over the center heated portion. Since insulation and radiation losses were difficult to calculate or measure precisely, but could rationally be assumed to be uniform over the full plate length, these were accounted for by obtaining a regression fit of the laminar range heat flow data to the laminar theory. This resulted in a vertical shift of the data to account for the stated losses. This could be done with confidence because the adherence of the experimental model to the laminar theory had already been verified, as discussed above. Agreement of the results with those of other investigators further substantiated this procedure.

Some temperature stratification was always present

in the ambient fluid during the experiments. This was accounted for by treating each data point individually in the calculation of the local wall-to-ambient temperature difference used in the reduction of data. Measurements of the ambient temperature near the base and top of the enclosure were made, using shielded thermocouples. The actual ambient temperature distribution was approximated for data reduction by a linear model passing through these two points. Computer programs were devised to provide comparisons among the present data and the various suggested correlations. The results of these computations are presented in Table A4, Appendix I.

Of immediate interest here is the comparison on customary terms of the experimental Nusselt number vs. Rayleigh number results with the results presented and correlated by others. Figures 26 and 27 give graphical representation to these data. Figure 26 demonstrates the good agreement of the present work with the theory in the laminar range, but gives poor representation of the better-known correlations for the turbulent case by the turbulent data. Figure 27 describes the turbulent data on an expanded scale, demonstrating the excellent agreement which was found with the correlation of Bayley(3). It shows two of the correlations, together with the present data and flat plate data for turbulent natural convection from the literature (see Saunders(40) and Griffiths and Davis(15)). The agreement with the data of Saunders is

Figure 26. Experimental Heat Transfer Data

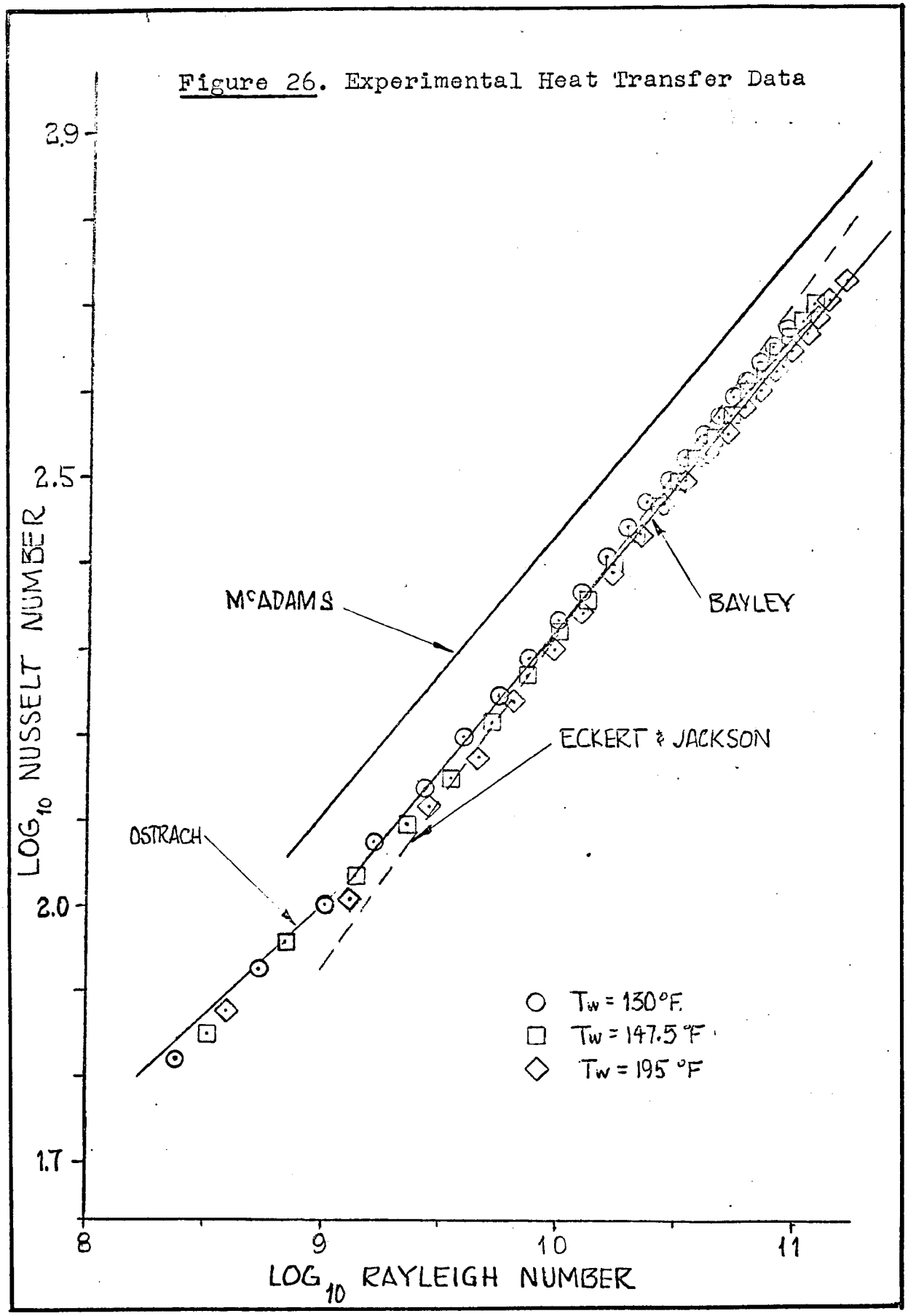
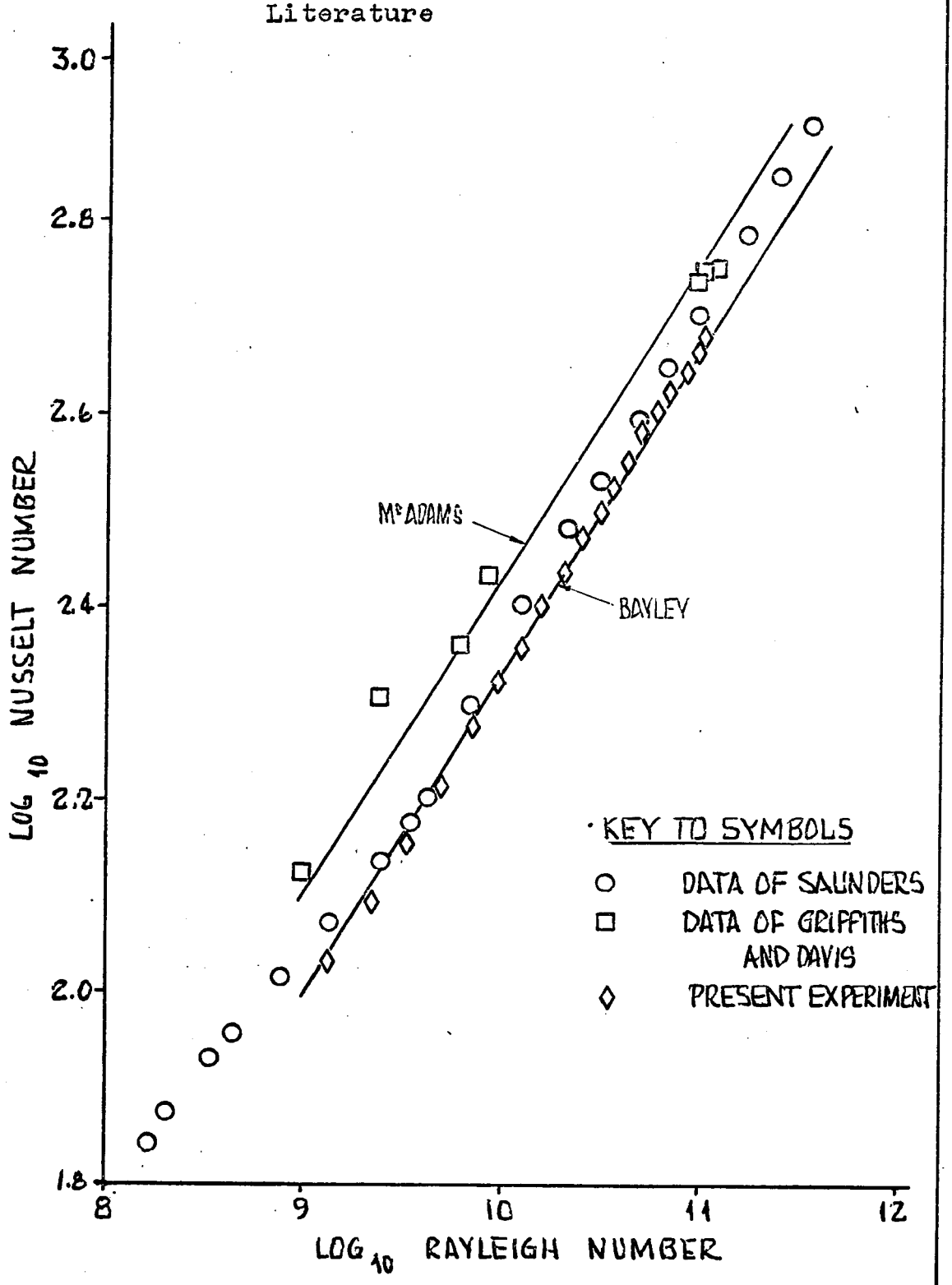


Figure 27. Heat Transfer Data Compared with Data and Correlations from the Literature



very good. The poor agreement with other data suggests a need for greater insight into the data and their sources. Before a further examination of these sources is undertaken, however, it is appropriate to be aware of the precautions taken to assure the reliability of the present data.

Besides the verification tests mentioned above, which gave assurance of a properly functioning apparatus, reproducibility checks on the heat flux data were made. Readings taken on different days showed less than three percent change in the recorded temperatures and power levels. This deviation could scarcely be detected in the logarithmic presentation. Further, eighty-two turbulent data points were employed in the verification of the recommended correlation.

The natural convection phenomenon has been stated or tacitly assumed by most investigators to be a two-dimensional flow field. Aside from the obvious departures from this picture introduced by random turbulence, further considerations regarding the mean flow, as they affect the assumptions made by many authors, deserve close attention.

Turbulence in a free convection boundary layer is capable of encouraging two kinds of three-dimensionalities. The most obvious effect is that each lump of fluid is subject to random motion in the third dimension, even though no average potential exists to encourage a mean flow in this dimension. By statistical treatment of the flow,

it is possible to visualize the real case in terms of a two-dimensional model. The more subtle effect of concern here is the increased mixing and heat transfer that may be expected to attend the turbulent motion. The entrainment inspired by this increased mixing has introduced errors into some of the data reported in the literature.

Consider a truly two-dimensional flow field. This may be approximated in reality in several ways. (One of the ways in which a parallel two-dimensional flow is commonly approximated is by the use of a vertical cylinder of sufficiently large diameter. For the boundary layer thicknesses considered here, this was not economically feasible.) The most common experimental means of approximating two-dimensional rectangular coordinate flow in natural convection is by the use of a wide flat plate. It is important to understand the the effect that would be seen if the ratio of the boundary layer thickness to plate width were to become too large. Although some of the published investigations did not report sufficient data to allow an estimate of this ratio, a good example of the problem is given by the data of Griffiths and Davis. In their work, a vertical sectioned plate of dimensions about two by nine feet was used for most of the turbulent measurements reported. The data taken indicated a thermal boundary layer thickness of about eight inches near the top of the plate. In this geometrical situation, one might expect a size-

able increase in heat transfer due to the entrainment of cooler air from the sides, as well as the front of the plate.

In the opinion of the present author, this is sufficient explanation for two things evident in Figure 27. First, the disagreement of Griffiths and Davis' data with that of Saunders and the present experiment can be easily understood. Second, since the McAdams correlation was based upon the best available data of its time, it was also probably biased by the Griffiths and Davis results, and is understandably displaced in the direction of higher heat transfer.

Here, as always, it is important that the obstacles presented by reality be properly understood, lest the valuable work of early contributors be too much belittled. The cumbersome experimental geometry required for turbulent natural convection research is just one of the problems to be considered. It is to their credit that Griffiths and Davis took the trouble to sectionalize their test surface, a justifiable inconvenience not suffered by many less patient researchers. (The importance of a sectionalized model in approaching the uniform-temperature mathematical case is suggested in Appendix VII.) The results of Griffiths and Davis are nothing short of remarkable when viewed in the perspective of their day. That they may have overlooked something that is plainly visible from our vantage in no way

destroys the value of their work.

Turning now to another interesting means of comparison, consider Figures 28 and 29. Here is seen the advantage of a sectionalized test surface. The actual power input is compared with the correaltions mentioned above. The trend of the data is much more obvious on this basis. In the figures, corrections have been made for insulation and radiation losses, and for thermal stratification of the ambient, as already discussed above. Here the correlations of McAdams, Eckert and Jackson, and Bayley have been transformed to the local coordinates.

The agreement of the data with the correlation of Bayley is perhaps even more strikingly demonstrated here, where the smoothing effect of the logarithmic coordinates is absent. The degree of accuracy with which the correlation of Bayley represents the local heat flux in both trend and magnitude lends significant credence to its use for natural convection boundary layers involving air and similar gasses.

D. Remarks Concerning the Measurement of Velocity

The original objectives of this research included the measurement of the full velocity field. It was hoped that in this way a rule similar to the law of the wall for turbulent forced convection might be established, paving the way for an analytical approach to natural convection patterned after the work of Spalding[48]. It was for this reason that atmospheric air was chosen

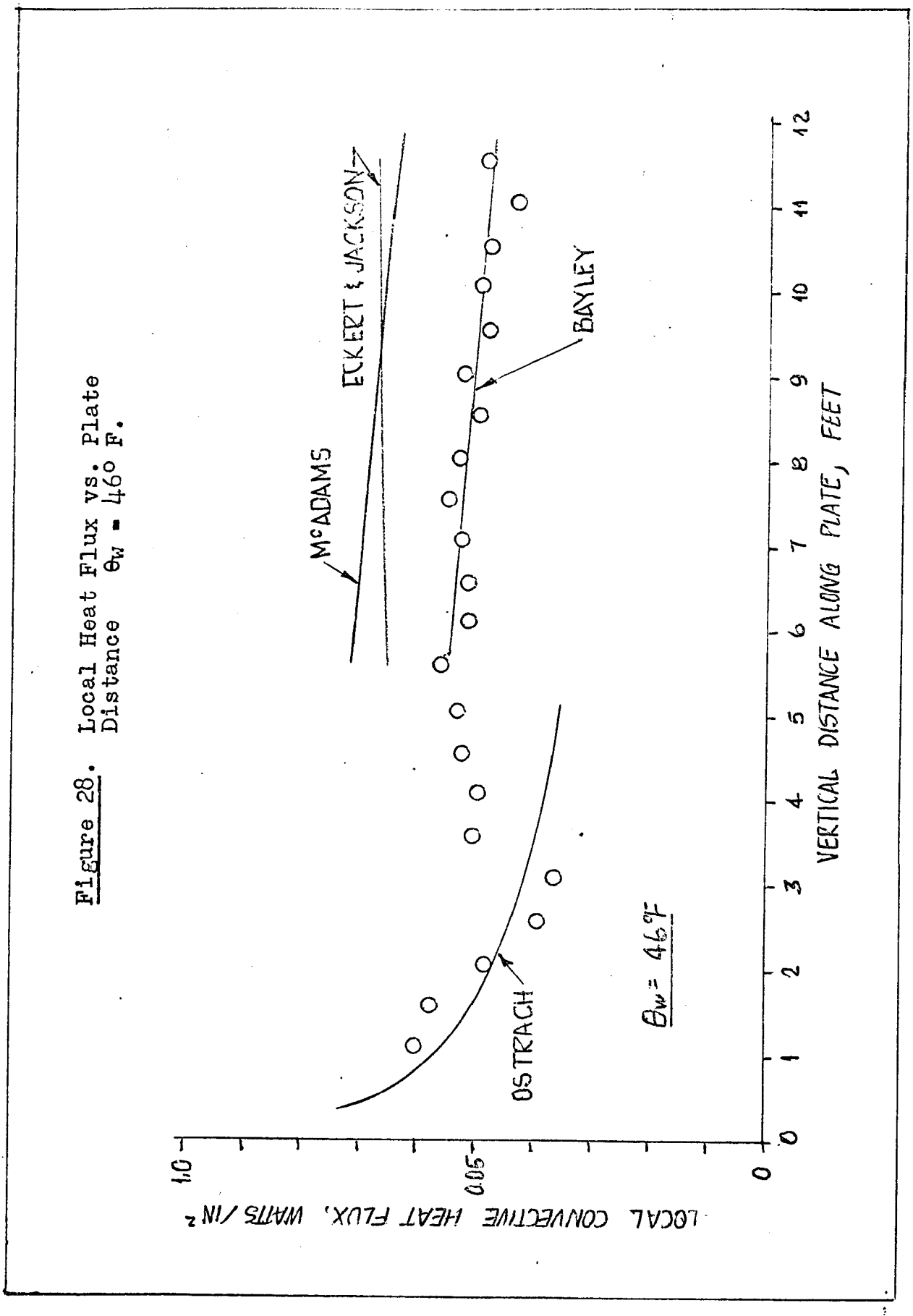


Figure 28. Local Heat Flux vs. Plate Distance θ_w = 46° F.

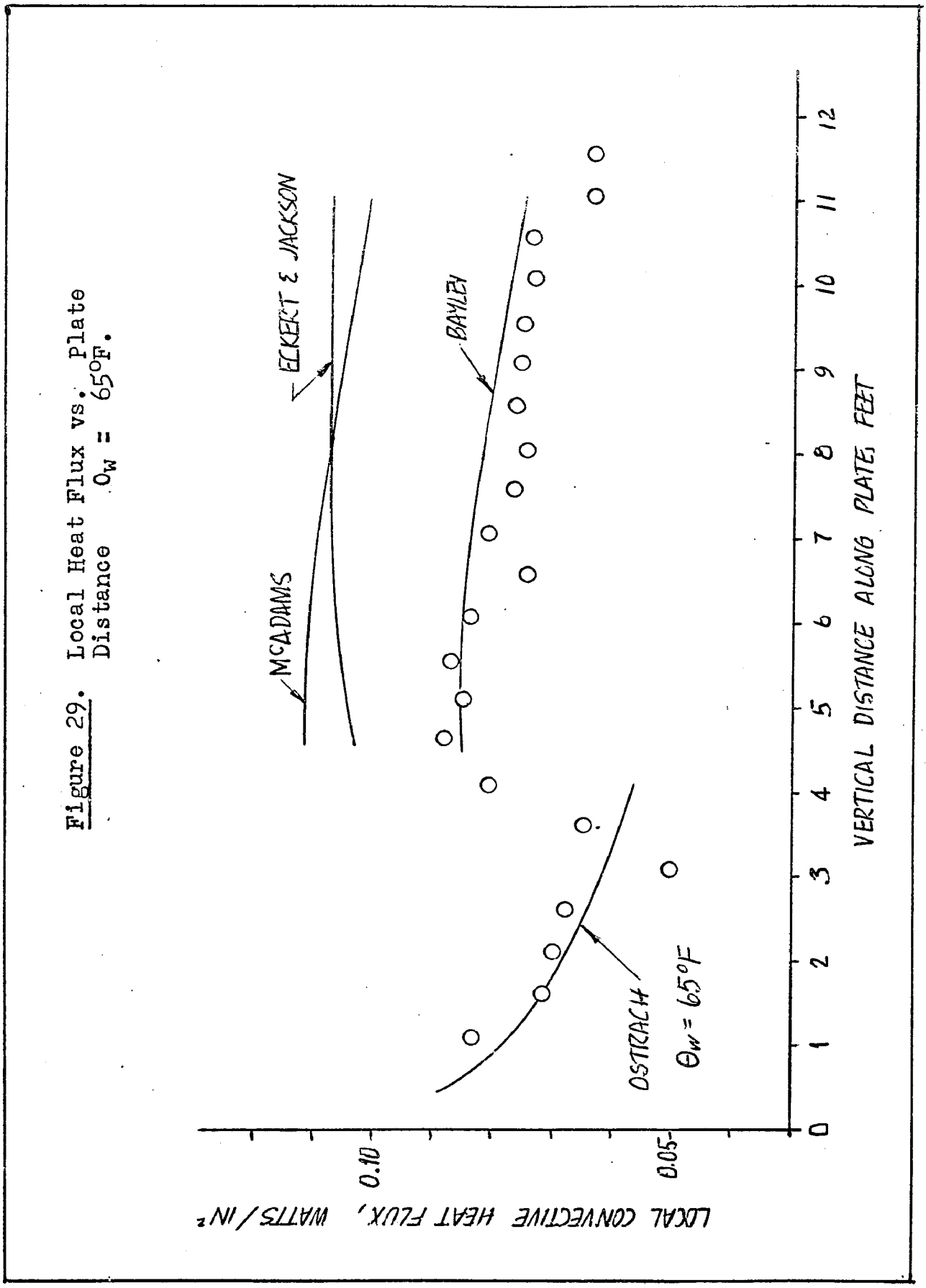


Figure 29. Local Heat Flux vs. Plate Distance θ_w = 65°F.

for the study; it appeared to be suited to velocity and turbulence measurements by virtue of the well-established techniques of hot-wire anemometry.

Griffiths and Davis[24] reported velocity measurements in the laminar and turbulent natural convection layers already discussed above. Their data points were quite widely spaced, but seemed to reflect an appropriate profile shape. The probe which they used and its calibration have already been discussed. It was suggested at that time that the probe was definitely in error for temperature measurements. Further it is possible to show by comparison with the laminar theory that the Griffiths and Davis velocity measurements admit a twenty-five percent error in that range. The desirability of improving the velocity data is therefore obvious. It is in the anemometry problem itself that the difficulty arises. One of the greatest frustrations of the present work was associated with the realization, born of thorough investigation, that this difficulty appears to admit no economical solution at present. Manageable methods for velocity measurement are unable to provide accurate measurements except in the vicinity of the velocity maxima. The region of primary interest very near the wall is completely beyond the capability of any anemometer known to the author. A full treatment of the velocity measurement problem in turbulent natural convection is given in Appendix IX.

The tools required to make significant improvements in the experimental data for velocity, especially in the critical region near the wall, do not appear to be in existence at present. In view of this, the velocity measurement objectives of this research could not be fulfilled.

V. CONCLUSIONS AND RECOMMENDATIONS

Until quite recently, forced convection heat transfer was consistently treated analytically by means of either integral methods or direct application of Reynolds' analogy, with a strong empirical flavor in either case.

The recent work of Spalding[48] constituted a very satisfactory step toward a more direct analytical approach, employing a convenient summary of the physics of the turbulent motion in terms of the well-known law of the wall. Early in the present study, it was hoped that a similar technique might be brought into focus for the case of turbulent natural convection. This will necessarily wait until more information can be gained about the nature of the velocity field in the near vicinity of the wall, which waits in turn upon the development of a satisfactory, practicable technique for measurement of very low velocities. A significant contribution will be made to the present state of knowledge about turbulent heat transfer when the velocity field is accurately measured.

The experimental results which were obtained in the present study allow the following conclusions.

(1) The correlations for heat transfer recommended by McAdams[33] and by Eckert and Jackson[15] are inferior to that of Bayley[3] for turbulent natural convection in

air, although that of McAdams gives a good representation of the slope of the experimental curve.

(2) The 1/7 power temperature profile adopted for use in analyses of turbulent natural convection is definitely not accurate for that case. It was based upon erroneous temperature readings.

(3) Except at the wall itself, the mean temperature is well represented on natural coordinates by a laminar profile over a great portion of the temperature drop.

(4) The primary effect of increased distance up the plate upon the temperature profiles appears to be a thickening of the thermal layer, with all profiles taking the same basic form for values of y less than 0.2 inch.

Beyond the measurement of velocity already recommended, there appears to be a need for verification of the established correlations at Prandtl numbers different than that treated here, with primary emphasis upon the Prandtl number range encompassed by liquid rocket propellants.

BIBLIOGRAPHY

1. Acrivos, A., "Modern Chemical Engineering, I. Physical Operations", Reinhold Publishing Co., New York (1963), pages 47-87.

2. Barakat, H. and J. A. Clark, "Transient, Laminar, Free-Convection Heat and Mass Transfer in Closed, Partially Filled Liquid Containers" Univ. of Michigan Heat Transfer Laboratory Report 04268-6-T. (1964).

3. Bayley, F.J., "An Analysis of Turbulent Free-Convection Heat Transfer", Inst. M.E. Proc. 169 (20), (1955), page 361.

4. Boussinesq, J. "Theorie de l' écoulement Tourbillant" Mem.prep.par div. Sav. 23, Paris (1877).

5. Carnahan, B. et.al., Applied Numerical Methods, Wiley, New York, (1966).

6. Carpenter, L.G. and A. C. Wassell, "The loss of Heat by Natural Convection from Parallel Vertical Plates in Air" Proc Inst M E, 128 (1934), page 439.

7. Clark, J.A., "A Review of Pressurization, Stratification, and Interfacial Phenomena", Paper No A-6, 1964 Cryogenic Engr. Conf. Philadelphia, Pa.

8. Collis, D. G., and M.J. Williams, "Two-dimensional Convection from Heated Wires at Low Reynolds Numbers" JFM 6, (1959), page 359.

9. Davis, A. H., "Natural Convective Cooling in Fluids" Phil Mag 44, (1922), page 920.

10. Deissler, R.G. "Turbulence in the Presence of a Vertical Body Force and Temperature Gradient", J. Geophys Res 67, (8), (1962), page 3049.

11. Deissler, R.G., "Analysis of Turbulent Heat Transfer, Mass Transfer, and Friction in Smooth Tubes at High Prandtl and Schmidt Numbers", NACA TR 1210 (1955) also see NACA TN 3145 (1954).

12. Deissler, R.G., "Turbulent Heat Transfer and Temperature Fluctuations in a Field with Uniform Velocity and Temperature Gradients", Int J. Heat and Mass Transfer 6, (1963). page 257.

13. Dotson, J.P., "Heat Transfer from a Vertical Plate by Free Convection" Purdue Univ. M.S. Thesis (1954).

14. Eckert, E.R.G., and A.J. Diagula, "Experimental Investigation of Free-Convection Heat Transfer in a Vertical Tube at Large Grashof Numbers" NACA TR 1211 (1955).

15. Eckert, E.R.G., and T.W. Jackson, "Analysis of Turbulent Free-Convection Boundary Layer on a Flat Plate", NACA TR 1015 (1951).

16. Eckert, E.R.G., and E.E. Soehngen, "Studies on Heat Transfer in Laminar Free Convection with the Zender-Mach Interferometer" AFTR 5747 (1948).

17. Eckert, E.R.G., and E.E. Soehngen, Interferometric Studies on the Stability and Transition to Turbulence of a Free-Convection Boundary Layer", IME/ASME General Discussion on Heat Transfer (1951), page 321.

18. Fujii, T. "An Analysis of Turbulent Free Convection Heat Transfer from a Vertical Surface", JapSME Bull 2, (8) (1959), page 559.

19. Fujii, T. "Experimental Studies of Free Convection Heat Transfer" op. cit., page 555.

20. Gardner, G.O., and J. Kestin, "Calculations of the Spalding Function over a Range of Prandtl Numbers" Int. J. H. M. Trans. 6 (1963), page 389.

21. Fox, L. "Numerical Solution of Ordinary and Partial Differential Equations", Addison-Wesley, Reading, Mass. (1962).

22. Goldstien, R.J., "Interferometric Study of the Steady- and Transient Free-Convection Thermal Boundary-Layers in Air and Water...", Univ of Minn. PhD Thesis (1959).

23. Goldstien, R.J. and E. R. G. Eckert, "The Steady and Transient Free Convection Boundary Layer on a Uniformly Heated Vertical Plate", Int. J. H.M.Trans. 4 (1960), page 208.

24. Griffiths, E. and A. H. Davis, "The Transmission of Heat by Radiation and Convection", British Food Inv. Bd. Spec. Rept. 9, D.S.I.R. (H.M.Stat Ofsc), London, (1922).

25. Hellums, J.D.and S.Churchill, "Computation of Natural Convection by Finite-Difference Methods", Int.Develop. Ht. Trans. , ASME (1961).

26. Hinze, J.O., "Turbulence", McGraw-Hill, New York, (1959)

27. Jakob, M., "Heat Transfer" Wiley, New York (1957).

28. Jakob, M. and W. Linke, Forschung. a. d. Geb. d. Ingenieurwes 4, (1933) page 75.

29. Kestin, J. and P.D. Richardson, "Heat Transfer Across Turbulent Incompressible Boundary Layers", Int.J.H.M. Trans. 6, (1963), page 147.

30. King, W.J. "The Basic Laws and Data of Heat Transmission: II. Natural Convection", Mech. Engr. 54, (1932), page 347.

31. Laufer, J. "The Structure of Turbulence in Fully-Developed Pipe Flow", NACA TR 1174 (1954).

32. Lumley, J. L. "The Constant-Temperature Hot-Thermistor Anemometer" ASME Symp. on Meas. Unst. Flow. (1962).

33. McAdams, W.H., "Heat Transmission", McGraw-Hill, New York (1954) 3rd Edition.

34. Nusselt, W. VDI - Zeitschr. 73 (1929), page 1475.

35. Nusselt, W., Gesundheitsingeneiur 38 (1915), page 477.

36. Ostrach, S., "Laminar Natural-Convection Flow and Heat Transfer of Fluids With and Without Heat Sources in Channels with Constant Wall Temperatures", NACA TN 2863 (1952).

37. Ostrach, S. "An Analysis of Laminar Free-Convection Flow and Heat Transfer About a Flat Plate Parallel to the Direction of the Generating Body Force", NACA TR 1111 (1953).

38. Reichardt, H. "The Principles of Turbulent Heat Transfer", NACA TM 1048 (translation) (1957).

39. Reynolds, W.C., et.al., "Heat Transfer in the Turbulent Boundary Layer" NASA Memo 12-4-58 (1958).

40. Saunders, O.A. "Effect of Pressure upon Natural Convection in Air", Proc Roy Soc A 157 (1936), Page 278.

41. Schlichting, H., "Boundary-Layer Theory", McGraw-Hill, New York, (1960), 4th Edition.

42. Schubauer, G.B., and C.M. Tchen, "Turbulent Flow", Princeton Univ. Press (1961).

43. Simmons, L.F.G., "A Shielded Hot-Wire Anemometer for Low Speeds" J. Sci. Inst. 26, (1942), Page 407.

44. Smith, A.G. and V.L. Shah, "The Calculation of Wall and Fluid Temperatures for the Incompressible Turbulent Boundary Layer with Arbitrary Distribution of Wall Heat Flux", Int. J. H. M. Trans. 8 (1962), page 1179.

45. Soehngen, E.E., "Interferometric Studies on Heat Transfer" IX Int. Cong. Appl. Mech. (1956).

46. Spalding, D.B., "A Single Formula for the Law of the Wall", J.A.M. 28, (1961), page 455.

47. Spalding, D.B., "A New Analytical Expression for the Drag of a Flat Plate, Valid for Both the Turbulent and Laminar Regimes", Int.J.H.M. Trans. 5, (1962), p. 1133.

48. Spalding, D.B., "Heat Transfer to Turbulent Stream from a Surface with a Stepwise Discontinuity in Wall Temperature", ASME/IME II Int. Dev. in H. T., Vol II, (1961), page 439.

49. Sparrow, E.M., and J.L. Gregg, "The Variable Fluid Property Problem in Free Convection", Trans. ASME 80, (1958), 879.

50. Szewczyk, C.C., "Stability and Transition of the Free-Convection Boundary Layer Along a Flat Plate", Int. J. H. M. Trans. 5, (1962), page 903.

51. Townsend, A.A. "The Structure of the Turbulent Boundary Layer" Proc. Camb. Phil. Soc. 47 (1951).

52. Tritton, D.J., "The Use of a Fibre Anemometer in Turbulent Flows", J.F.M. 16, (1963), page 269.

53. Vliet, G.C. "Stratified Layer Flow Model - A Numerical Approach to Temperature Stratification in Liquids Contained in Heated Vessels", AIAA Aerospace Sciences Mtg., New York, (1964), Preprint No. 64-37.

54. Wills, J.A.B., "The Correction of Hot-Wire Readings for Proximity to a Solid Boundary", J.F.M. 12, (1962), page 388.

APPENDIX I. EXPERIMENTAL TEMPERATURE FIELD

The following two tables present printed listings of the temperature field within the boundary layer. Table A1 gives the corrected actual temperatures in degrees Fahrenheit, while Table A2 presents ratios of excess temperature. Tabular values of y are in inches, values of x in feet. Figure A1 gives geometrical meaning to the tabular values.

Table A3 reports the data used for computation of the heat flux values reported herein. Tables A4a to A4d present the results of the Nusselt Number-Rayleigh Number computations. In these tables, the headings LNUM, LNUT, and LNUD represent the logarithms of the Nusselt Number values for McAdams' correlation, Eckert and Jacksons' correlation, and the experimental data, respectively (see references 15 and 33). The symbol Gr', as used in these tables, refers to the Grashof number divided by the numerical value $\cdot 10^{10}$.

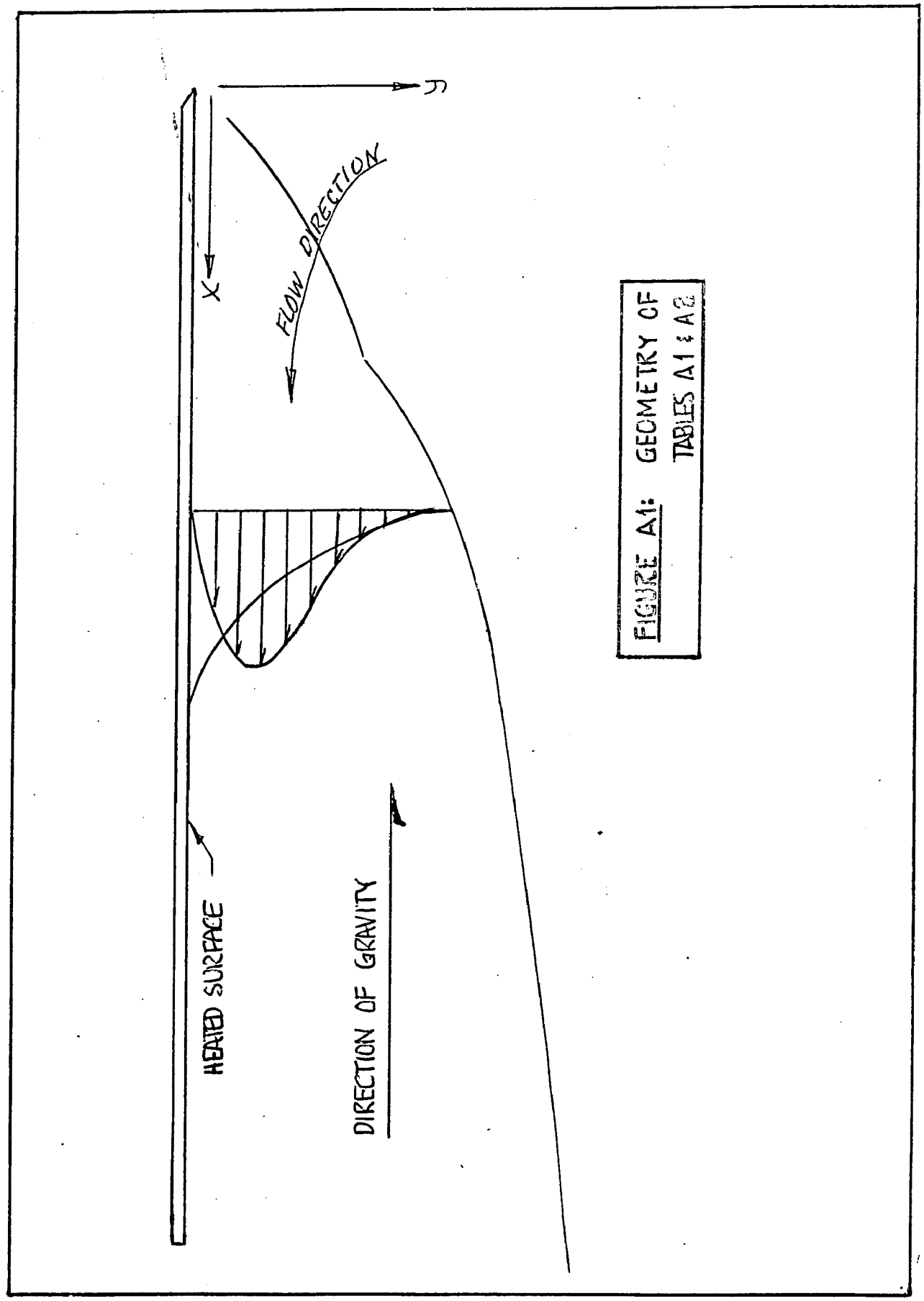


FIGURE A1: GEOMETRY OF TABLES A1 & A2

TABLE A1 -- TEMPERATURE FIELD IN BOUNDARY LAYER, DEGREES F

X	11.50	9.00	7.00	5.00	4.00	3.00	2.50	2.00	1.50	1.00	.67
DELT	58.34	56.27	60.73	63.48	64.60	66.75	66.31	66.63	67.40	67.43	66.42
GR'	14.1600	6.6530	3.4260	1.3270	.6931	.3049	.1755	.0910	.0384	.0114	.0003
Y					TEMPERATURES						
.000	144.90	141.50	142.90	142.80	143.20	143.60	143.10	142.50	144.30	143.80	142.70
.001	145.00	141.50	142.80	142.60	142.80	143.40	143.10	142.30	143.90	143.40	142.30
.002	144.70	141.40	142.70	142.40	142.70	143.30	143.00	142.30	143.90	143.40	142.40
.003	144.50	141.30	142.60	142.20	142.60	143.30	143.00	142.20	143.90	143.40	142.50
.004	144.30	141.20	142.40	142.10	142.50	143.30	142.90	142.20	143.90	143.40	142.50
.005	144.20	141.00	142.30	142.10	142.40	143.30	142.80	142.20	143.80	143.30	142.40
.006	144.10	140.90	142.10	142.00	142.40	143.20	142.70	142.20	143.80	143.30	142.40
.007	144.00	140.80	141.50	141.70	142.20	143.20	142.70	142.10	143.60	143.20	142.20
.008	143.80	140.80	141.60	141.50	142.10	143.00	142.70	142.00	143.60	143.00	142.20
.009	143.60	140.70	141.90	141.40	141.70	143.00	142.60	141.90	143.50	142.90	142.30
.010	143.30	140.60	141.60	141.30	141.60	142.90	142.40	141.80	143.20	142.90	142.00
.012	143.10	140.20	141.00	141.00	140.70	142.70	142.20	141.50	143.10	142.70	141.70
.014	142.80	139.80	140.40	140.70	140.50	142.10	142.00	141.90	143.00	142.30	141.50
.016	142.50	139.40	140.40	140.50	140.80	142.10	141.60	141.20	142.60	141.90	141.20
.018	142.10	139.20	139.80	140.20	140.40	142.00	141.60	140.90	142.50	141.60	141.20
.020	141.70	138.90	139.10	139.80	140.20	141.70	141.30	140.80	142.10	141.10	140.30
.025	141.20	137.40	138.80	138.70	140.00	140.90	140.70	140.20	141.70	140.60	139.80
.030	140.30	136.80	137.80	138.30	139.60	140.80	139.90	139.30	140.70	139.60	138.40
.035	139.10	136.10	136.50	136.40	138.80	139.80	139.00	138.00	140.10	138.30	137.60
.040	138.00	134.80	134.60	134.30	138.50	139.20	138.60	137.50	139.20	137.50	135.90
.045	137.20	133.40	134.10	133.40	138.10	138.20	137.60	136.80	138.00	136.50	135.60
.050	136.50	132.60	133.10	132.80	137.90	136.80	137.10	135.80	136.20	135.10	134.10
.060	133.90	129.80	130.30	128.80	135.20	135.90	135.70	134.30	134.50	133.20	131.60
.070	131.70	127.70	127.50	126.70	132.70	134.70	134.20	131.90	132.70	131.60	129.90

.... CONTINUATION OF TABLE ....(TABLE A1)

.080	128.60	126.70	126.20	125.30	129.10	132.60	132.10	131.20	131.10	129.00	128.20
.090	126.10	123.90	124.90	126.30	128.80	131.40	129.40	128.00	129.70	127.20	125.50
.100	124.40	121.70	122.70	121.90	126.70	128.90	128.80	127.20	127.80	125.40	122.30
.150	120.10	115.30	113.00	109.90	122.70	122.10	119.70	119.10	119.10	114.60	110.80
.200	113.30	109.20	107.10	105.60	114.70	112.90	113.20	111.40	110.50	105.20	100.70
.250	109.50	106.80	103.70	102.10	105.70	107.80	105.20	102.50	102.10	98.64	96.90
.300	107.20	103.10	102.70	100.00	101.80	101.40	99.85	96.74	96.19	92.70	89.58
.400	104.60	99.34	97.49	98.81	96.71	91.34	91.37	85.54	89.17	84.04	81.18
.500	98.94	97.61	95.99	96.48	91.63	84.63	82.44	82.44	82.44	78.81	78.69
.600	97.52	96.02	94.51	93.55	90.11	82.03	79.83	77.87	78.84	78.25	76.82
.700	96.34	95.49	93.64	92.64	89.50	79.80	79.31	77.17	77.79	76.94	76.41
.800	95.94	93.80	92.08	90.35	86.04	77.20	77.99	76.53	77.35	76.65	76.47
.900	95.25	92.78	91.63	89.82	84.13	77.41	76.94	76.03	76.68	76.18	76.18
1.000	94.71	92.61	90.52	88.35	82.41	77.03	76.82	76.03	76.68	76.30	76.18
1.250	92.64	91.03	90.20	85.68	79.13	77.14	76.62	75.55	.00	.00	.00
1.500	91.51	90.71	90.11	84.95	79.60	77.00	.00	.00	.00	.00	.00
1.750	91.17	89.73	86.33	83.37	79.54	77.00	.00	.00	.00	.00	.00
2.000	91.03	89.41	86.33	83.08	78.60	76.65	.00	.00	.00	.00	.00
2.250	90.74	87.97	86.33	83.55	78.60	76.91	.00	.00	.00	.00	.00
2.500	90.20	87.58	85.86	81.88	78.60	.00	.00	.00	.00	.00	.00
3.000	89.17	87.01	84.19	80.39	.00	.00	.00	.00	.00	.00	.00
3.500	88.35	86.24	84.19	79.80	.00	.00	.00	.00	.00	.00	.00
4.000	88.00	86.10	83.11	79.07	.00	.00	.00	.00	.00	.00	.00
4.500	87.49	86.24	83.11	79.07	.00	.00	.00	.00	.00	.00	.00
5.000	87.52	85.77	82.17	.00	.00	.00	.00	.00	.00	.00	.00
6.000	86.81	85.63	82.17	.00	.00	.00	.00	.00	.00	.00	.00
7.000	86.78	85.16	82.17	.00	.00	.00	.00	.00	.00	.00	.00
8.000	86.70	85.42	.00	.00	.00	.00	.00	.00	.00	.00	.00
9.000	86.67	85.07	.00	.00	.00	.00	.00	.00	.00	.00	.00
10.000	86.73	85.36	.00	.00	.00	.00	.00	.00	.00	.00	.00
11.000	86.56	85.23	.00	.00	.00	.00	.00	.00	.00	.00	.00

TABLE A2 -- NONDIMENSIONAL TEMPERATURE FIELD - θ/θ_{WALL}

X	11.50	9.00	7.00	5.00	4.00	3.00	2.50	2.00	1.50	1.00	.67
DELT	58.34	56.27	60.73	63.48	64.60	66.75	66.31	66.63	67.40	67.43	66.42
GR'	14.1600	6.6530	3.4260	1.3270	.6931	.3049	.1755	.0910	.0384	.0114	.0003
Y					. . . . TEMPERATURES						
.000	144.90	141.50	142.90	142.80	143.20	143.60	143.10	142.50	144.30	143.80	142.70
.001	1.0030	.9995	.9974	.9962	.9929	.9964	1.0010	.9963	.9951	.9932	.9939
.002	.9968	.9970	.9960	.9927	.9916	.9960	.9991	.9958	.9951	.9932	.9961
.003	.9935	.9955	.9951	.9896	.9903	.9956	.9982	.9954	.9951	.9932	.9969
.004	.9901	.9940	.9909	.9882	.9889	.9956	.9972	.9954	.9951	.9932	.9969
.005	.9876	.9910	.9900	.9882	.9881	.9951	.9959	.9954	.9931	.9928	.9961
.006	.9872	.9890	.9858	.9869	.9872	.9947	.9946	.9950	.9931	.9928	.9956
.007	.9847	.9875	.9756	.9820	.9846	.9934	.9938	.9937	.9905	.9915	.9935
.008	.9814	.9865	.9784	.9789	.9824	.9912	.9938	.9924	.9896	.9885	.9922
.009	.9779	.9850	.9825	.9771	.9763	.9912	.9929	.9908	.9888	.9862	.9939
.010	.9734	.9840	.9788	.9758	.9750	.9893	.9891	.9886	.9849	.9858	.9901
.012	.9695	.9755	.9681	.9709	.9605	.9868	.9861	.9844	.9832	.9829	.9858
.014	.9644	.9689	.9579	.9669	.9584	.9775	.9844	.9903	.9819	.9774	.9829
.016	.9591	.9624	.9579	.9625	.9627	.9775	.9776	.9793	.9758	.9720	.9782
.018	.9528	.9589	.9477	.9589	.9557	.9767	.9772	.9759	.9737	.9670	.9782
.020	.9450	.9526	.9361	.9522	.9540	.9716	.9733	.9738	.9679	.9598	.9646
.025	.9373	.9269	.9320	.9341	.9496	.9597	.9644	.9641	.9620	.9519	.9565
.030	.9218	.9165	.9147	.9282	.9448	.9576	.9520	.9514	.9473	.9368	.9361
.035	.9000	.9026	.8934	.8985	.9318	.9432	.9384	.9321	.9385	.9183	.9238
.040	.8823	.8810	.8624	.8647	.9269	.9335	.9329	.9247	.9251	.9059	.8975
.045	.8686	.8553	.8547	.8520	.9210	.9186	.9171	.9139	.9065	.8908	.8937
.050	.8555	.8409	.8373	.8419	.9177	.8977	.9095	.8994	.8802	.8708	.8701
.060	.8111	.7919	.7928	.7786	.8754	.8845	.8882	.8761	.8548	.8424	.8334
.070	.7744	.7536	.7462	.7453	.8381	.8669	.8656	.8407	.8290	.8190	.8076

.... CONTINUATION OF TABLE .... (TABLE A2)

.080	.7210	.7365	.7239	.7241	.7818	.8348	.8345	.8305	.8047	.7801	.7817
.090	.6780	.6864	.7025	.7400	.7763	.8166	.7944	.7823	.7842	.7535	.7408
.100	.6491	.6479	.6671	.6696	.7444	.7793	.7852	.7693	.7552	.7269	.6930
.150	.5750	.5339	.5067	.4807	.6822	.6782	.6472	.6477	.6262	.5671	.5204
.200	.4590	.4252	.4097	.4139	.5580	.5405	.5491	.5334	.4994	.4279	.3680
.250	.3940	.3824	.3551	.3588	.4198	.4633	.4291	.4001	.3743	.3301	.3106
.300	.3546	.3167	.3371	.3260	.3584	.3682	.3479	.3130	.2864	.2420	.2004
.400	.3085	.2506	.2520	.3069	.2802	.2171	.2199	.1450	.1822	.1137	.0738
.500	.2122	.2198	.2275	.2702	.2016	.1165	.0851	.0985	.0821	.0361	.0364
.600	.1878	.1917	.2030	.2240	.1781	.0775	.0458	.0301	.0288	.0279	.0082
.700	.1676	.1822	.1887	.2097	.1686	.0442	.0379	.0196	.0131	.0084	.0021
.800	.1607	.1522	.1630	.1736	.1150	.0052	.0181	.0100	.0066	.0041	.0030
.900	.1490	.1342	.1556	.1653	.0856	.0083	.0022	.0024	-.0033	-.0029	-.0015
1.000	.1396	.1311	.1374	.1422	.0588	.0026	.0004	.0024	-.0033	-.0011	-.0015
1.250	.1041	.1030	.1321	.1002	.0081	.0044	-.0026	-.0048	.0000	.0000	.0000
1.500	.0848	.0975	.1307	.0887	.0154	.0022	.0000	.0000	.0000	.0000	.0000
1.750	.0790	.0800	.0684	.0638	.0145	.0022	.0000	.0000	.0000	.0000	.0000
2.000	.0765	.0743	.0684	.0592	.0000	-.0031	.0000	.0000	.0000	.0000	.0000
2.250	.0716	.0487	.0684	.0666	.0000	.0009	.0000	.0000	.0000	.0000	.0000
2.500	.0623	.0418	.0607	.0403	.0000	.0000	.0000	.0000	.0000	.0000	.0000
3.000	.0447	.0317	.0332	.0169	.0000	.0000	.0000	.0000	.0000	.0000	.0000
3.500	.0306	.0180	.0332	.0077	.0000	.0000	.0000	.0000	.0000	.0000	.0000
4.000	.0246	.0154	.0154	-.0038	.0000	.0000	.0000	.0000	.0000	.0000	.0000
4.500	.0159	.0180	.0154	-.0038	.0000	.0000	.0000	.0000	.0000	.0000	.0000
5.000	.0164	.0097	.0000	.0000	.0000	.0000	.0000	.0000	.0000	.0000	.0000
6.000	.0042	.0071	.0000	.0000	.0000	.0000	.0000	.0000	.0000	.0000	.0000
7.000	.0037	-.0012	.0000	.0000	.0000	.0000	.0000	.0000	.0000	.0000	.0000
8.000	.0023	.0035	.0000	.0000	.0000	.0000	.0000	.0000	.0000	.0000	.0000
9.000	.0018	-.0028	.0000	.0000	.0000	.0000	.0000	.0000	.0000	.0000	.0000
10.000	.0028	.0024	.0000	.0000	.0000	.0000	.0000	.0000	.0000	.0000	.0000
11.000	.0000	.0000	.0000	.0000	.0000	.0000	.0000	.0000	.0000	.0000	.0000

TABLE A3. HEAT FLUX MEASUREMENTS

TWALL	130.0000	147.5000	194.7000	195.0000
TAMB	80.0000	77.5000	86.0000	86.0000
DTAMB	8.0000	10.5000	10.0000	10.0000
X, FEET		POWER INPUTS, WATTS		
.625	13.1000	13.5500	25.0000	24.5000
1.125	10.2000	9.0000	15.4000	15.0000
1.625	10.0000	8.1500	13.8000	13.5000
2.125	9.3000	8.1000	12.6000	12.4000
2.625	8.6000	7.8500	13.6000	13.3000
3.125	8.3000	6.5500	13.8000	13.6000
3.625	9.3000	7.6500	14.1000	13.8000
4.125	9.2500	8.8000	18.5000	17.5000
4.625	9.4000	9.3000	18.2000	17.9000
5.125	9.4500	9.0500	17.0000	16.7000
5.625	9.6000	9.2000	16.2000	15.9000
6.125	9.2000	8.9000	15.9000	15.7000
6.625	9.2000	8.3000	15.2000	15.2000
7.125	9.3000	8.7000	14.8000	14.5000
7.625	9.4000	8.4000	14.7000	14.5000
8.125	9.2500	8.3000	15.8000	15.5000
8.625	8.9500	8.4000	15.0000	14.9000
9.125	9.1500	8.3000	14.9000	14.8000
9.625	8.7500	8.3000	14.0000	13.8000
10.125	8.8500	8.1000	14.3000	13.1000
10.625	8.7000	8.1000	14.9000	13.3000
11.125	8.4000	7.4000	15.3000	13.2000
11.625	8.6500	7.4000	12.7000	12.6000
12.125	9.8000	10.6000	20.2000	19.7000

TABLE A4a. HEAT FLUX DATA REDUCTION RESULTS

NUSSELT -- RAYLEIGH DATA: **Twall = 130. ° F.**

X	QIN	DT	GR	LRA	LNUT	LNUD	LNUM
.6250	13.1000	49.5876	.1925E 08	.7150E 01	.1532E 01	.1411E 01	.1532E 01
1.1250	10.2000	49.2577	.1114E 09	.7912E 01	.1722E 01	.1662E 01	.1722E 01
1.6250	10.0000	48.9278	.3330E 09	.8387E 01	.1841E 01	.1819E 01	.1841E 01
2.1250	9.3000	48.5979	.7385E 09	.8733E 01	.1928E 01	.1927E 01	.1928E 01
2.6250	8.6000	48.2680	.1381E 10	.9005E 01	.1924E 01	.2008E 01	.2113E 01
3.1250	8.3000	47.9381	.2310E 10	.9229E 01	.2014E 01	.2074E 01	.2187E 01
3.6250	9.3000	47.6082	.3577E 10	.9419E 01	.2090E 01	.2139E 01	.2250E 01
4.1250	9.2500	47.2784	.5226E 10	.9583E 01	.2156E 01	.2195E 01	.2305E 01
4.6250	9.4000	46.9485	.7305E 10	.9729E 01	.2214E 01	.2246E 01	.2354E 01
5.1250	9.4500	46.6186	.9857E 10	.9859E 01	.2266E 01	.2292E 01	.2397E 01
5.6250	9.6000	46.2887	.1292E 11	.9976E 01	.2313E 01	.2335E 01	.2436E 01
6.1250	9.2000	45.9588	.1654E 11	.1008E 02	.2356E 01	.2372E 01	.2472E 01
6.6250	9.2000	45.6289	.2075E 11	.1018E 02	.2395E 01	.2407E 01	.2505E 01
7.1250	9.3000	45.2990	.2559E 11	.1027E 02	.2432E 01	.2440E 01	.2535E 01
7.6250	9.4000	44.9691	.3110E 11	.1036E 02	.2465E 01	.2471E 01	.2563E 01
8.1250	9.2500	44.6392	.3730E 11	.1044E 02	.2497E 01	.2499E 01	.2589E 01
8.6250	8.9500	44.3093	.4423E 11	.1051E 02	.2527E 01	.2526E 01	.2614E 01
9.1250	9.1500	43.9794	.5191E 11	.1058E 02	.2554E 01	.2551E 01	.2637E 01
9.6250	8.7500	43.6495	.6038E 11	.1065E 02	.2581E 01	.2574E 01	.2659E 01
10.1250	8.8500	43.3196	.6966E 11	.1071E 02	.2605E 01	.2597E 01	.2680E 01
10.6250	8.7000	42.9897	.7978E 11	.1077E 02	.2629E 01	.2618E 01	.2699E 01
11.1250	8.4000	42.6598	.9075E 11	.1082E 02	.2651E 01	.2637E 01	.2718E 01
11.6250	8.6500	42.3299	.1026E 12	.1088E 02	.2673E 01	.2657E 01	.2736E 01
12.1250	9.8000	42.0000	.1154E 12	.1093E 02	.2693E 01	.2678E 01	.2753E 01

TABLE A4b. HEAT FLUX DATA REDUCTION RESULTS

NUSSELT -- RAYLEIGH DATA: Twall = 147.5 °F.

X	QIN	DT	GR	LRA	LNUT	LNUD	LNUM
.6250	13.5500	69.4588	.2550E 08	.7272E 01	.1562E 01	.1494E 01	.1562E 01
1.1250	9.0000	69.0258	.1475E 09	.8034E 01	.1753E 01	.1716E 01	.1753E 01
1.6250	8.1500	68.5928	.4410E 09	.8510E 01	.1872E 01	.1851E 01	.1872E 01
2.1250	8.1000	68.1598	.9781E 09	.8855E 01	.1958E 01	.1954E 01	.1958E 01
2.6250	7.8500	67.7268	.1829E 10	.9127E 01	.1973E 01	.2035E 01	.2153E 01
3.1250	6.5500	67.2938	.3060E 10	.9351E 01	.2063E 01	.2093E 01	.2228E 01
3.6250	7.6500	66.8608	.4737E 10	.9541E 01	.2138E 01	.2153E 01	.2291E 01
4.1250	8.8000	66.4278	.6923E 10	.9705E 01	.2204E 01	.2213E 01	.2346E 01
4.6250	9.3000	65.9948	.9677E 10	.9851E 01	.2263E 01	.2269E 01	.2394E 01
5.1250	9.0500	65.5619	.1306E 11	.9981E 01	.2315E 01	.2318E 01	.2438E 01
5.6250	9.2000	65.1289	.1712E 11	.1010E 02	.2362E 01	.2362E 01	.2477E 01
6.1250	8.9000	64.6959	.2192E 11	.1021E 02	.2405E 01	.2402E 01	.2512E 01
6.6250	8.3000	64.2629	.2750E 11	.1030E 02	.2444E 01	.2436E 01	.2545E 01
7.1250	8.7000	63.8299	.3392E 11	.1040E 02	.2480E 01	.2469E 01	.2576E 01
7.6250	8.4000	63.3969	.4121E 11	.1048E 02	.2514E 01	.2499E 01	.2604E 01
8.1250	8.3000	62.9639	.4943E 11	.1056E 02	.2546E 01	.2527E 01	.2630E 01
8.6250	8.4000	62.5309	.5862E 11	.1063E 02	.2575E 01	.2554E 01	.2655E 01
9.1250	8.3000	62.0979	.6882E 11	.1070E 02	.2603E 01	.2579E 01	.2678E 01
9.6250	8.3000	61.6649	.8006E 11	.1077E 02	.2630E 01	.2603E 01	.2700E 01
10.1250	8.1000	61.2320	.9237E 11	.1083E 02	.2654E 01	.2625E 01	.2721E 01
10.6250	8.1000	60.7990	.1058E 12	.1089E 02	.2678E 01	.2646E 01	.2740E 01
11.1250	7.4000	60.3660	.1204E 12	.1095E 02	.2700E 01	.2665E 01	.2759E 01
11.6250	7.4000	59.9330	.1361E 12	.1100E 02	.2722E 01	.2683E 01	.2777E 01
12.1250	10.6000	59.5000	.1531E 12	.1105E 02	.2742E 01	.2708E 01	.2794E 01

TABLE A4c. HEAT FLUX DATA REDUCTION RESULTS

NUSSELT -- RAYLEIGH DATA: Twall = 194.7 °F.

X	QIN	DT	GR	LRA	LNUT	LNUD	LNUM
.6250	25.0000	108.1845	.3232E 08	.7375E 01	.1588E 01	.1536E 01	.1588E 01
1.1250	15.4000	107.7722	.1875E 09	.8138E 01	.1779E 01	.1745E 01	.1779E 01
1.6250	13.8000	107.3598	.5619E 09	.8615E 01	.1898E 01	.1874E 01	.1898E 01
2.1250	12.6000	106.9474	.1250E 10	.8962E 01	.1907E 01	.1965E 01	.2098E 01
2.6250	13.6000	106.5351	.2342E 10	.9235E 01	.2016E 01	.2046E 01	.2189E 01
3.1250	13.8000	106.1227	.3930E 10	.9460E 01	.2106E 01	.2116E 01	.2264E 01
3.6250	14.1000	105.7103	.6101E 10	.9651E 01	.2182E 01	.2177E 01	.2328E 01
4.1250	18.5000	105.2979	.8940E 10	.9816E 01	.2249E 01	.2247E 01	.2383E 01
4.6250	18.2000	104.8856	.1253E 11	.9963E 01	.2307E 01	.2306E 01	.2432E 01
5.1250	17.0000	104.4732	.1696E 11	.1009E 02	.2360E 01	.2355E 01	.2475E 01
5.6250	16.2000	104.0608	.2229E 11	.1021E 02	.2408E 01	.2397E 01	.2515E 01
6.1250	15.9000	103.6485	.2862E 11	.1032E 02	.2451E 01	.2435E 01	.2551E 01
6.6250	15.2000	103.2361	.3601E 11	.1042E 02	.2491E 01	.2469E 01	.2584E 01
7.1250	14.8000	102.8237	.4455E 11	.1051E 02	.2528E 01	.2499E 01	.2615E 01
7.6250	14.7000	102.4113	.5429E 11	.1060E 02	.2562E 01	.2527E 01	.2644E 01
8.1250	15.8000	101.9990	.6532E 11	.1068E 02	.2594E 01	.2556E 01	.2670E 01
8.6250	15.0000	101.5866	.7769E 11	.1076E 02	.2624E 01	.2582E 01	.2696E 01
9.1250	14.9000	101.1742	.9148E 11	.1083E 02	.2653E 01	.2606E 01	.2719E 01
9.6250	14.0000	100.7619	.1067E 12	.1089E 02	.2680E 01	.2627E 01	.2741E 01
10.1250	14.3000	100.3495	.1235E 12	.1096E 02	.2705E 01	.2649E 01	.2763E 01
10.6250	14.9000	99.9371	.1419E 12	.1102E 02	.2729E 01	.2670E 01	.2783E 01
11.1250	15.3000	99.5247	.1620E 12	.1107E 02	.2752E 01	.2690E 01	.2802E 01
11.6250	12.7000	99.1124	.1838E 12	.1113E 02	.2774E 01	.2707E 01	.2820E 01
12.1250	20.2000	98.7000	.2073E 12	.1118E 02	.2795E 01	.2732E 01	.2837E 01

TABLE A4d. HEAT FLUX DATA REDUCTION RESULTS

NUSSELT -- RAYLEIGH DATA: Twall = 195.0 °F.

X	QIN	DT	GR	LRA	LNUT	LNUD	LNUM
.6250	24.5000	108.4845	.3237E 08	.7375E 01	.1588E 01	.1537E 01	.1588E 01
1.1250	15.0000	108.0722	.1878E 09	.8139E 01	.1779E 01	.1745E 01	.1779E 01
1.6250	13.5000	107.6598	.5628E 09	.8615E 01	.1898E 01	.1874E 01	.1898E 01
2.1250	12.4000	107.2474	.1252E 10	.8963E 01	.1907E 01	.1966E 01	.2098E 01
2.6250	13.3000	106.8351	.2347E 10	.9236E 01	.2016E 01	.2047E 01	.2189E 01
3.1250	13.6000	106.4227	.3937E 10	.9460E 01	.2106E 01	.2117E 01	.2264E 01
3.6250	13.8000	106.0103	.6112E 10	.9651E 01	.2183E 01	.2178E 01	.2328E 01
4.1250	17.5000	105.5979	.8956E 10	.9817E 01	.2249E 01	.2245E 01	.2383E 01
4.6250	17.9000	105.1856	.1255E 11	.9964E 01	.2308E 01	.2305E 01	.2432E 01
5.1250	16.7000	104.7732	.1699E 11	.1010E 02	.2360E 01	.2354E 01	.2476E 01
5.6250	15.9000	104.3608	.2233E 11	.1021E 02	.2408E 01	.2397E 01	.2515E 01
6.1250	15.7000	103.9485	.2867E 11	.1032E 02	.2451E 01	.2435E 01	.2551E 01
6.6250	15.2000	103.5361	.3608E 11	.1042E 02	.2491E 01	.2469E 01	.2585E 01
7.1250	14.5000	103.1237	.4463E 11	.1051E 02	.2528E 01	.2500E 01	.2615E 01
7.6250	14.5000	102.7113	.5439E 11	.1060E 02	.2562E 01	.2528E 01	.2644E 01
8.1250	15.5000	102.2990	.6544E 11	.1068E 02	.2595E 01	.2557E 01	.2671E 01
8.6250	14.9000	101.8866	.7784E 11	.1076E 02	.2625E 01	.2583E 01	.2696E 01
9.1250	14.8000	101.4742	.9165E 11	.1083E 02	.2653E 01	.2607E 01	.2719E 01
9.6250	13.8000	101.0619	.1069E 12	.1089E 02	.2680E 01	.2629E 01	.2742E 01
10.1250	13.1000	100.6495	.1238E 12	.1096E 02	.2705E 01	.2649E 01	.2763E 01
10.6250	13.3000	100.2371	.1422E 12	.1102E 02	.2729E 01	.2668E 01	.2783E 01
11.1250	13.2000	99.8247	.1623E 12	.1108E 02	.2752E 01	.2686E 01	.2802E 01
11.6250	12.6000	99.4124	.1841E 12	.1113E 02	.2774E 01	.2703E 01	.2820E 01
12.1250	19.7000	99.0000	.2077E 12	.1118E 02	.2795E 01	.2729E 01	.2838E 01

APPENDIX II. THERMOCOUPLE PROBE DESIGN CONSIDERATIONS

The following simplified one-dimensional analysis provides a criterion for assignment of values to the dimension parameters of a temperature probe.

Let us adopt for the mathematical representation of the sensitive element of the probe a one-dimensional fin with insulated end and a base temperature θ_b, equal to the maximum expected temperature gradient multiplied by the distance b (see Figure A2). The analysis then proceeds as follows:

(1) Calculate

From the severest gradient near the wall

$$-\left.\frac{\partial T}{\partial y}\right|_0 = q''_0/k_f = \frac{Nu_x}{x}(T_w - T_\infty) \doteq 0.1\, Ra_x^{1/3}\left(\frac{T_w - T_\infty}{x}\right)$$

$$-\left.\frac{\partial T}{\partial y}\right|_0 = 0.1\left(\frac{g\beta Pr}{\nu^2}\right)^{1/3}(T_w - T_\infty)^{4/3}$$

So

$$\theta_b \doteq b\left.\frac{\partial T}{\partial y}\right|_0 = 0.1\, b\left(\frac{g\beta Pr}{\nu^2}\right)^{1/3}(T_w - T_\infty)^{4/3}$$

(2) Calculate the relationship among the properties, the length ℓ, and θ_b.

$$\frac{\partial^2\theta}{\partial z^2} - m^2\theta = 0, \qquad m = \frac{4h}{kd}$$

$$\theta(0) = \theta_e, \quad \theta'(0) = 0, \quad \theta(\ell) = \theta_b,$$

so

$$\theta_e = \theta_b / \cosh m\ell.$$

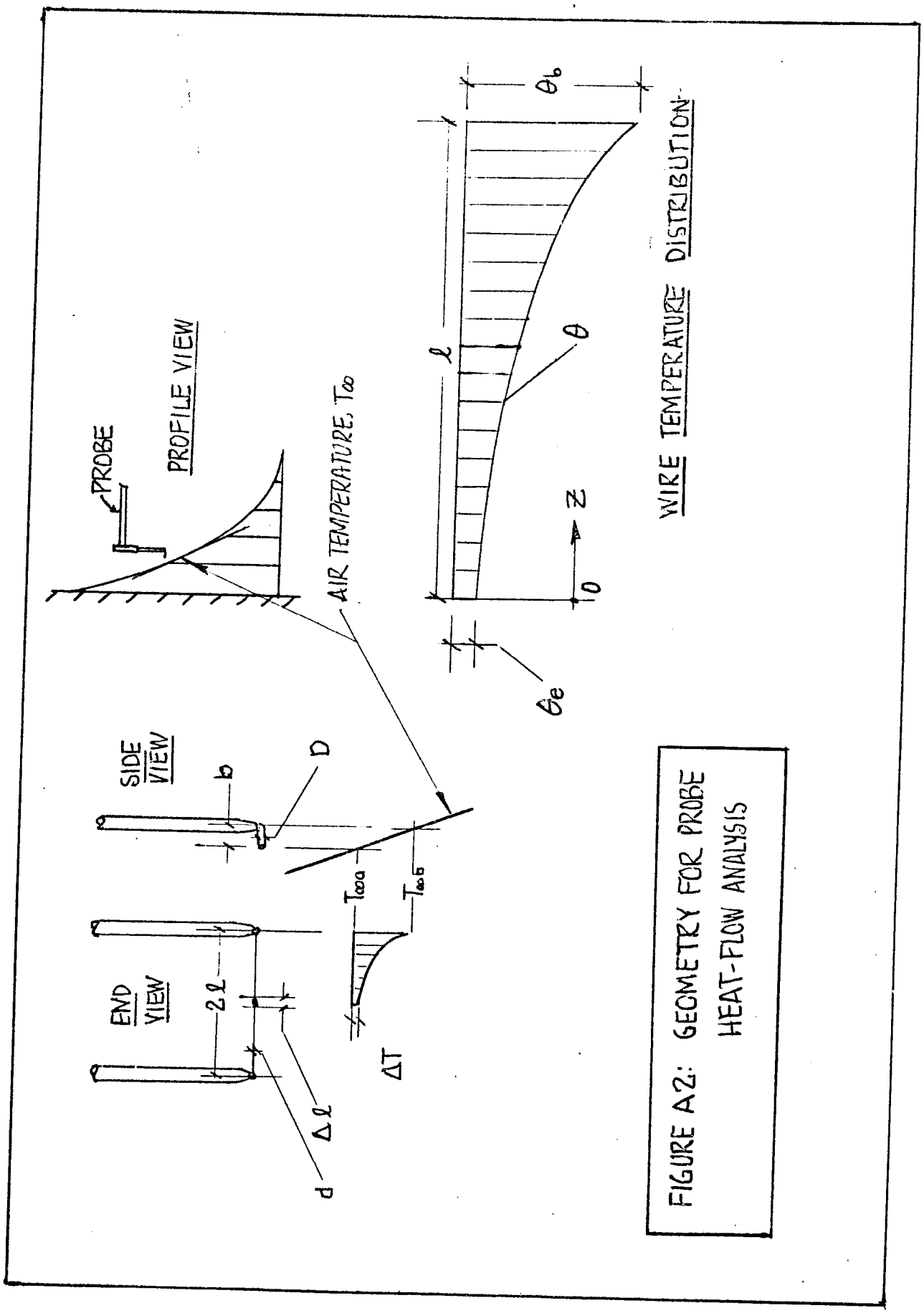


FIGURE A2: GEOMETRY FOR PROBE HEAT-FLOW ANALYSIS

(3) After specifying the limits on θ_e, calculate ℓ.

$$\theta_e \leq \theta_{e(max)}$$

$$\ell \geq \frac{1}{2}\sqrt{\frac{kd}{h}}\ \operatorname{arccosh}\left\{\frac{0.1b\left(\frac{g\beta P_r}{\nu^2}\right)^{1/3}(T_w - T_\infty)^{4/3}}{\theta_{e(max)}}\right\}$$

The computational procedure is then as follows:

(1) Recognize constraints

(a) Temperatures of wall and fluid,

(b) Desired probe diameter (b, Fig. A2),

(c) Fluid and solid properties,

(d) Allowable temperature variation, $\theta_{e(max)}$.

(2) Calculate film coefficient, h.

(3) Calculate ℓ from the equation derived above.

Using this procedure, a length of $2\ell = 1$ inch was estimated for the natural convection case, with $d = 0.0005$ inch and $b = 0.2$ inch, and with $\theta_{e(max)} = 0.5°F$.

APPENDIX III. THERMOCUPLE FIXED-POINT CALIBRATIONS

The converted temperature indications of the copper-constantan and chromel-constantan thermocouples used in this study were corrected by the equations developed below. The deviation equations are based upon measurements of known temperatures, taken with thermocouples constructed of the same materials and spools as those built into the apparatus. The following table gives the pertinent basic data.

TABLE A5. BASIC THERMOCOUPLE CALIBRATION DATA

Data Point	Reference Temperature and source	response	
		Cu-Co	Ch-Co
		LN 8662	LN K-2
1	Room temperature: Plat Resist Therm $T = 70.707^{\circ}F.$	0.810	1.2225
2	Steam Point: Hypsometer. $P_{atm} = 29.225''$, $T_s = 210.81^{\circ}F.$	4.255	6.2888
3	Ice Point: Distilled water ice bath. $T_i = 32.0^{\circ}F.$	0.0	0.0

The following deviation equations were derived from this data.

$$DEV_{CH-CO} = -.03621\ T_c + 1.844 \times 10^{-4}\ T_c^2$$

$$DEV_{CU-CO} = (6.378\ T_c - 1.29036\ T_c^2) \times 10^{-6}$$

APPENDIX IV. PROBE POSITIONING MECHANISM CALIBRATIONS

Position calibration data for the probe positioner in both electrically controlled directions is given in the following table.

Table A6. Position Calibrations

y, inches	Reading	y, inches	Reading
0.0 to 1.0	not used: directly read	3.5	228
		4.0	251
		4.5	274
1.0	118	5.0	297
1.25	128	6.0	342
1.50	139	7.0	387
1.75	151	8.0	432
2.00	162	9.0	477
2.25	173	10.0	522
2.50	184	11.0	566
3.00	206		

z, inches	Reading	z, inches	Reading
5	70	-1	427
4	128	-2	486
3	188	-3	546
2	248	-4	606
1	307	-5	666
0	368	-6	725

APPENDIX V. EMISSIVITY DATA

Table A7 presents the emissivity measurements recorded at various positions on the polished plate. The average wall temperature during these measurements was 275°F.

TABLE A7. PLATE EMISSIVITY DISTRIBUTION

x, ft	Emissivity of Surface					
------	mean	z=-5	z=-3	z= 0	z= 3	z= 5
11.5	.226	.237	.224	.224	.230	.243
9.5	.229	.237	.230	.227	.231	.234
7.5	.223	.246	.223	.219	.228	.230
5.5	.232	.228	.231	.231	.236	.236
4.5	.222	.223	.219	.218	.228	.231
3.5	.221	.219	.217	.219	.226	.222
2.5	.217	.215	.213	.215	.222	.225
1.5	.215	.217	.215	.214	.217	.214

APPENDIX VI. ALLOWABLE PLATE TEMPERATURE VARIATIONS

Two assumptions upon which the experimental results are based have to do with the temperature variations which exist within the heated plate. These are discussed here. First, as a criterion of the design, it was necessary to know what proportion of the back surface of the heated sections needed to be covered with electrical heaters such that the plate temperature itself within that section would not vary too much. Secondly, for the desired accuracy of heat flux readings, a tolerance on section-to-section temperature difference was needed. Since the first result depends upon the second, they are treated here in reverse order.

Because the theoretical heat flux due to convection, and hence the total theoretical heat flux (other losses are uniform in x) for a constant temperature plate reaches its minimum shortly before transition, this is the most critical region for measurement accuracy. If all measurements of heat flux are wanted to be within t%, then the maximum allowable loss from any section is equal to t% of the local heat flux $q_{c_{(min)}}$ at incipient transition.

Each plate section may be represented as a two-dimensional slab as shown in Figure A3. The amount of heat lost to the guard section of the plate per unit length per unit time is given by

$$q_k \doteq -k \frac{b}{L_k} (T_{WM} - T_{WG})$$

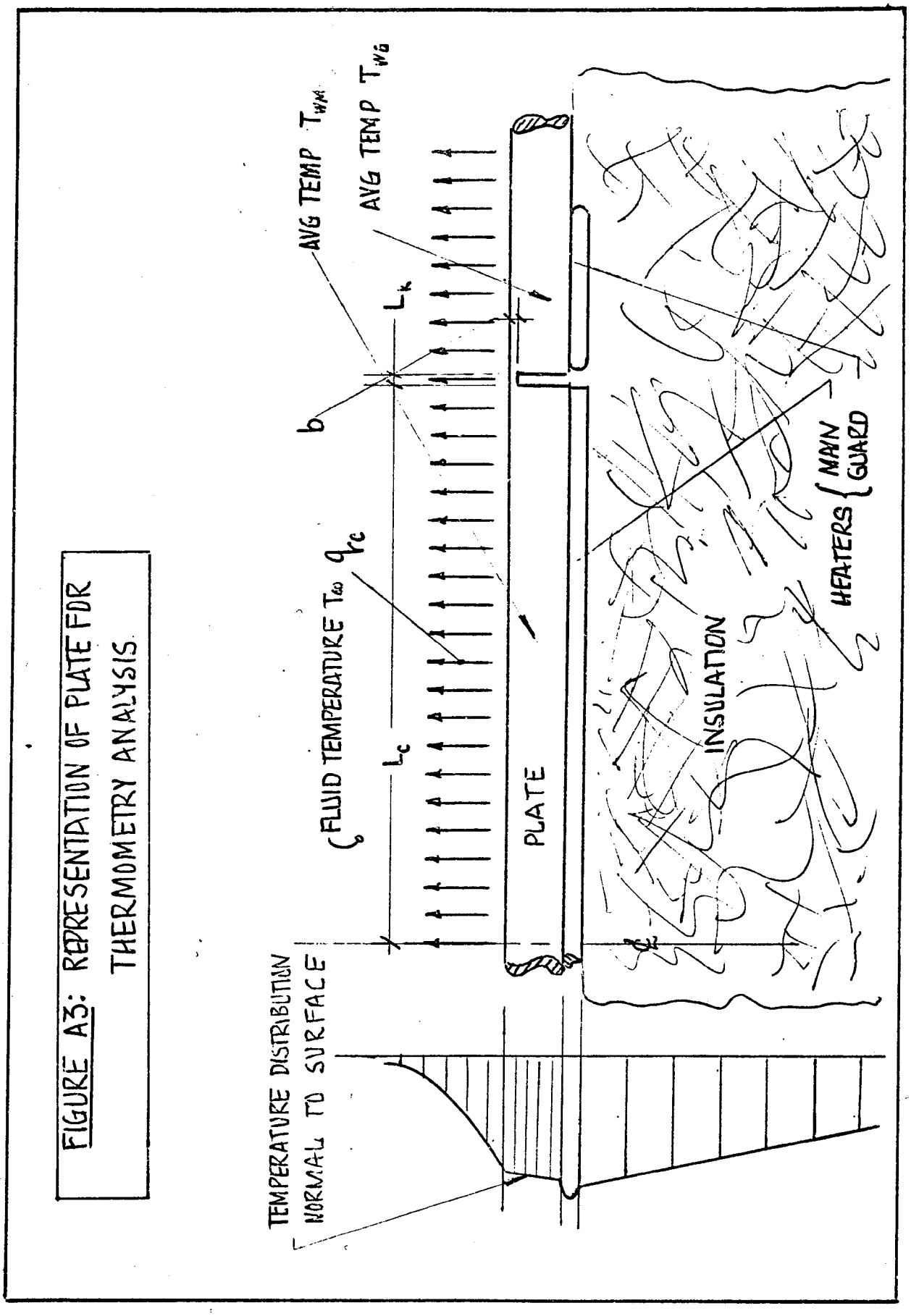


FIGURE A3: REPRESENTATION OF PLATE FOR THERMOMETRY ANALYSIS

whereas the heat loss by convection from the plate surface is

$$q_c = h L_c (T_w - T_\infty).$$

From the Ostrach theory

$$h^* = \frac{Nu_x^* k_f}{x^*} = \frac{0.416 (G_r^* P_r)^{1/3}}{x^*} \doteq 37.5 k_f.$$

Thus, if the local convection losses are to be held within t%:

$$\frac{|T_{WM} - T_{WG}|}{(T_w - T_\infty)} \leq \frac{t}{100} \left\{ \frac{37.5 k_f}{k_w} \frac{L_c L_K}{b} \right\}.$$

For the present case, a 2% error limit at an operating temperature difference of 100°F requires

$$|T_{WM} - T_{WG}| \leq 0.4\,^\circ F.$$

(Note that this is perhaps a supercritical test of accuracy in the turbulent range, since the relative magnitude of the heat transfer due to convection is much larger there.)

The second phenomenon requiring investigation as a design criterion was the distribution of temperature over the plate surface inspired by the relative size and orientation of the heaters affixed to it. An estimate of these requirements may also be obtained from a one-dimensional model. Figure A4 illustrates the geometry of this model.

If we assign $\theta = T_w - T_\infty$, the formulation of this model becomes

$$\frac{d^2\theta}{dx^2} - m^2\theta = -n, \quad n = \begin{cases} 0, & x \geq 0 \\ N, & x < 0, \end{cases}$$

where

$$m^2 = \frac{h}{kb},$$

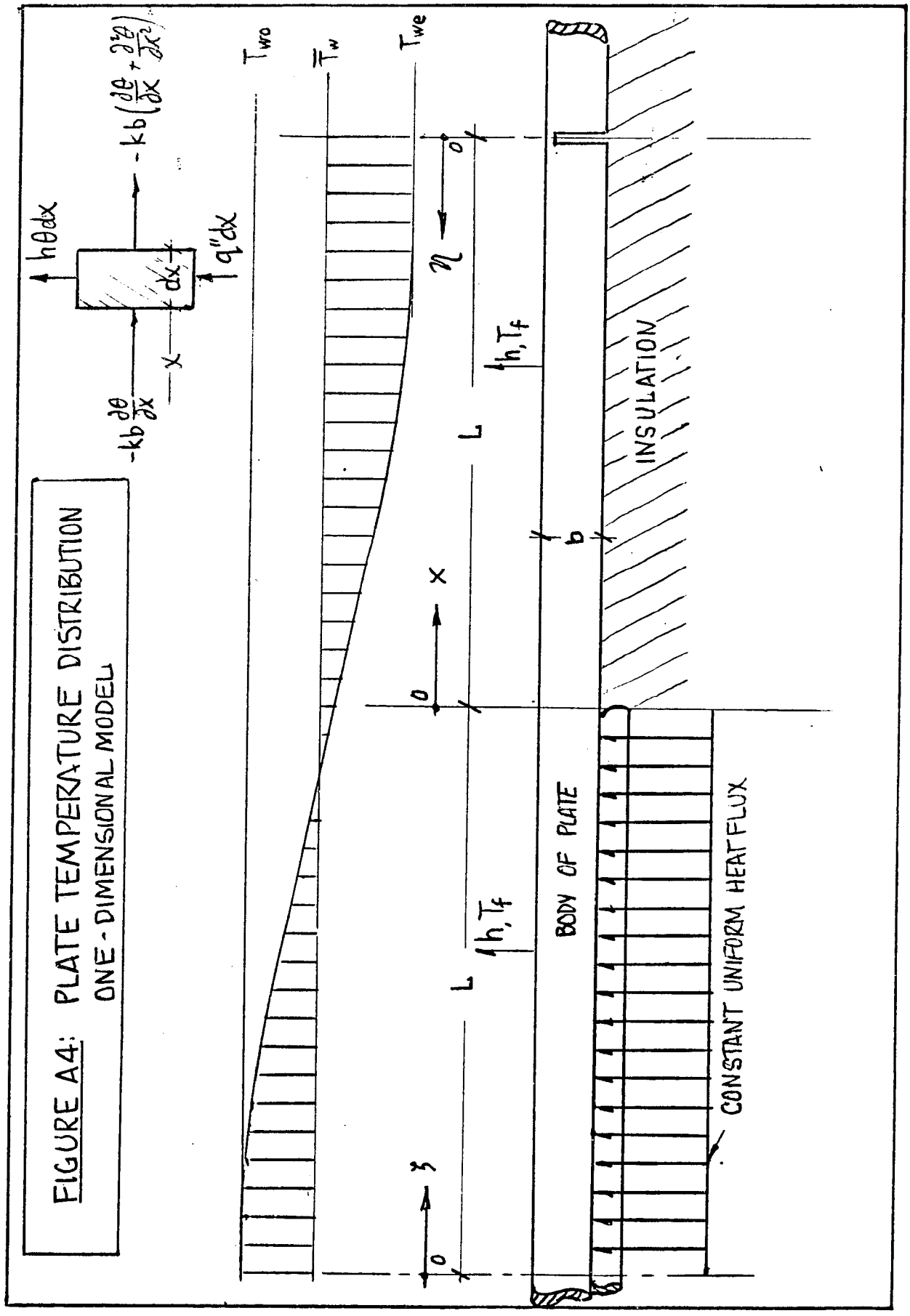


FIGURE A4: PLATE TEMPERATURE DISTRIBUTION
ONE-DIMENSIONAL MODEL

and $$N = q''/kb$$

The boundary conditions are

$$\frac{d\theta}{dx}(\pm L) = 0, \quad \theta(L) = \theta_0, \quad \theta(-L) = \theta_e$$

Actually, this system is most conveniently handled as two fin problems, matched at the center (x = 0).

For $x \geq 0$,

$$\theta_R = A \cosh m\eta + B \sinh m\eta,$$

$$\theta_R(\eta) = \theta_e \cosh m\eta,$$

and for $x < 0$,

$$\theta_L = C \cosh m\xi + D \sinh m\xi + N/m^2$$

$$\theta_L(\xi) = N/m^2 (1 - \cos n\xi) + \theta_0 \cosh m\xi$$

Since at the center $\theta_L = \theta_R$, we may write

$$\theta_e \cosh mL = N/m^2 [1 - \cosh m\xi] + \theta_0 \cosh mL$$

or

$$(\theta_0 - \theta_e)/\theta_0 = 2 [1 - 1/\cosh mL]$$

Inserting the values 2.0, 120., and 1/24, for h, k, and b, respectively gives m = 0.3165, and

$$(\theta_0 - \theta_e)/\theta_0 = 2(1. - 0.954) \doteq 0.1°F.$$

The thermocouples used in this study were accurate to within 0.5°F. It is reasonable to require that the maximum temperature fluctuation within a section be of the same order of magnitude as the allowable difference across an isolation groove. This is satisfied by the design.

APPENDIX VII. TYPICAL PLATE TEMPERATURE DISTRIBUTIONS

A. Results of Constant Heat-flux Test

Because the majority of the research reported in the literature deals with self-heated one piece plates, for which a uniform temperature was assumed, the following data was gathered. It was hoped that this data would give basis for evaluation of the uniform-temperature assumption. The plate heaters were adjusted to a uniform heat input, such as might be expected to exist in a one-section test surface, and the resulting plate temperature distribution in x was recorded. As may be seen from Figure A5, the distribution of temperature is far from uniform. The impact of these temperature distributions upon the resulting heat transfer data would make an interesting study.

B. Constant-Temperature Plate Data

Table A8 shows a typical distribution of thermocouple readings as they appeared during a heat-flux test in the present study.

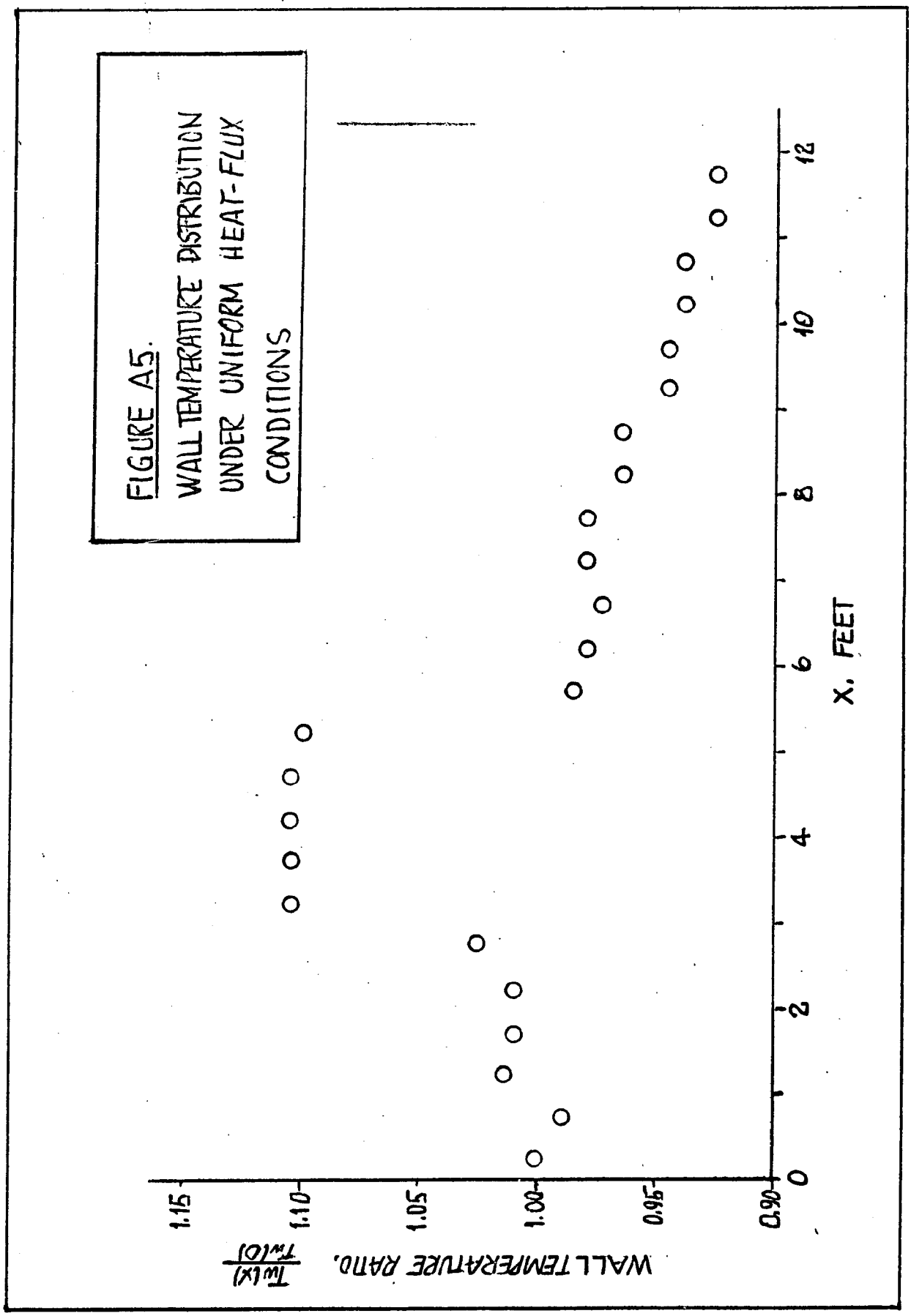


FIGURE A5.
WALL TEMPERATURE DISTRIBUTION UNDER UNIFORM HEAT-FLUX CONDITIONS

TABLE A8. TYPICAL PLATE TEMPERATURE DISTRIBUTION

Station	Temperatures, Cu-Co millivolts			
-------	Left Guard	Main A	Main B	Right Guard
12	2.69	2.69	2.68	2.68
11	2.68	2.68	2.68	2.69
10	2.69	2.68	2.69	2.69
9	2.68	2.68	2.68	2.68
8	2.69	2.69	2.68	2.69
7	2.69	2.68	2.68	2.69
6	2.68	2.68	2.68	2.68
5	2.68	2.68	2.68	2.68
4	2.68	2.68	2.69	2.68
3	2.69	2.69	2.69	2.69
2	2.69	2.69	2.69	2.69
1	2.68	2.69	2.69	2.68

(Data from Run of 12 Apr 66 - 2000 hrs)

APPENDIX VIII. LIST OF EXPERIMENTAL EQUIPMENT

The following table reports pertinent data relative to the major experimental equipment used in the measurements reported in the text.

TABLE A9. EQUIPMENT LIST

Item & Mfgr	Model	Serial #	Range	Accuracy
Portable Precision Potentiometer (L & N)	8662	1151909	0 - 75 mv.	10 microvolts
"	7552	752431	0 - 0.1 vdc	1 microvolt
Galvanometer (L & N)	2430C	1329831	25 ohms	3.9 μa/m
"	"	1654526	500 ohms	3.5 μa/m
Resist. Therm. (L & N)	8163	1639558		
Bridge (L&N)	8069	1605421	100 ohms	1 milliohm
Wattmeter (SenResIns)	DW	955527	200 watts	¼ % fs
Std Cell (Eppley)		661279	1.01926 v.	0.01 %
Thermopile (Cenco)		81070		
Dial Gage (Federal)			0 - 1 inch	0.0002 inch
Miller Telescope (R. Heiser)			3 - 10X	
Galvanometer (GMI)	570	204	0 - 60μv	

APPENDIX IX. VELOCITY MEASUREMENT IN NATURAL CONVECTION

The following is a brief discussion of the problems involved in accurate measurement of local fluid velocities in turbulent natural convection. It is presented in four parts, vis. (1) The requirements placed upon any anemometer by the physics of natural convection, (2) the low-speed limitations of the hot-wire anemometer, (3) comments on some other possible techniques, and (4) recommendations regarding the measurements in question.

A. Natural Convection Anemometer Problems

The experimental challenge presented by the measurement of velocity in natural convection is composed of several separate problems. Primary among these is the magnitude of the velocities to be measured. The general shape of the natural convection velocity profile is well known (consult Figure 1 of the text). It is significant that for laminar natural convection in air, the maximum velocity measured has been on the order of 0.5 feet per second. Approximate early measurements in the turbulent regime (Rayleigh Number of 10^{10}) indicated a velocity maximum in the vicinity of 2 ft/sec. (24) The low relative potentials thus constitute a significant challenge to measurement, in and of themselves.

The problem is further complicated by the changing direction of the average total velocity vector with distance through the boundary layer, due to the combined in-

fluence of the u and v velocities. A satisfactory instrument must thus be capable of directional discrimination.

The superposition of the temperature profile further complicates matters. The desired instrument must also separate its velocity and temperature responses in some way.

For accurate measurements near the wall, the interaction of wall and instrument must be, at least, capable of mathematical correction. Wills[54] describes and discusses this problem and its solution for a particular class of instruments.

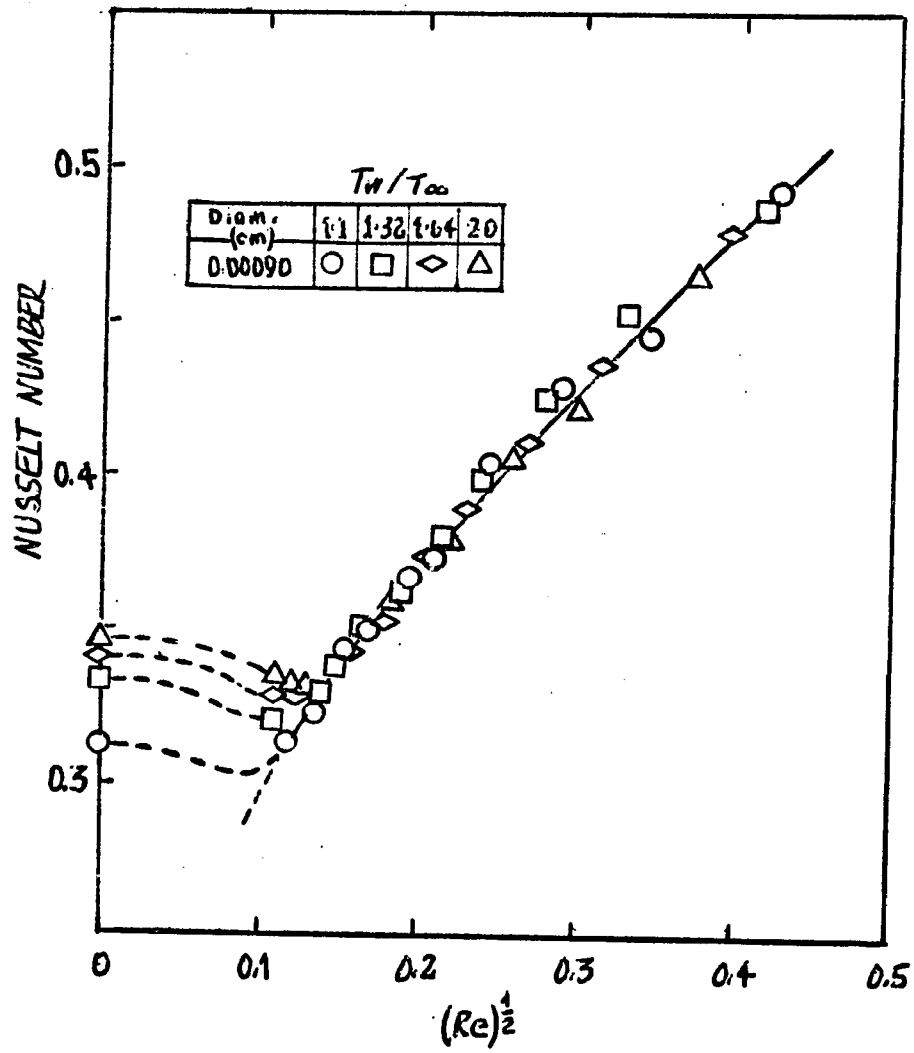
Perhaps the most significant problem in the turbulent regime of the flow is the turbulence itself. The fluctuations introduced into all measurable variables present an added burden upon the instrumentation: it must here be capable of discriminating between mean and fluctuation. This is particularly severe in the case of natural convection, where fluctuations are relatively large, and frequencies are small.

The sum of the problems listed presents a formidable obstacle, especially in the turbulent case. Because of its widespread success in forced convection, the hot-wire anemometer seems at first to provide the obvious solution. As will shortly be seen, some subtleties of its heat transfer physics also preclude its use.

B. Obstacles to the Application of the Hot-Wire Anemometer to Natural Convection

The majority of the problems mentioned above have been successfully attacked by hot-wire anemometry in the case of forced convection. By the employment of two or more wires in special geometrical and thermal configurations, the various effects of crossed velocity and temperature fields may be singled out. Although fluctuations greater than 20% of the mean would require a new data handling technique to allow the measurement of intensities and correlations, mean velocity should be easily within the range of capablility. The real challenge of turbulent natural convection is rooted in the magnitude of the velocities themselves. At Reynolds Numbers below one the sensitivity of the hot-wire anemometer decreases rapidly to zero (and actually becomes negative in the limiting case). This is due to the interaction of the forced convection problem caused by the velocity field to be measured with the free convection problem inspired by the overheat in the wire. This problem has received thorough treatment in the experimental work of Collis and Williams[8]. Their data for this interaction problem is partially reproduced here as Figure A6. For the experimental case described in the text, $(Re)^{\frac{1}{2}} = 0.2$ corresponds roughly to a cooling velocity of 0.4 feet per second. As is shown in Figure A6, the lower limit of sensitivity increases with overheat. Further information from the paper indicates that it also increases with

FIGURE A6. FORCED-FREE CONVECTION INTERACTION DATA FOR HOT WIRES (FROM COLLIS & WILLIAMS [8])



wire diameter. The same effects were noted earlier by Simmons[43].

Comparison of the instrument limitations with the expected velocity magnitudes, as discussed above, reveals the difficulty clearly. Even for an isothermal case, only velocities near the maximum would be capable of accurate measurement by this technique. The presence of the temperature field renders the highly temperature-sensitive hot-wire useless as an anemometer in this low-velocity range.

In view of what is now knownabout hot-wire physics, the velocities measured by Griffiths and Davis[24] are indeed suspect, and although no better measurements have been published to date, we accept them with reservation.

C. Other Anemometery Possibilities

With a full awareness of the limitations of the hot-wire anemometer, methods which previously seemes cumbersome and unnecessarily complicated are seen in a more favorable light.

The pioneering velocity measurements for the laminar case were made with the quartz-fibre anemometer. This instrument is thoroughly discussed by Tritton[52]. Although cumbersome in application, it has the advantage of a very low sensitivity to temperature changes, and thus sufficed for the laminar case. The reference cited gives a good bibliography for laminar applications. This initial recommendation to its use for turbulent flows is rather

forcefully counterbalanced by the greatly complicated procedure required for its application to the fluctuation-ridden measurements characteristic of those flows.

A search of the literature suggested the following alternatives: (1) a hot-thermistor anemometer[32], (2) timed observations of smoke or particle trajectories, (3) a pulsed hot-wire, or pulsed-spark anemometer.

Experimental trials of alternative (3) suggested a very poor sensitivity to low velocities here as well. It would be surprising indeed to find a different heat transfer behavior in the larger, hotter heated thermistor than in the hot-wire anemometer. The interminable observations which are suggested by the particle-trajectory technique for low-frequency, fluctuating flows appears to rule out alternative (2). The remaining possibility within the stated scope is that of the quartz-fibre anemometer. The extensive investigation of this instrument made by Tritton[52] shows that it can probably be adapted to turbulent flow, but at high cost in terms of optical instrumentation and observation, compilation and interpretation labor, since all data must be taken visually. Moreover, calibration is a very exacting and troublesome process, since the natural frequencies of each element must be separately determined for proper interpretation of results. The sum of these precluded the use of this instrument in the experimental program reported in the text.

As a result of the study outlined above, it was concluded that measurements of velocity were beyond the scope of the present study.

D. Recommendations for Velocity Measurements

It is recommended that the fibre anemometer and particle-trajectory techniques be further investigated. The use of one of these methods to obtain information about the fields of velocity in turbulent natural convection would constitute a valuable contribution to the literature.